Seasonal Variability of Sediment Oxygen Demand and Biogeochemistry on The Namibian Inner Shelf

Warren R. Joubert
B.Sc (Hons.) (Chemistry) (University of Stellenbosch)

Submitted in fulfilment of the requirements for the degree of
Master of Science
(Geochemistry)

Department of Geological Sciences


UNIVERSITY OF CAPE TOWN

2006

Supervisors:
Dr. Alakendra. N. Roychoudhury
Dr. Pedro.M.S Monteiro

DECLARATION

This thesis reports the seasonal variability in sediment oxygen demand and its relation to biogeochemical fluxes on the Namibian inner shelf sediments. It forms part of the SEDYN project under the BENEFIT programme, Project No: GTZ 2001/007. Sediment sampling coincided with monthly oceanographic monitoring cruises conducted by Namibian National Marine Information and Research Centre (NatMIRC) and was carried out between November 2002 and November 2003. The ideas presented in this thesis are largely my own, the chemical data was collected and processed with the help of people listed in the acknowledgements.

The data from this work contributed to following journal article accepted for publication in *Geophysical Research Letters*:

P.M.S. Monteiro, A. van der Plas, V. Mohrholz, E. Mabille, A. Pascall, W.R. Joubert, The variability of natural hypoxia and methane production in a coastal upwelling system: oceanic physics or shelf biology?

I, Warren Ryan Joubert, declare that this work has not been submitted for a degree at any other university and any assistance I received throughout my studies is fully acknowledged.

_____ _____

Date

ACKNOWLEDGEMENTS

A number of people were instrumental in making this project a success. And it is with appreciation that I express my gratitude to the following:

Dr Alakendra Roychoudhury (UCT), for taking on this project at such a late stage and for his guidance, enthusiasm and advice, throughout the project. Dr Pedro Monteiro (CSIR), for the opportunities created to pursue a carreer in biogeochemistry. Also for his thought provoking discussions and guidance throughout the project.

The staff at CSIR (Stellenbosch), Dr Marten Grundlingh and the marine ecosystems group. Mr Andrew Pascal, Mr Sebastian Brown, Mr Alistair Adonis (CSIR) and Mr Eugane Mabille for assistance in field sampling logistics and sampling analysis. Also for their encouragement and willingness to listen to frustrations.

Anja van der Plas (NatMirc, Namibia), for the the use of laboratory facilities at Natmirc and also Kaarina Nkandi and Suzie Christoff from Natmirc for their assistance in the laboratory. And for making my stay in Swakopmund a welcome one.

The BENEFIT secretariat (www.benefit.org) for their financial assistance and investing in the capacity of young researchers in the Benguela region and also CSIR for financial assistance thought their parliamentary grant program.

The Officers and crew of the Namibian fisheries research vessel, *RV Welwitchia*, for their assistance and patience during multi-core sampling.

To my parents, family and friends, for their support, encouragement and prayers throughout. Lastly, Brigetta, for your belief, understanding, support and love. You're my reason for being.

Abstract

The Central Benguela inner shelf is characterised by hypoxic to anoxic sub-thermocline water conditions on a semi-permanent basis. Historical understanding of the incidence of hypoxia is that the inner shelf area off Namibia is one of the main areas of formation of low oxygen water (LOW) in the Benguela upwelling system. Local biogeochemical remineralization of organic matter mostly related to the primary production in surface waters (Chapman and Shannon. 1985) is thought to drive seasonal variability in sediment oxygen demand. New understanding of the system suggests that shelf hypoxia is driven by a remotely forced equatorial hypoxic boundary condition thought to trigger anaerobic remineralization and increased sediment fluxes of reduced metabolites (Monteiro *et. al. in press.*). The study focused on seasonal variability of sediment oxygen demand on the Namibian inner shelf and its relation to particulate organic carbon and reduced metabolite fluxes.

Seasonal variability of total sediment oxygen demand measurements were conducted from November 2002 – November 2003 on sediments from one station (23°S, 14°E) on the Namibian organic rich inner continental shelf. Total sediment oxygen demand (TSOD) was compared with vertical fluxes of POC and reduced metabolites at the sediment-water interface to assess their role as drivers of TSOD.

A seasonal trend in sediment oxygen demand (TSOD) from the core incubations were observed, which peaked at 20.10 mmol $O_2.m^{-2}.day^{-1}$ during austral winter/early spring (May to Sep 2003). Particulate Organic Carbon (POC) fluxes however peaked during austral summer months (Nov – Dec 2002 and Nov 2003) at 7 – 10 $mmolC.m^{-2}.d^{-1}$. During summer months a good stoichiometric agreement between POC flux and

TSOD were observed, however, TSOD increased beyond the oxidation of POC/PON during winter months. The anomaly in the austral winter period suggested that TSOD controls lie in a biogeochemical response of the sediment and not in POC forcing. It was expected that reduced metabolite fluxes govern sediment oxygen demand.

Ammonium diffusive fluxes peaked during austral summer (Nov – Dec 2002) months at 3 – 5 $mmolN.m^{-2}.d^{-1}$ in the direction of the water column indicating highest remineralization rates during these months. Small concentration gradients of hydrogen sulphide were observed with little seasonal variability in hydrogen sulphide fluxes with only a spike in July 2006 which was in agreement with the increased TSOD in austral winter.

This study clarifies some of the important biogeochemical characteristics of seasonal variability in sediment oxygen demand on the Namibian inner shelf. Although POC and ammonium fluxes play a role in seasonal TSOD in austral summer months, neither of these fluxes explain the TSOD increase in winter. Increased biogeochemical activity, coupled to remote forcing signal are thought to be responsible for this.

TABLE OF CONTENTS

Declaration i

Acknowledgements ii

Abstract iii

List of Figures ix

List of tables xiii

Chapter 1 1

Introduction and literature review 1

1.1 Context: Fisheries and ecosystem services..... 1

1.2 Central Benguela shelf sediment characteristics. 5

1.3 Remineralization of organic matter..... 8

1.4 Redox zonation within the sediment (oxic, suboxic and anoxic). 13

1.5 Oxidation of reduced inorganic metabolites..... 16

1.6 Flux across the sediment-water interface..... 16

1.7 Summary of processes affecting sediment oxygen demand..... 22

1.8 The aim of this project. 23

1.9 Approach. 23

Chapter 2 25

Materials and sampling methods 25

2.1 Introduction..... 25

2.2 Site description. 25

2.2.1 Geographic setting and main characteristics 25
2.3 Sediment sample collection. 28
2.4 Sediment oxygen demand measurements 30
2.5 Interstitial water 33
2.6 Diffusive fluxes at the sediment water interface. 34
2.7 Sediment core incubations. 35
2.8 Brief description of analytical methods used for determining solute concentrations 35
2.9 Particulate Organic Carbon (POC) and Particulate Organic Nitrogen (PON). 36
2.10 Sediment traps 36

Chapter 3 38

Results 38

3.1 Sediment interstitial water profiles. 38
3.1.1 Ammonium porewater profiles. 46
3.1.2 Nitrate porewater profiles. 46
3.1.3 Sulphate porewater profiles. 46
3.1.4 Hydrogen sulphide porewater profiles. 47
3.1.5 Ortho phosphate porewater profiles. 47
3.1.6 Ortho silicate porewater profiles. 48
3.2 Particulate Organic Carbon (POC) and Particulate Organic Nitrogen (PON). 48
3.3 Calculated diffusive fluxes of dissolved species. 53
3.3.1 Ammonium diffusive fluxes. 54
3.3.2 Nitrate diffusive fluxes. 55

3.3.3 Sulphate diffusive fluxes. 56
3.3.4 Hydrogen sulphide diffusive fluxes. 57
3.3.5 Phosphate diffusive fluxes. 58
3.3.6 Dissolved silicate diffusive fluxes 59
3.4 Sedimentation fluxes of particulate organic carbon (POC) and nitrogen (PON). 60
3.5 Total sediment oxygen demand. 61
3.6 Fluxes of dissolved species measured in incubation experiments. 64

Chapter 4 65
Discussion 65
Temporal variability in sediment oxygen demand and biogeochemical fluxes 65
4.1 Seasonal oxygen and oxygen flux variability. 65
4.2 Seasonal POC/PON fluxes. 66
4.3 Reduced metabolite diffusional fluxes. 69
4.3.1 Diffusive ammonium fluxes. 69
4.3.2 Diffusive hydrogen sulphide fluxes. 71
4.3.3 Diffusive Sulphate flux. 74
4.4 Fluxes of other metabolites 75
4.4.1 Diffusive nitrate flux. 75
4.4.2 Diffusive phosphate flux. 76
4.4.3 Diffusive silicate flux 77

Chapter 5 79

Findings and Conclusions 79

References:..... 82

Appendix A - **Description of analytical methods** 90

- Dissolved Oxygen. 90
- Dissolved Nitrate. 90
- Dissolved Total Ammonium. 90
- Dissolved Reactive Phosphate. 91
- Dissolved Reactive Silicate 91
- Sulphate. 92
- Hydrogen sulphide. 92

Appendix B – Raw data for Chapter 3. 93

Table B.1: Porewater concentrations of sediment cores collected in 2003. 93

Table B.2: Areal oxygen uptake rates calculated from raw data. 96

Table B.3: Particulate organic carbon (POC) and particulate organic nitrogen (PON) concentration profiles with sediment depth from November 2002 to November 2003. 97

LIST OF FIGURES

Figure no.	***Figure Caption***	*Page*
Figure 1.1	A conceptual summary of the main processes governing the distribution of low oxygen waters in the Benguela system (Chapman and Shannon, 1985).	*4*
Figure 1.2	Depicts the spatial distribution of large-scale high- and low-POM bands along the Namibian shelf (taken from Monteiro *et. al.* 2005). It shows the highest concentration (POM up to 25%) at the inshore belt. The mid-shelf belt terminates just south of 23°S where the double shelf break feature also ends. The insert shows the position of Namibia relative to Africa.	*6*
Figure 1.3	Sequence of microbially mediated redox reactions. Arrows point in the direction of the spontaneous redox reaction and no information is contained in the relative length of the arrow. (Taken from *Aquatic Chemistry*, Stumm and Morgan (1996) by John Wiley and Sons, Inc., New York.	*10*
Figure 1.4	Idealized representation of depth profiles of O_2, NO_3^-, $MnO_2(s)$, Mn^{2+}, Fe^{2+}, SO_4^{2-}, HS^- and CH_4 in marine sediments (Adapted from Froelich *et. al.* 1979 and Libes, 1992). Reactions generally occur in the sequence down the depth of the sediment.	*15*
Figure 1.5	Schematic representation of box model normally used to depict bioturbation. Within the box there is perfect mixing and uniformity of concentration (Adapted from Berner, 1980).	*21*
Figure 1.6	Conceptual model of processes affecting sediment oxygen demand.	*22*
Figure 2.1	Depicts the sample location at Station A as well as the spatial distribution of the large-scale high- and low POM bands along the Namibian shelf (In Monteiro, et. al. 2005, adapted from Bremner, 1983). It shows two parallel POM rich belts the highest concentration (POM up to 25%) at the inshore belt.	*26*
Figure 2.2	Multicorer device deployed over the side of the *RV Welwitschia* during a sampling cruise.	*30*
Figure 2.3	Schematic diagram of sediment core oxygen incubation measurements. Oxygen concentrations were monitored in the overlying water over a period of 24 hours. The diagram is not to scale.	*32*
Figure 2.4	Reeburgh Teflon squeezing apparatus (Rheeburgh, 1967).	*33*

Figure 2.5	Retrieval of sediment traps deployed at Station A.	*37*
Figure 3.1	Interstitial water profiles of dissolved ammonium in sediment cores collected at Station A between Oct 2002 and Nov 2003. Ammonium concentrations of the overlying water were chosen at the sediment-water interface (Z = 0cm). Below Z = 0cm, ammonium concentrations were orders of magnitude greater than at the interface and indicated flux in the direction of the water column.	*40*
Figure 3.2	Interstitial water profiles of nitrate in sediment cores collected at Station A between Oct 2002 and Sep 2003. Nitrate concentrations of the overlying water were chosen at the sediment-water interface (Z = 0cm). Peak nitrate concentrations were observed between Z = 1cm and Z = 5 cm which were unexpectedly high in certain cases, possibly due to sample handling which introduced oxygen into the sediment cores.	*41*
Figure 3.3	Interstitial water profiles of sulphate in sediment cores collected at Station A between Feb 2003 and Nov 2003. Sulphate concentrations at the sediment-water interface were chosen as the overlying water concentration. Higher sulphate concentrations in the water column indicated sulphate flux into the sediment.	*42*
Figure 3.4	Interstitial water profiles of dissolved hydrogen sulphide in sediment cores collected at Station A between Feb 2003 and Nov 2003. Dissolved hydrogen sulphide concentrations increased towards the bottom of the cores from Feb 2003 – May 2003 and indicated fluxes in the direction of the water column. Sep 2003 and Nov 2003 showed little concentration variability with sediment depth. July 2003 shows an unexpected maximum in the concentration profile.	*43*
Figure 3.5	Interstitial water profiles of dissolved phosphate in sediment cores collected at Station A between Oct 2002 and Nov 2003. Phosphate concentrations within the sediment (below Z =1cm) were orders greater than at the sediment-water interface (Z = 0cm) which implied flux in the direction of the water column.	*44*
Figure 3.6	Interstitial water profiles of dissolved ortho-silicate in sediment cores collected at Station A between October 2002 and November 2003. Dissolved silicate concentrations within the sediment (below Z =1cm) were orders greater than at the sediment-water interface (Z = 0cm) which implied flux in the direction of the water column.	*45*
Figure 3.7	Depth profiles of % organic carbon and nitrogen of sediment cores collected on the Namibian inner shelf in November 2002.	*49*
Figure 3.8	Depth profiles of % organic carbon and nitrogen of sediment cores collected on the Namibian inner shelf in February 2003.	*49*
Figure 3.9	Depth profiles of % organic carbon and nitrogen of sediment cores collected on the Namibian inner shelf in March 2003.	*50*
Figure 3.10	Depth profiles of % organic carbon and nitrogen of sediment cores collected on the Namibian inner shelf in May 2003.	*50*

Figure 3.11	Depth profiles of % organic carbon and nitrogen of sediment cores collected on the Namibian inner shelf in July 2003.	*51*
Figure 3.12	Depth profiles of % organic carbon and nitrogen of sediment cores collected on the Namibian inner shelf in November 2003.	*51*
Figure 3.13	Plot of diffusive ammonium flux on the Namibian inner shelf sediments from Oct 2002 to Nov 2003. Diffusive fluxes are expressed in mmolN.m^{-2}.d^{-1}. Data suggests highest ammonium flux in summer months and lowest ammonium flux in winter months. Negative scale indicated flux to the water column.	*54*
Figure 3.14	Plot of diffusive nitrate flux on the Namibian inner shelf sediments from Oct 2002 to Nov 2003. Diffusive fluxes are expressed in mmolN.m^{-2}.d^{-1}. The data show no clear seasonal trend in nitrate flux. Negative scale indicated flux to the water column which is unexpected in the anoxic environment.	*55*
Figure 3.15	Plot of diffusive sulphate flux on the Namibian inner shelf sediments from Feb 2003 to Nov 2003. Diffusive fluxes are expressed in mmolS.m^{-2}.d^{-1}. Highest fluxes were observed from May 2003 – Sep 2003. Positive scale indicates flux into the sediment.	*56*
Figure 3.16	Plot of diffusive hydrogen sulphide flux on the Namibian inner shelf sediments from Feb 2003 to Nov 2003. Diffusive fluxes are expressed in mmolS.m^{-2}.d^{-1}. No seasonal trend was observed in hydrogen sulphide fluxes only a spike was of elevated sulphide flux in July 2003. The negative scale indicates flux to the water column.	*57*
Figure 3.17	Plot of diffusive phosphate flux on the Namibian inner shelf sediments from Oct 2003 to Nov 2003. Diffusive fluxes expressed in mmolP.m^{-2}.d^{-1}. The negative scale indicates flux to the water column.	*58*
Figure 3.18	Plot of diffusive silicate flux on the Namibian inner shelf sediments from Oct 2003 to Nov 2003. Diffusive fluxes are expressed in mmolSi.m^{-2}.d^{-1}. The negative scale indicates flux to the water column.	*59*
Figure 3.19	Plot of depositional C_{org} and N_{org} flux on the Namibian inner shelf from Nov 2002 to Nov 2003. Fluxes of both C_{org} and N_{org} peaked during summer months. Rates are expressed in mmol $Cm^{-2}day^{-1}$.	*61*
Figure 3.20	Plot of total oxygen consumption on the Namibian inner shelf between Nov 2002 and Nov 2003. TSOD peaked between May 2003 and Sep 2003.	*63*
Figure 3.21	Water column dissolved oxygen profile time series at sample Station A from Oct 2002 – Nov 2003. Water depth (m) is plotted on the y-axis and oxygen concentration per individual month on the x-axis. It shows that anoxic conditions peaked between Feb 2002 and Jul 2003 while hypoxic conditions prevailed during summer months. (Data courtesy of NATMIRC).	*63*

Figure 4.1	*a*) Plot of total oxygen demand on the Namibian inner shelf between Nov 2002 and Nov 2003. TSOD peaked between May 2003 and Sep 2003. Rates are expressed in mmol $O_2m^{-2}day^{-1}$; *b*) Water column dissolved oxygen profile time series at sample Station A from Oct 2002 – Nov 2003. It showed the maximum anoxia is in winter months.	*66*
Figure 4.2	Plot of seasonal relationship between POC export flux and C:N molar ratios: 2002 – 2003. It shows highest input of fresh POC fluxes (C:N ~7) during summer months, while winter months showed the slowest POC fluxes with higher C:N ratios. POM with higher C:N ratios is and indication of 'older' relict POM.	*67*
Figure 4.3	Plot comparing TSOD and POC flux during 2002 – 2003. It shows that peak POC fluxes during summer months (Nov 2002 – Mar 2003) do not coincide with peak TSOD during winter to early spring (May 2003 – Sep 2003).	*68*
Figure 4.4	Comparison of PON flux and NH_4 flux at the sediment water interface. It shows that PON fluxes are smaller than NH_4 fluxes.	*71*
Figure 4.5	Plot showing the hydrogen sulphide and sulphate diffusive fluxes (in mmol $S.m^{-2}.d^{-1}$) between Feb 2003 and Nov 2003. It shows that the highest sulphide fluxes into the water column (Jul 2003) had little relation to sulphate fluxes over the period.	*74*
Figure 4.6	Plot of phosphate diffusive flux vs ammonium diffusive flux. It shows the linear relationship between ammonium and phosphate. The line represents the 16:1 N:P Redfield stoichiometry. It shows the linear relationship between ammonium and phosphate flux and its typical Redfield behaviour.	*77*
Figure 5.1	Plot comparing TSOD and POC flux during 2002 – 2003. It shows that peak TSOD (winter to early spring; Mar - Sep) does not coincide with peak POC fluxes (during summer months; Nov - Feb).	*80*

LIST OF TABLES

Table no.	***Table Caption***	*Page*
Table 1.1	Low oxygen water (LOW) terminology, concentrations and impacts (Taken from Monteiro *et. al.* 2004)	*2*
Table 1.2	Stoichiometric relationship between oxidant and organic matter (Taken from Froeliech *et. al.*1979).	*11*
Table 1.3	Oxidation reactions of educed compounds.	*12*
Table 2.1	Summary of sampling schedule, positions, water depth and water column properties in the benthic boundary layer (BBL; <5m overlying the sediment) determined with Seabird 911*plus* CTD-O (courtesy NATMIRC).	*28*
Table 3.1	Concentration of oxygen, ammonia, nitrate, sulphate and sulphide in the bottom boundary layer (BBL; <5m above sediment) collected with Niskin bottles during each sampling interval.	*39*
Table 3.2	C:N molar ratios down the depth of the sediment cores over the course of the year (Nov 2002 – Nov 2003). Highest ratios (>9) were observed during summer months indicating relict organic matter.	*52*
Table 3.3	Summary of calculated diffusive fluxes calculated using Fick's 1st Law. For concentration gradients (dC/dx), *interface* indicated gradients calculated from the difference between Z = 0 cm and Z =1cm while for the *gradient* the linear slope down the length of the core were used. Negative flux rates refered to diffusive flux in the direction of the water column while positive values implied flux in the direction of the sediment.	*53*
Table 3.4	Quasi-monthly depositional flux (total suspend solids, POC flux and PON flux) from sediment traps moored at Station A (22°59'S 14°03'E). The <200 µm fraction results are presented in both mg.m^{2-} $\cdot$d^{-1} and mmol.m^{-2}.d^{-1}.	*61*
Table 3.5	Areal flux of ammonium, nitrate, sulphate, hydrogen sulphide, phosphate and silicate measured in sediment cores collected on the Namibian inner shelf sediments from Nov 2002 till Nov 2003. Negative rates indicate decrease in concentration while positive rates indicate increase. Standard deviations in brackets suggest that the replicate samples were not reproducible.	*64*

Chapter 1

Introduction and literature review

1.1 Context: Fisheries and ecosystem services.

Fisheries in Namibia is the second largest contributor to the country's GDP and therefore are of great importance to its economy (10% of the GDP in 2000, www.bclme.org). Fisheries habitats are largely constrained by the temporal and spatial variability of hypoxia and anoxia (Monteiro and Van der Plas 2004). Low oxygen water (LOW) characterises most of the Namibian inner shelf (Wattenberg 1938, 1939; Copenhagen 1953; Hart and Currie 1960; Bubnov 1972; Chapman and Shannon 1985; Bailey 1985, 1991; Monteiro *et. al.* 2004) causing a significant problem for fisheries management.

Ecosystem services include primary productivity and suitable habitat. High primary productivity supports abundant resources (Hutchings 1992; Hocutt and Verheye 2001). Habitat suitability however, is influenced significantly by oxygen availability. The impacts of hypoxic/anoxic conditions include the periodic mortalities of fish (Copenhagen 1953) and the recruitment failures as observed near Walvis Bay in 1992 and 1994 (Hamukuaya *et. al.*, 1998; Woodhead *et. al.*1998). Avoiding hypoxic areas is a common response of marine organisms and may play an important role in determining their abundance, distribution, catchability and availability (Monteiro *et. al.* 2004). Habitat modification due to hypoxia has also triggered adaptive behavioural and physiological responses in the local biota. Juvenile Cape hake *Merluccius capensis*, which inhabit the Walvis Bay inner shelf, tolerate low levels of dissolved oxygen (Woodhead *et. al.* 1998). Offshore spawning of Cape hake *M. capensis* just

above the bottom where oxygen concentrations are at a minimum, have been proposed to minimise egg predation (Sunby *et. al.* 2001). It was also shown that hake tolerate oxygen levels down to 44.6 µmol $O_2.l^{-1}$ ($1ml.l^{-1}$) due to high haematocrit and relatively high haemoglobin concentrations in their blood (Woodhead *et. al.* 1998). Low oxygen water (LOW) terminology are used in this document are summarised in Table 1.1.

Table 1.1: Low oxygen water (LOW) terminology, concentrations and impacts (Taken from Monteiro *et. al.* 2004):

Oxygen State	**Oxygen concentration**	**Impacts**
Super Saturated	>100% saturation	Out-gassing to the atmosphere: typical in high surface primary production
Saturated	100% saturation	Equilibrium with the atmosphere
Under Saturated	30 – 100% saturation	Range over which biological responses should be insignificant
Depleted	89.2 – 133.8 $\mu mol.l^{-1}$	Biological impacts at behavioural level
Critical Hypoxia	44.6 - 89.2 $\mu mol.l^{-1}$	Organisms require physiological adaptation to survive.
Hypoxic	22.3 – 44.6 $\mu mol.l^{-1}$	Extreme stress and mortality in organisms (denitrification compete with aerobic respiration)
Anoxic	< 22.3 $\mu mol.l^{-1}$	Respiration dominated by anaerobes and sulphide/methane fluxes

Two mechanisms are thought to drive the distribution of low oxygen water (LOW) in the Benguela marine ecosystem:

- A remote forcing hypothesis based on the premise that wherever LOW events are observed, mostly on the shelf, they are forced by poleward advection of

low oxygen water from the eastern tropical South Atlantic system (Hart and Currie 1960; Bubnov 1972; Morholtz 2001).

- Local generation of low oxygen water through the biogeochemical remineralization of organic matter mostly related to the primary production in the surface water (Visser 1970; Bailey 1979, 1987; Brüchert *et. al.* 2003).

Monteiro *et. al.* (2004) proposed a coupling of these two mechanisms to understand and predict LOW variability in the Central Benguela Ecosystem. A conceptual summary of the main processes governing the distribution of low oxygen waters in the Benguela system in 1985 (Chapman and Shannon 1985) are depicted in Figure 1.1. For the purposes of this work, only the biogeochemistry on the Namibian inner shelf will be considered.

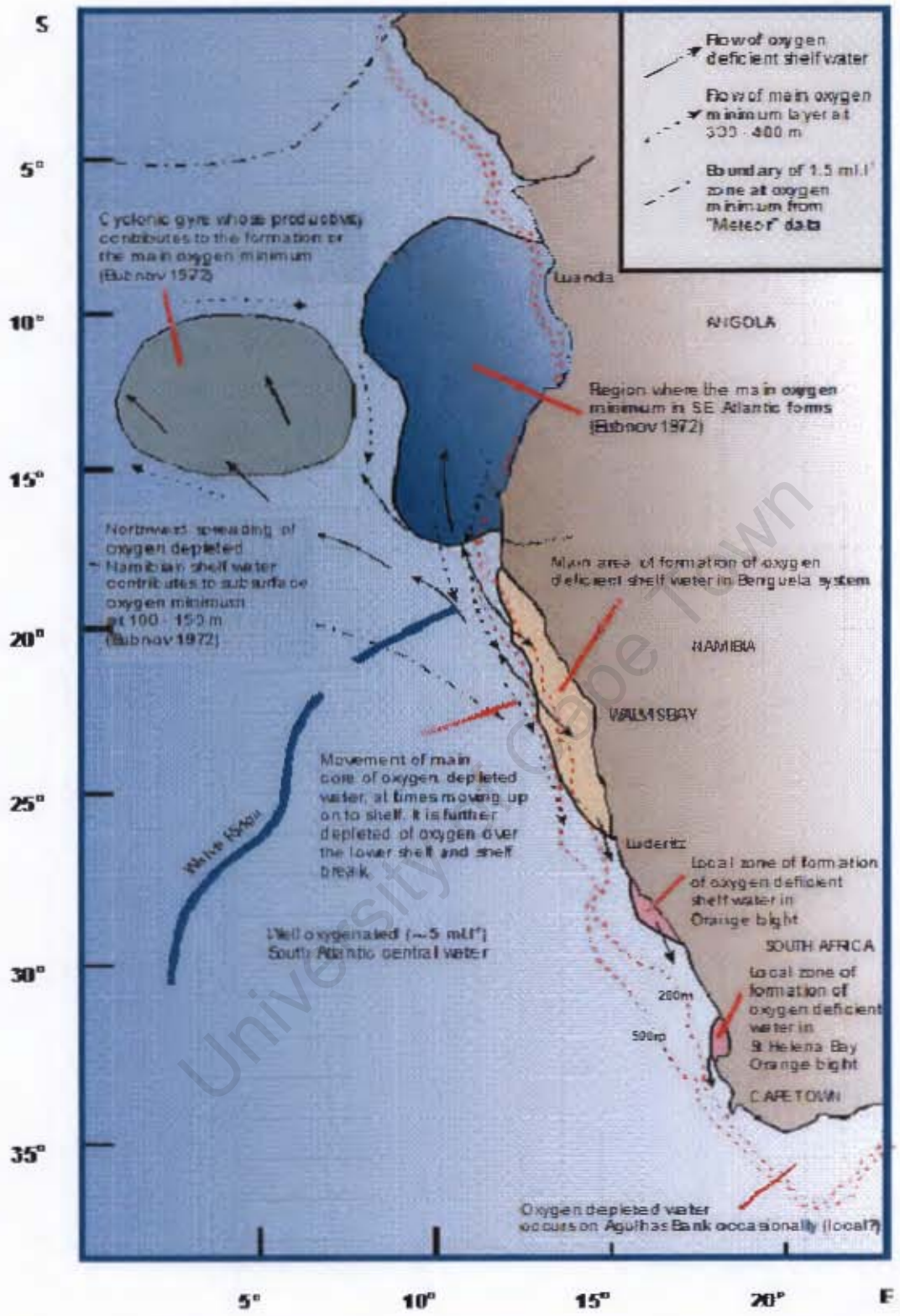

Figure 1.1: A conceptual summary of the main processes governing the distribution of low oxygen waters in the Benguela system in 1985 (Chapman and Shannon 1985).

1.2 Central Benguela shelf sediment characteristics.

The Namibian shelf sediment characteristics are determined by factors such as wind driven coastal upwelling and nutrient enrichment of the euphotic zone, orientation of the coastline and the Coriolis Effect, topography with double shelf break, water body flow patterns, and the deposition of particulate organic carbon (POC) equatorward of upwelling centers. Upwelling of nutrient rich water provides a supply of nutrients such as nitrate and phosphate to the euphotic zone and leads to high primary productivity of organic matter in the overlying water column. It has been hypothesized previously that the depositional flux of particulate organic carbon (POC) over the Namibian inner shelf drives the formation of anoxic conditions (through remineralization) and low oxygen water (LOW) is linked to the seasonal primary production signal (Bailey 1991).

Globally, marine shelf areas (depth < 200m) have two salient biogeochemical characteristics:

- 30% - 100% of particulate carbon export flux reaches the sediments (Middelburg *et. al.* 1993) over shelf areas, focussing most of the remineralization flux within the benthic environment rather than the water column.
- Shelf areas have the greatest turnover of organic matter. Shelf systems occupy 9% of ocean surface area but account for 83% of carbon remineralization (Middelburg *et. al.* 1993).

These two characteristics are also typical of the Namibian shelf when one considers the prevalent LOW overlying the sediments (Bailey 1991) and the high POC (up to 25%) in the sediments (Bremner 1983; Monteiro *et. al.* 2005). Sediments with high

POC concentrations are distributed along three well-defined long shore belts along the Namibian coast depicted in Figure 1.2 (Monteiro *et. al.* 2005). Favourable conditions exist for the observed banding effect of high organic matter; a perennially active upwelling cell and associated high productivity (Bailey 1991), little degradation through the short water column, and the shelf topography (Monteiro *et. al.* 2005).

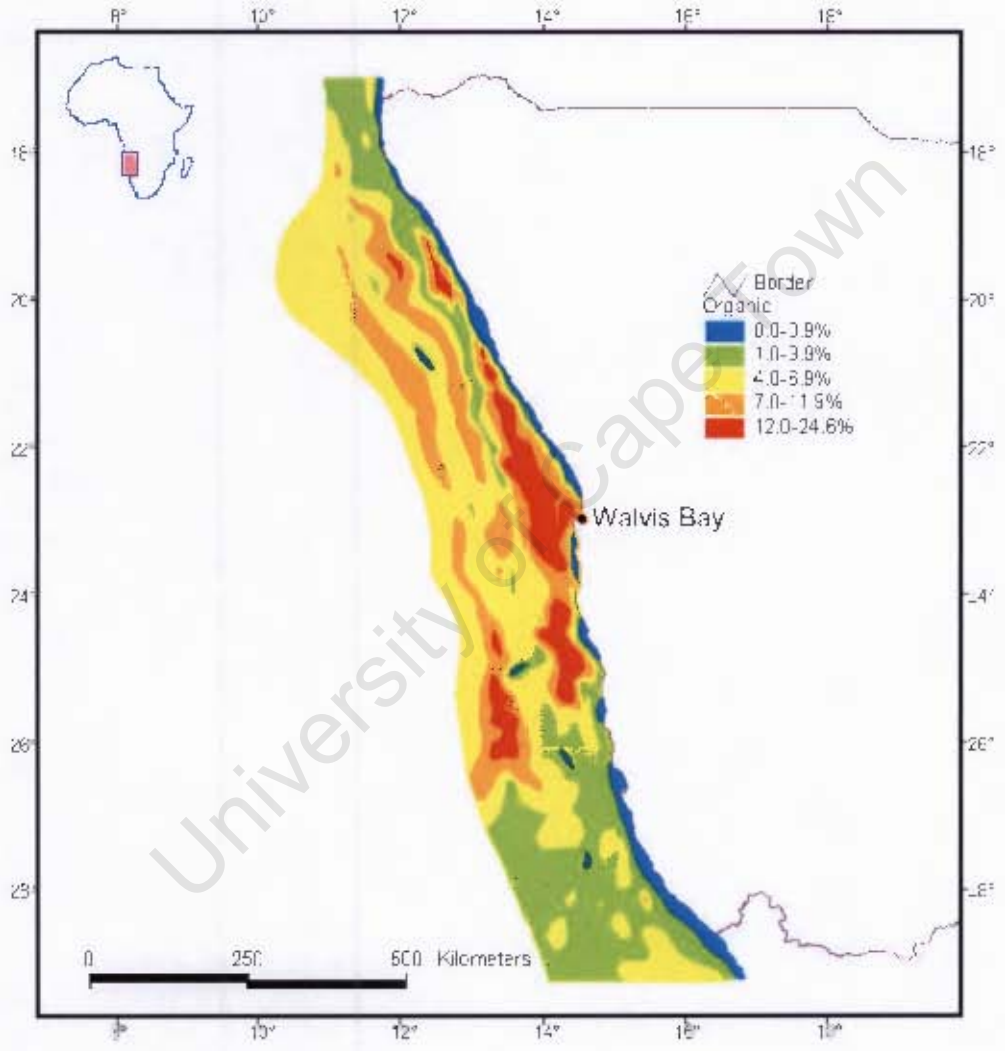

Figure 1.2: Depicts the spatial distribution of large-scale high- and low-POM bands along the Namibian shelf (taken from Monteiro *et. al.* 2005). It shows the highest concentration (POM up to 25%) at the Inshore belt. The mid-shelf belt terminates just south of 23°S where the double shelf break feature also ends. The insert shows the position of Namibia relative to Africa.

Two views exist for the depositional fluxes of particulate matter observed on the Central Benguela continental shelf; the Ekman transport model (Bremner 1983; Giraudeau *et. al.* 2000) and a turbulence-resuspension-deposition model (Monteiro *et. al.* 2005). Bremner, (1983) and Giraudeau *et. al.* (2000) proposed that the three layered water column (surface Ekman/boundary layer, bottom Ekman layer and a return or compensatory flow layer which carry the water to be upwelled) structure dynamics, induced by upwelling to be responsible for the distribution of biogenic material on the shelf. The transfer processes for settling over the upper slope during the upwelling season requires aged biogenic material, advecting off-shore in the surface Ekman layer, and relict material is transported at depth from the outer shelf through the offshore bottom boundary layer down the slope, while fresh biogenic particles produced in the surface waters over the shelf-break and slope are deposited on the shelf (Giraudeau *et. al.* 2000).

The turbulence-resuspension model proposed that the inshore high POC mud belt is sustained by the combined effect of phytoplankton productivity and persistently low average benthic boundary layer current velocities (Monteiro et. al. 2005). It was shown that the deeper long shore high POC belts are outside the upwelling front from where new production is exported and the POC in the mid- and outer shelf belts have higher C:N ratio's (>9) (Monteiro *et. at.* 2005). Re-suspension of biogenic material at the shelf break and deposition of relict detritus in adjacent areas are responsible for the observed POC distribution of the mid- and outer belts rather than from surface phytoplankton export production (Monteiro *et. at.* 2005). The POM banding effect is thus caused by surface productivity in the inshore zone, re-suspension of POC deposited in the shelf break zone and re-deposition in low turbulence areas adjacent to the shelf break zone. Because of the high organic content of the inshore high POC (up to 25% wt) belt and its remineraliztion activity it was chosen as the study area this work.

1.3 Remineralization of organic matter.

The composition of organic matter (OM) is governed by primary production and the remineralization thereof (Libes 1992). Particulate organic matter (POM) is derived mainly from primary producing organisms namely phytoplankton through photosynthesis. During photosynthesis, inorganic compounds such as carbon dioxide and nitrate are transformed by light energy to form organic cell material and oxygen. The idealized stoichiometry of constituents for marine derived particulate organic matter is:

$$(CH_2O)_{106}(NH_3)_{16}PO_4$$

This generic form of carbon serves as an electron donor available for heterotrophic microrganism to utilize as an energy source. The elemental ratio of carbon to nitrogen to phosphorus that is present in average phytoplankton is usually 106:16:1 and is referred to as the ***Redfield ratio***, (Redfield et al. 1963). The Redfield ratio specifies the stoichiometry of biogenic organic matter and is an important indicator of the trends in organic matter transformations in the marine environment. Formation and decomposition of organic matter influences the distribution of nutrients such as nitrate, ammonia and phosphate in the water column (Libes, 1992). During the process of photosynthesis, nutrients from the water column are assimilated into cell material while remineralization releases nutrients in their respective soluble forms.

Heterotrophic microrganisms extract energy from organic matter for physiological functioning, via the remineralization of organic matter (Froelich *et. al.* 1979; Libes 1992). Within the sediment environment, remineralization of organic matter proceeds via a series of chemical reactions, resulting in fluxes of dissolved species across the sediment-water interface. A continuum of redox states exists ranging from oxic to

anoxic. Remineralization over the range of redox conditions contributes to sediment oxygen demand. Under aerobic conditions, aerobic organisms utilize oxygen as electron acceptor while under anaerobic conditions other oxidants such as nitrate, iron- and manganese oxides and sulphate are utilized (Berner 1980). Aerobic respiration continues until sufficient oxygen has been consumed to drive the redox potential low enough to favour the next most efficient oxidant. Reactions with different oxidants yield different metabolic energy and the reaction with most favourable energy yields occurs preferentially. Relative oxidation energies of other oxidants in seawater are presented in Figure 1.3 (taken from Stumm and Morgan 1981) and their reaction stoichiometry in Table 1.2 and 1.3. These particulate organic matter breakdown reactions generally occur in the sequence indicated in Table 1.2, however, in nature, overlap in reactions are possible.

Organic matter such as phytoplankton or zooplankton varies in its elemental composition. The selective degradation of various groups of organic substances (such as phytoplankton or zooplankton) causes changes in the composition of organic matter and affects remineralization rates (Wang and Van Cappellen 1996, Anrosti and Homer 2003). Different groups of organic matter are oxidised in direct proportion to their reactivity and concentration (Berner 1980). Labile organic matter fractions are oxidised preferentially over less readily oxidizable organic matter leading to the sequential utilization of substrates (Middelburg *et. al.* 1993). A set of carbohydrates could be decomposed faster aerobically than say anaerobically through sulphate reduction. The total degradation rate of decomposable organic matter in the sediments is equal to the sum of the degradation rates of the individual groups ("one-*G*" model; Berner 1980). Experiments in which similar organic matter is mineralised under oxic and anoxic conditions indicated that aerobic and anaerobic remineralisation rates were not significantly different (Lee 1992).

Within the sediments on the Namibian shelf, it is expected that anaerobic remineralization dominate sediment OM breakdown processes as permanent anoxic conditions are observed (Chapman and Shannon 1985; Brüchert *et. al.* 2003). Sulphate reduction in particular is considered the major remineralization process (Fossing *et. al.* 1999; Ferdelman *et. al.* 1999; Brüchert *et. al.* 2003). The effect of the flux of reduced compounds on low oxygen variability is yet to be fully understood, particularly how the seasonal signal is related to the fluxes of reduced compounds.

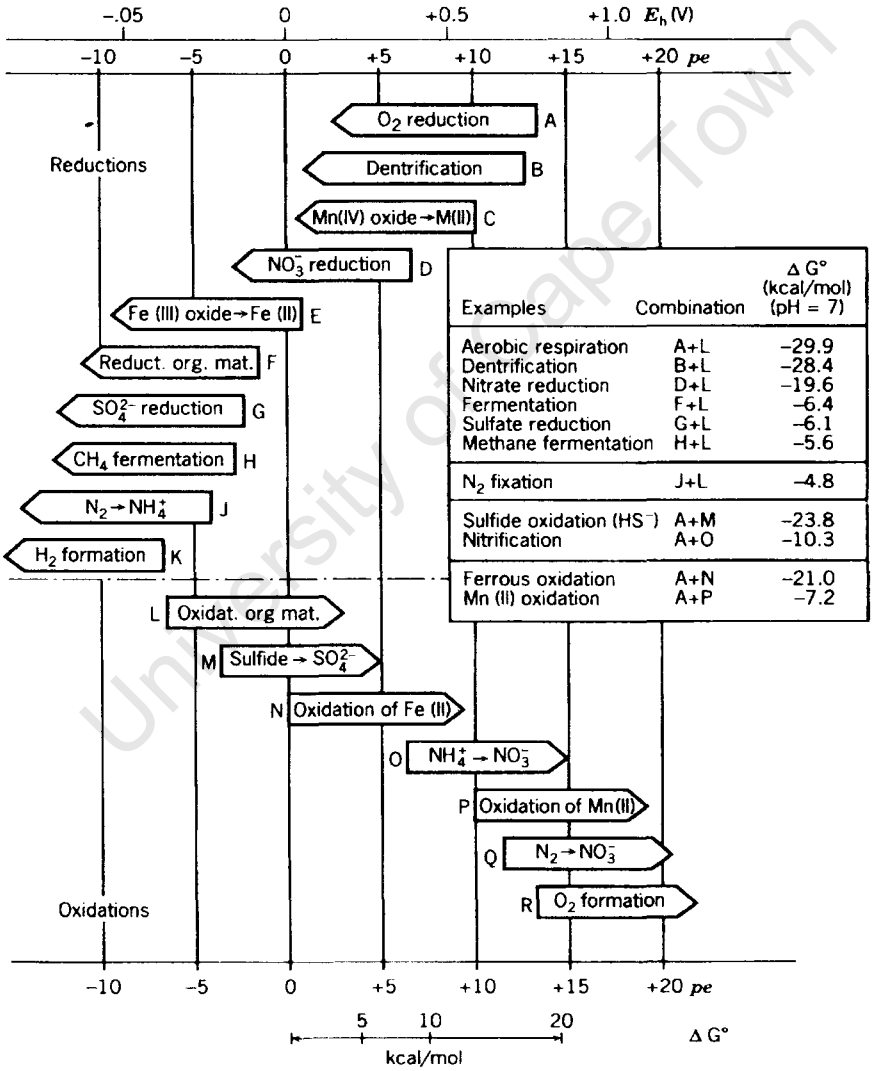

Figure. 1.3. Sequence of microbially mediated redox reactions. Arrows point in the direction of the spontaneous redox reaction and no information is contained in the relative length of the arrow. (Taken from *Aquatic Chemistry*, Stumm and Morgan (1981) by John Wiley and Sons, Inc., New York)

Table 1.2 : Stoichiometric relationship between oxidant and organic matter (Taken from Froeliech *et. al.*1979)

Oxidant	Reaction	ΔG^0 (*kcal.mol^{-1} of glucose*)	
O_2	$(CH_2O)_{106}(NH_3)_{16}(H_3PO_4) + 106\ O_2 \rightarrow 106\ CO_2 + 16\ HNO_3 + H_3PO_4 + 106\ H_2O$	- 762.4	(1)
NO_3	$(CH_2O)_{106}(NH_3)_{16}(H_3PO_4) + 84.8\ HNO_3 \rightarrow 106\ CO_2 + 16\ NH_3 + H_3PO_4 + 148.4\ H_2O + 42.4\ N_2$	- 657.3	(2)
MnO_2	$(CH_2O)_{106}(NH_3)_{16}(H_3PO_4) + 236\ MnO_2 + 474H^+ \rightarrow 106\ CO_2 + 8\ N_2 + H_3PO_4 + 366\ H_2O + 236\ Mn^{2+}$	- 697.9	(3)
FeOOH	$(CH_2O)_{106}(NH_3)_{16}(H_3PO_4) + 424\ FeOOH + 848\ H^+ \rightarrow 106\ CO_2 + 16\ NH_3 + H_3PO_4 + 742H_2O + 424\ Fe^{2+}$	- 317.9	(4)
SO_4	$(CH_2O)_{106}(NH_3)_{16}(H_3PO_4) + 53\ SO_4 + 53\ H^+ \rightarrow 106\ CO_2 + 16\ NH_3 + H_3PO_4 + 106\ H_2O + 53\ HS^-$	- 90.8	(5)
CO_2	$(CH_2O)_{106}(NH_3)_{16}(H_3PO_4) \rightarrow 53\ CO_2 + 53\ CH_4 + 16\ NH_3 + H_3PO_4$	- 83.7	(6)

Reactions are not proton balanced

Table 1.3: Oxidation reactions of reduced inorganic compounds[a] (Libes 1992)

Description	Reaction			ΔG^0 (*kcal.mol^{-1}*)	
Sulphide oxidation	$H_2S + 2O_2$	$\rightarrow$	$SO_4^{2-} + 2H^+$	- 23.5	(7)
Iron oxidation	$4Fe^{2+} + O_2 + 20H_2O$	$\rightarrow$	$4Fe(OH)_3(s) + 8H^+$	- 21.0	(8)
Nitrification	$2NH_4^+ + 3O_2$	$\rightarrow$	$2NO_2^- + 2H_2O + 4H^+$	- 10.8	(9)
	$2NO_2^- + O_2$	$\rightarrow$	$2NO_3^-$	- 9.0	(10)
Manganese oxidation	$2\ Mn^{2+} + O_2 + H_2O$	$\rightarrow$	$2\ MnO_2(s) + 4\ H^+$	- 7.2	(11)

[a] Accomplished by chemoautotrophs, mostly autotrophs.

Reactions are not proton balanced.

1.4 Redox zonation within the sediment (oxic, suboxic and anoxic).

Redox conditions within the sediments are controlled by the relative supply of organic matter and electron acceptors (Berner 1980). Oxygen is supplied through diffusion from the water overlying the sediment. In sediments where benthic remineralization is fast, suboxic and anoxic conditions occur within the sediment, and the redox interface could lie within the upper few millimetres at the sediment water interface but it also extends into the bottom waters due to high POM fluxes. A simple three layer conceptual model can be used to view the sediment whereby the top layer of the sediment is aerobic, a middle suboxic layer and the bottom layer is the anaerobic layer. An idealized illustration is presented in Figure 1.4 (adapted from Froelich *et.al.*1979). The depth of the aerobic layer is determined by the diffusive flux of oxygen into the sediment, which is dependent on the concentration gradient of oxygen between the water and sediment as well as the porosity of the sediment (Berner 1980). Reactions 1, and 7 - 10 (Table 1.2 and 1.3) occur in the oxic (aerobic) zone, reactions 2 - 4 and 11 occur in the suboxic zone while reactions 5 – 6 occur in the anoxic (anaerobic) zone.

As the oxygen concentration in the sediments decreases, the concentration of nitrate increases to a maximum, then decreases to zero. The nitrate maximum result from the oxygen flux and ammonium flux from opposite directions. In this zone nitrification of ammonium with oxygen proceed via Eq. 9 (Table 1.3) (Berner 1980). In the absence of oxygen, anaerobic ammonium oxidation (Anammox) with nitrate/nitrite is also possible in this zone (Devol 2003; Kuypers *et. al.* 2003). Below the nitrate maximum, nitrate diffuses downward to be reduced to N_2 through denitrification. If denitrification occurs via reaction 2 (Table1.2), some overlap in metabolic free energy yield of reactions 2 and 3 occur, depending on the Mn-phase being reduced, and it is expected that nitrate and manganese dioxide reduction might occur simultaneously

(Froelich 1979). After consumption of nitrate and manganese dioxide, reduction of iron proceeds, followed by sulphate reduction. Sulphate reduction does not proceed until oxygen is completely depleted because the energy yield form sulphate reduction is so low that sulphate cannot effectively compete for organic matter in the presence of oxygen (Berner 1980). Oxygen also appears to "poison" sulphate-reducing enzymes (Libes 1992). The zone of sulphate reduction is much thicker than for other oxidants due to the abundance of sulphate in seawater and takes much longer to be completely consumed (Berner 1980). Eventually at sediment depths where all oxidants are consumed, organic matter is oxidized through a disproportionation reaction in which some of the carbon is oxidized to carbon dioxide and some reduced to methane. This is termed the methane fermentation or methanogenesis (Libes 1992).

The thermodynamic stratification model presented (Froelich 1979) is an idealised sequence of the remineralization reactions and is often not the case in the natural environment. As most of these reactions are microbially mediated and involves enzymes, microbial ecology could be adapted in such a way that lower energy yielding reactions could occur preferentially due to better adaptation. Sulphate reduction on the Namibian shelf was suggested to be more common than denitrification due to the relative abundance of sulphate as an electron acceptor (Tyrell and Lucas 2002).

Anoxic sediments usually have well defined concentration gradients which provide valuable information regarding the diffusional fluxes of solutes that can be extracted from the shape of the pore-water profiles. The solute concentration is controlled by diffusion from the source depending on the direction of the gradient. A gradient that is convex (eg. the oxygen profile Figure 1.4) will result from the chemical removal or downward advection of the solute in the pore-water (Libes 1992). A gradient that is

concave (eg. HS^-, Mn^{2+} and Fe^{2+}) will result from chemical production or upward advection of the solute in the pore-water. A pore-water profile with a maximum such as MnO_2 indicates production at the maximum, and *vice versa*.

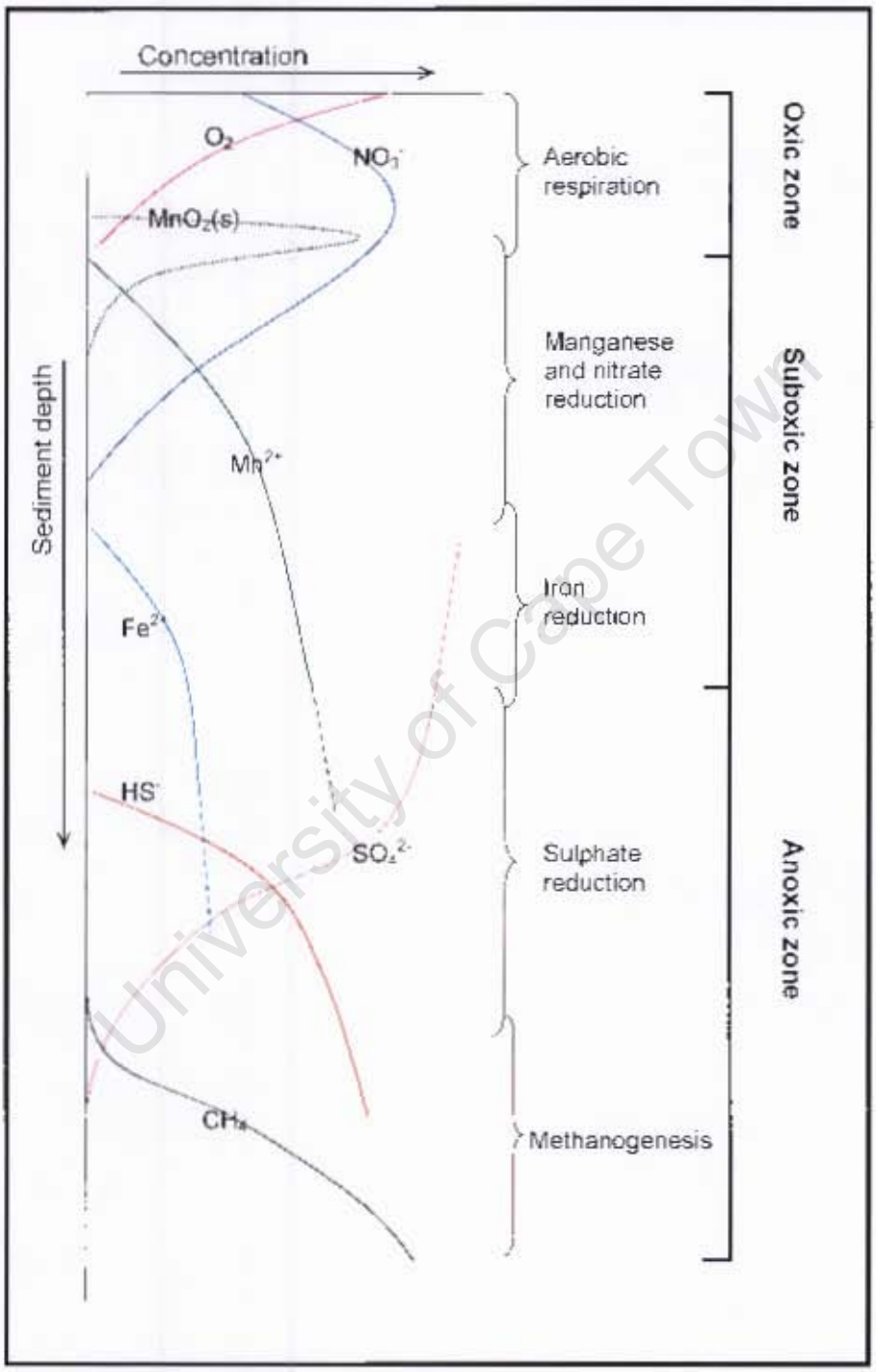

Figure 1.4: Idealized representation of depth profiles of O_2, NO_3^-, $MnO_2(s)$, Mn^{2+}, Fe^{2+}, SO_4^{2-}, HS^- and CH_4 in marine sediments (Adapted from Froelich *et. al.* 1979 and Libes 1992). Reactions generally occur in the sequence down the depth of the sediment.

1.5 Oxidation of reduced inorganic metabolites.

As the reduced species diffuse upward through pore-water along the concentration gradient they are reoxidised in the oxic zone. Chemical equations 7 – 11 (Tables 1.3) are possible reactions for the oxidation of reduced compounds formed through the oxidation of organic matter. For instance, ammonium is readily oxidised in oxic water to nitrite and then to nitrate by marine bacteria *Nitrosomas* and *Nitrobacter* respectively through nitrification (Stumm and Morgan 1981; Libes 1992). The re-oxidation of reduced compounds such as Fe^{2+}, Mn^{2+}, $HS^{-}(H_2S)$, NH_4^{+} and CH_4, which are products of anaerobic remineralization in deeper parts of the sediments, can make a significant contribution to the low oxygen conditions in the water overlying the sediments (Ferdelman *et. al.* 1999; Ogrinc *et.al.* 2003; Monteiro *et. al.* 2004; Brüchert *et. al.* in press). It was estimated that up to 55% of sulphide oxidation was mediated by large nitrate-storing sulphur bacteria *Thiomargarita namibiensis* in sulphidic bottom water over the shelf (Brüchert *et. al.* 2003) and sulphide oxidation to sulphate can account for up to 2/3 of oxygen consumption (Ogrinc *et. al.* 2003). However, it is difficult to estimate the total contribution of these reactions to the sediment oxygen demand as the reduced species may participate in secondary redox reactions, be absorbed on sediment particles, or precipitate as authigenic hydroxides, carbonate or sulphide minerals through precipitation and dissolution reactions (Wang and Van Cappellen 1996).

1.6 Flux across the sediment-water interface.

The boundary between water column and sediment plays an important role in determining the chemical composition of the overlying water column. It provides an environment whereby chemical species can interchange between the water column

and the sediment. If diagenetic chemical reactions (i.e. OM remineralization) occur close enough to the sediment water interface, fluxes of dissolved species between sediment and overlying water occur along concentration gradients between the sediment-water interface. Two types of flux occur between the sediment and water column, namely diffusive and advection. Diffusion is the net motion of dissolved species from a region of higher concentration to lower concentration in the absence of an external force while advection refers to the bulk unidirectional flow of porewater relative to an adopted reference frame at the sediment-water interface due to an impressed force such as pressure (Berner 1980). The generalised expression depicting the two flux components is:

$$J_i = -D\frac{\partial C_i}{\partial z} + \omega C_i \qquad (12)$$

where J_i is the total (diffusive and advective) flux of component i (mmol.m^{-2}.day^{-1});

D_i is the molecular diffusion coefficient of i (m^2.day^{-1});

C_i is the solute concentration and (mmol.L^{-1});

z is the direction of maximum concentration gradient (m).

ω is the velocity of flow relative to the sediment-water interface

In the sediment environment, the advective component arises from the loss of water due to the compression as a result of deposition of sediment. The effect of compaction on flux in fine-grained muds is very slow, and the advection term in equation 12, thereby, is usually omitted (Berner 1980). The diffusion term can be divided into four categories: molecular diffusion, dispersion, eddy diffusion and bioturbation. Dispersion due to flow is negligible, and one can assume that once depths below zones of bioturbation and current stirring are reached, oxidants and remineralization flux of solutes are mainly controlled through the process of

molecular diffusion (Berner 1980). Fluxes of solutes across the sediment water interface can therefore be calculated from the concentration gradient according to Fick's first law of diffusion (Stumm and Morgan 1981; Berner 1980):

$$J_i = -D_i \frac{\partial C_i}{\partial z}, \qquad (13)$$

Before applying Fick's law of diffusion directly to sediments, several modifications must be made. For instance, for charge effects, because major species that undergo diffusion in the porewaters are ions. An ion migrates in response to its own concentration gradient, as well as the electrical potential gradient brought about by concentration gradients of other ions (Berner 1980). Ion flux cannot result in a pile up of charge, so the electroneutrality relation has to be considered. The molecular diffusion coefficient therefore is made up of two components, one depending on mobility and temperature, and the other on electrical effects due to other ions. Additionally, inter-ion effects brought about by ion pairing influences diffusion. When a diffusing ion is considered, generally the sum of all the major species containing the ion is included. For the sulphate ion in seawater this would include sulphate as well as the ion pairs $MgSO_4$, $CaSO_4$, $NaSO_4^-$ and KSO_4^-.

Appreciable changes in diffusion coefficients of ions can be brought about by electrical effects, but an even greater effect arises in the sediment due to tortuosity, resulting from the presence of solid particles. In the sediment, an ion is not free to diffuse in any direction, but it is hindered by collision with the particles as it follows a tortuous path (Berner 1980; Boudreau 1996). Tortuosity is defined as:

$$\theta = \frac{dl}{dz}, \qquad (14)$$

where θ = tortuosity;

dl = length of the actual sinuous path over depth interval dz.

The relation used to calculate tortuosity from measurements of electrical resistivity and on natural sediments and porewaters separately (Berner 1980), is given by:

$$\theta^2 = \phi F, \qquad (15)$$

where F = formation factor = R/R_O;

R = electrical resistivity of the sediment;

R_O = electrical resistivity of the pore water alone.

A simple relation between R/R_O and porosity for a wide variety of sediment is $F \cdot \phi^{-n}$. When n = 2, this equation is known as Archie's law (Li and Gregory 1974).

The diffusion coefficient for sediment is corrected for tortuosity as follows:

$$D_s = \frac{D}{\theta^2}, \qquad (16)$$

where D_s = whole sediment diffusion coefficient in terms of area of sediment per unit time.

When applying values of D_s to the sediments, an additional factor, sediment porosity (ϕ) must be included. Fick's First Law for sediments is thus:

$$J_s = -\phi D_s \frac{\partial C_s}{\partial z}, \qquad (17)$$

Where J_s = diffusion flux in sediments in terms of mass per unit area of sediment per unit time.

Temperature also affects molecular diffusion (Berner 1980). Higher temperature causes greater molecular motion and therefore higher diffusion coefficients.

Corrections for temperature should be made. The temperature dependency of viscosity and self-diffusion of water in the temperature range of 0 – 100°C is adequately described by the Stokes-Einstein relation, (Li and Gregory 1974) namely:

$$\left(\frac{D^0\eta^0}{T}\right)_{T_1} = \left(\frac{D^0\eta^0}{T}\right)_{T_2} \qquad (18)$$

where η^0 = the viscosity of water.

T = the absolute temperature.

Bioturbation is the process of sediment mixing through the activity of benthic organism, such as macrofauna crawling through the sediments or polychaete worms burrowing into the sediments (Libes 1992) and is commonly described as a diffusive process (Boudreau 1996). A "box model" approach is adopted to describe such fast mixing process. Over a certain depth, all sediment properties are uniform from the sediment-water interface to this fixed depth (Berner 1980). Changes in properties of sediment added at the sediment water interface are immediately sensed at the bottom of the "box" (Figure 1.5). Mathematically this box model is represented by equation (19):

$$\frac{dC}{dt} = \frac{J(t) - \omega C_S}{L} \qquad (19)$$

where C_S is the concentration in the zone of bioturbation (box) of solid substance under study (solids + porewater);

$J(t)$ is the depositional flux to the sediment;

ω is the rate of depositional burial of total sediment;

L is the thickness (depth) of the box.

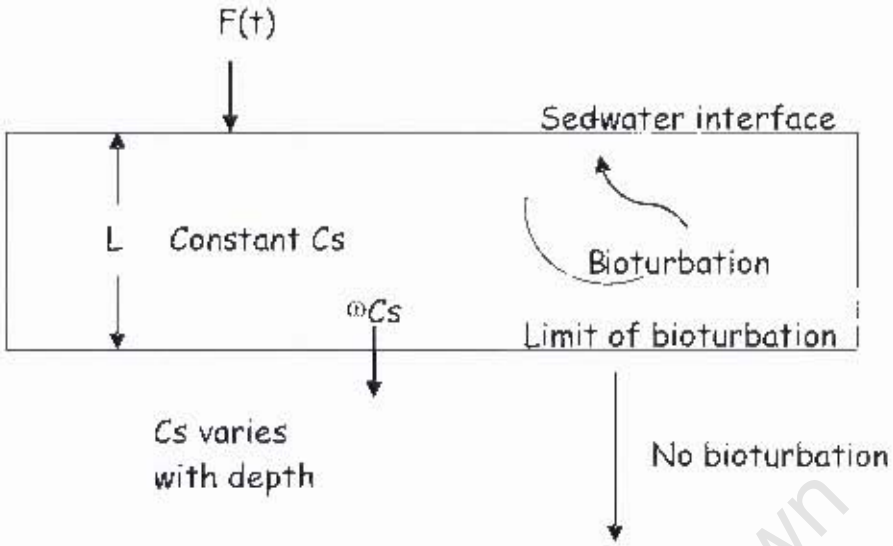

Figure 1.5: Schematic representation of box model normally used to depict bioturbation. Within the box there is perfect mixing and uniformity of concentration (Adapted from Berner 1980).

The effect of bioturbation on total oxygen uptake rates measured *in situ* and calculated diffusive uptake rates in South East Atlantic sediment (*Z* ranging between 400 and 4000m) indicated that *in situ* oxygen uptake rates were always higher than diffusive uptake rates (Glud *et. al.* 1994). A strong correlation between total oxygen uptake rates and dry weight macrofauna in the sediment was observed in that study, and when macrofauna were absent total and diffusive oxygen uptake rates were in good agreement. The authors concluded that the abundance of benthic foraminifera increased the total oxygen uptake rate by a factor of up to 3 and even at Z = 3095m, the presence of macrofauna (dominated by polychaeta) doubled the rate of sediment oxygen demand (Glud *et.al.* 1994).

1.7 Summary of processes affecting sediment oxygen demand.

The processes affecting sediment oxygen demand and essentially the distribution of water column constituents described in the previous sections are conceptually summarised as follows (see Figure 1.6):

- Organic matter depositional flux,
- Remineralization of organic matter (aerobic and anaerobic),
- Fluxes of constituents between the sediment and the water column,
- Physical environmental conditions.

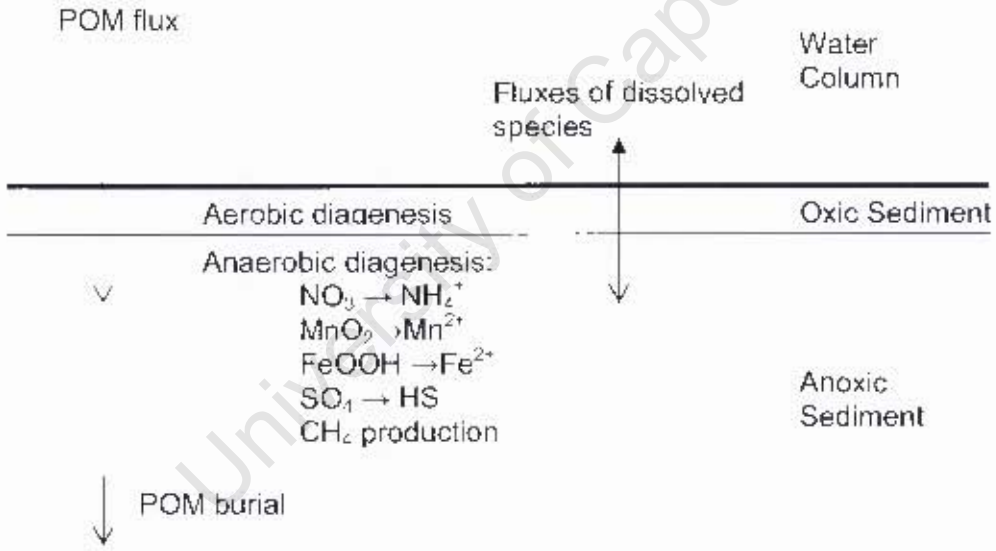

Figure 1.6: Conceptual model of processes affecting SOD.

1.8 The aim of this project.

The variability in water column oxygen concentration over the Namibian inner shelf is thought to be influenced by biogeochemical remineralisation of organic rich sediments. High primary productivity rates and particulate organic matter fluxes, high organic content (up to 25% wt) of the sediments, high remineralisation rates and accompanied fluxes of reduced compounds all contribute to the observed hypoxia variability. This project focussed on understanding the dynamics of hypoxia linked to biogeochemical fluxes, specifically on seasonal characteristics in sediment oxygen demand over the Namibian inner shelf. Secondly, the relation of sediment oxygen demand to water column particulate fluxes and fluxes of products of primary biodegradation processes near the sediment water interface. Two key questions are articulated as follows:

- What are the characteristics of seasonal variability of sediment oxygen demand on the Namibian inner shelf mud belt?

- How is seasonal variability in sediment oxygen demand related to the vertical sediment biogeochemical fluxes?

1.9 Approach.

A quasi-monthly observational programme was adopted to address the research questions posed above, to determine seasonal variability in sediment oxygen demand, through a series of incubated sediment cores collected on the Namibian inner shelf. This was achieved through:

- Undertaking a yearlong quasi-monthly collection of sediment cores on the Namibian inner shelf at 23°S, 14°E,
- Determining the total oxygen demand from core incubations,
- Measuring particulate fluxes through moored sediment traps,
- Measuring interstitial water concentrations of nutrients (nitrate, ammonium, sulphate, hydrogen sulphide, phosphate and silicate) with sediment depth and calculating sediment diffusional fluxes,
- Quantifying the observed sediment oxygen demand fluxes with diffusional fluxes of reduced constituents through their stoichiometric relationships.

Chapter 2

Materials and sampling methods

2.1 Introduction.

One site on the Namibian inner shelf (23°S, 14°E ~130m water depth) was chosen for the investigation within one of the main areas of oxygen deficient water in the Benguela system (Figure 2.1). Sampling coincided with the monthly oceanographic monitoring programme on the research vessel *RV Welwitschia* conducted by National Marine Information and Research, (NatMIRC) Ministry of Fisheries and Marine Resources, Namibia and extended from November 2002 to November 2003.

2.2 Site description.

2.2.1 Geographic setting and main characteristics

The Namibian coastline runs in a general SSE – NNW direction (Figure 2.1). The continental shelf is 100 – 160km wide, with a double shelf break between 21°00'S and 23°30'S in central Namibia. The inner shelf has a gently sloping surface from the coast to roughly 13°5'E with the first shelf break at Z: ~160m and a steeply sloping outer shelf break at 13°0'E (Z: ~ 350m), separating the continental margin to an inner (Z: 50 – 140m), mid-shelf (Z: 200 - 300m) and outer shelf (Z: 500 – 1400m) regions (Bremner 1983; Shannon and Nelson 1996). The inner shelf break feature ends just south of 23°S.

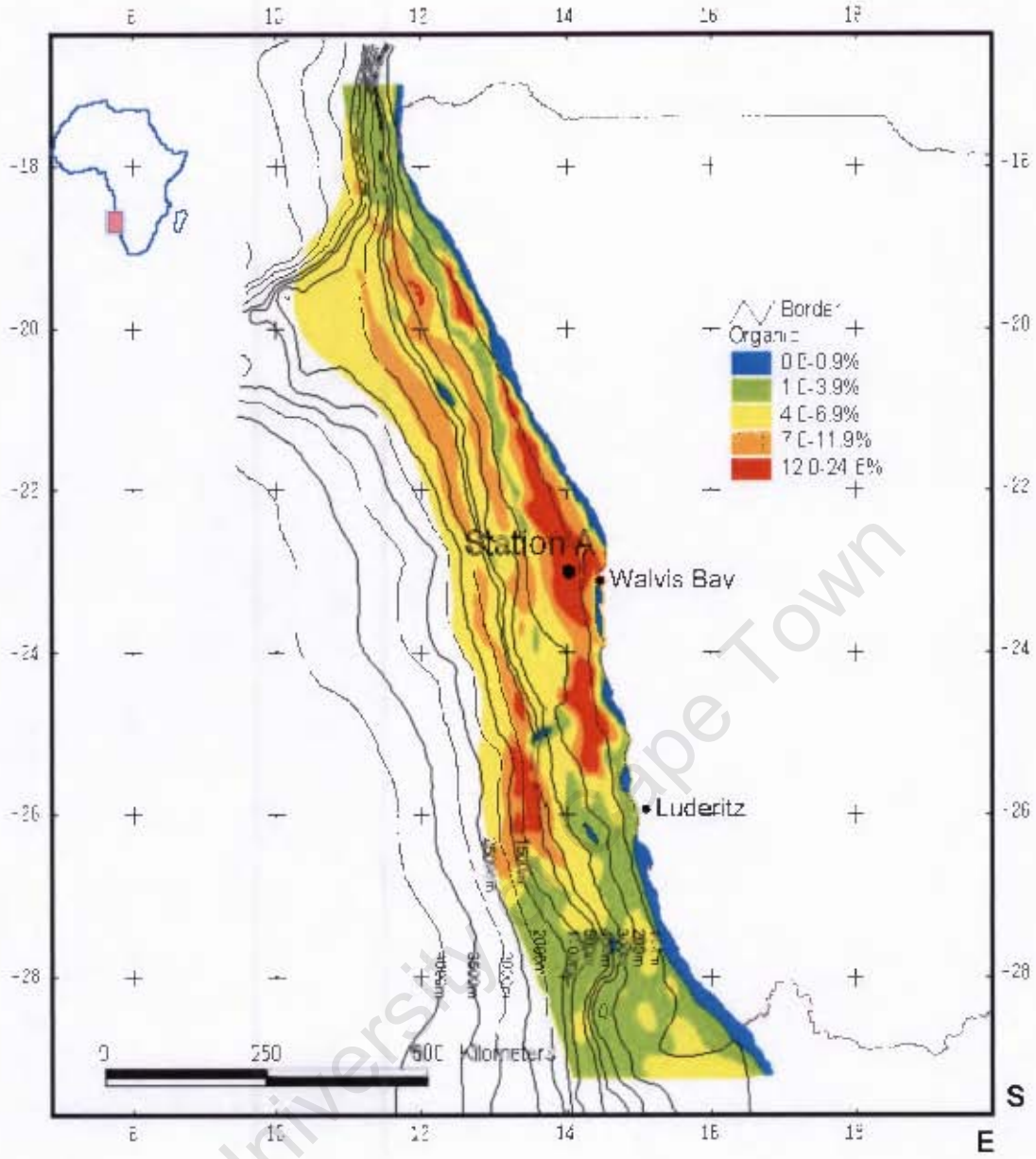

Figure 2.1 Depicts the sample location at Station A as well as the spatial distribution of the large-scale high- and low POM bands along the Namibian shelf (In Monteiro, et. al. 2005, adapted from Bremner 1983). It shows two parallel POM rich belts the highest concentration (POM up to 25%) at the inshore belt.

The shelf area is rich in diatomaceous detritus (three bands indicated in Figure 2.1) and exceptionally rich in organic matter (up to 20% organic carbon) mainly of planktonic origin (Bremner 1983; Chapman and Shannon 1985; Bailey 1991, Van der Plas and Monteiro, *in press*). Copenhagen (1953) described this as the azoic zone;

"extremely fluid, olive green muds containing hydrogen sulphide and lacking benthos". The shelf break indicates the boundary for sulphidic bottom water (Brüchert *et. al.* 2003). Three parallel bands (measuring between 500 - 800km in length) of alternating high and low POM appear between 19°S and 26°S, with the highest concentration inshore near Walvis Bay (Figure. 2.1) (Bremner 1983; Monteiro *et. al.*, 2005). Water below the thermocline over the inner shelf off Walvis Bay water contains dissolved oxygen concentrations of less than 20 μM (or $<0.5 ml.L^{-1}$) throughout the year and are often completely anoxic (Chapman and Shannon 1985; Bailey 1991).

The continental margin is overlain by the Benguela Current, which is a sluggish northward to north-westward flowing body of water with average surface velocities of 10 – $20 cm.s^{-1}$. The main current flows westward away from the coast at WalvisBay (23°S) then split into three narrow ancillary branches parallel to the coast named the Benguela Coastal Current (BCC) (Shannon and Nelson 1996). In the northern part of Namibian continental margin, the southward flowing warmer-water Angola current (AC) converges with the eastern branch of the Benguela current (BCC) to form the Angola-Benguela Front (ABF) located between 14°S and 17°S which is also the northern boundary of the coastal upwelling system. The location of the ABF shifts between these latitudes on a seasonal basis. Southward movement of the front is usually associated with austral summer conditions when longshore wind stress and upwelling in the Northern Benguela are reduced (Shannon and Nelson 1996). The southward flowing Angola current continues poleward below the thermocline over the central Benguela shelf (Shannon and Nelson 1996).

Three perennial upwelling cells are located on the Namibian coast. These are located around Cape Frio in the north, WalvisBay (23 °S) in the middle and Lüderitz (26°S – 27°S) which is also the largest. The Lüderitz upwelling cell effectively divides the

Benguela system into the southern and northern Benguela sub-systems. Periods of peak upwelling in these two sub-systems are out of phase, with maximum upwelling occurring during late winter/early spring in the northern Benguela and in the summer in the southern Benguela (Bailey 1991).

2.3 Sediment sample collection.

The sampling position, Station A (23°S, 14°E; Z ~130m water depth) depicted in Figure 2.1 is well within the upwelled waters generated by the Walvis Bay cell. Sampling dates, water depth and water properties in the benthic boundary layer during the sampling exercise are summarised in Table 2.1.

Table 2.1: Summary of sampling schedule, positions, water depth and water column properties in the bottom boundary layer (BBL; <5m overlying the sediment) determined with Seabird 911*plus* CTD-O (courtesy NATMIRC).

Date	Position	Depth (m)	Temp (°C)	Salinity (ppt)	DO ($\mu mol.l^{-1}$)
01/10/2002	22°58.96'S, 14°02.65'E	125	11.3	35.01	14.4
29/10/2002	22°59.96'S, 14°02.65'E	129	11.2	34.98	2.6
05/12/2002	23°00.00'S, 14°04.40'E	123	11.6	35.05	12.7
01/02/2003	22°59.80'S, 14°02.50'E	127	12.4	35.13	2.0
04/03/2003	22°59.80'S, 14°02.50'E	129	12.8	35.18	6.6
13/05/2003	22°59.80'S, 14°02.42'E	124	12.3	35.14	5.8
02/07/2003	23°00.00'S, 14°02.43'E	126	11.9	35.10	5.0
04/09/2003	22°59.80'S, 14°02.42'E	125	11.6	35.05	21.6
01/10/2003	22°59.80'S, 14°02.42'E	122	11.5	35.02	4.5

Sediment samples were collected for core incubations for determination of total sediment oxygen uptake rates, diffusional fluxes of nitrate, ammonium, sulphate, hydrogen sulphide, phosphate and silicate at the sediment-water interface. Sediment

traps were anchored at 60m and 80m from the sea surface for determining particulate organic matter export flux. Diffusional fluxes were determined from porewater profiles as well as incubated sediment cores.

Sediment coring was conducted with an Ocean Instrument (MC-200) multicorer device (Figure. 2.2). This method has been used extensively by various authors (Bailey *et. al.* 1987, Glud *et. al.* 1994, Fossing *et. al.* 2000, Brüchert *et. al.* 2003). Polycarbonate core tubes (30 cm length, 7cm i.d) were inserted into the multicorer device (Figure 2.2). The multicorer was lowered to the bottom and allowed to settle on the sediment surface. A gravity mechanism then extruded the open core tubes into the sediment which also triggered a closing of the core tubes (foot and top). Sediment samples were then retrieved with roughly 20 cm sediment and 10 cm overlying water. Immediately after the sediment cores were recovered, they were closed with rubber stoppers and stored in a portable temperature regulated refrigerator at *in situ* temperature (10 – 12°C). The cores were allowed to settle over 24hrs and transported to a land based laboratory for further processing. The sediment cores with overlying water intact were used mainly for oxygen incubations. Core tubes with the least overlying water, were used to determine the interstitial water profiles. It was noted that the September 2003 interstitial water core were completely filled with sediment. Here it was assumed that the top of the core was the sediment-water interface. Completely filled sediment cores were also used for nitrate, ammonium, sulphate, hydrogen sulphide, phosphate and silicate incubations. To prepare the cores for incubations, some sediment was released from the bottom of the core tube and carefully filled with replacement water. The replacement water was collected in Niskin bottles from the bottom boundary layer water overlying, < 5m above the sediment, transferred to 2.5L plastic screwtop bottles and siphoned into the cores using Tygon tubing.

Figure 2.2: Multicorer device deployed over the side of the *RV Welwitschia* during a sampling cruise.

2.4 Sediment oxygen demand measurements.

Sediment oxygen demand has been widely used to measure the total rate of benthic remineralization. It is done by enclosing an area of sediment and measuring the change in oxygen concentration in the overlying water (Bailey, 1991; Glud, 1994). This gives an indication of the total sediment oxygen demand. There are generally 3 methods of determining sediment oxygen demand:

- Laboratory incubations of recovered intact sediment cores,
- *In situ* measurements with benthic flux chambers placed over the sediment and
- Estimation by diffusive oxygen fluxes calculated from vertical profiles of dissolved oxygen on sub-thermocline waters.

Diffusive oxygen flux calculations are generally lower than laboratory and *in situ* incubations because it excludes the impact of bioturbation on the oxygen uptake rate (Glud *et. al.* 1994). Little or no bioturbation are expected for the inner shelf mud belt as the anoxic conditions makes it devoid of benthic infauna. SOD measured *in situ* have the advantage of measuring oxygen and nutrient fluxes simultaneously from the same core. In the present study, laboratory incubations were used to determine the total sediment oxygen demand (TSOD). No such data is currently available for the study area.

The change in oxygen concentration over time was measured in the water volume overlying the sediment. An air-tight bung was manufactured with three holes; one for a microelectrode oxygen sensor (YSI model 56), one for a mechanical stirrer and a small bleed hole.

In situ waters overlying the sediments generally contained dissolved oxygen concentrations less than 22 µM and in order to measure an oxygen consumption rate in the overlying water, dissolved oxygen is required in this water. To overcome this, the oxygen deficient water overlying was partially aerated by leaving the cores open to the atmosphere for 10 - 15 minutes prior to incubations. This would elevate the oxygen concentration to roughly 100 µM. After a 2 point calibration, the oxygen electrode was inserted into the bung and the whole bung-probe assembly was inserted into the overlying water volume of the reactor (Figure.2.3). The reactor was stirred at a constant speed (3 ¾ rpm) whilst maintaining *in situ* temperature (10-12°C) and light conditions. The oxygen concentration was logged every minute for a period of 24 hours and the total SOD rate was determined. Three cores per site were analysed sequentially and the average was used in the results.

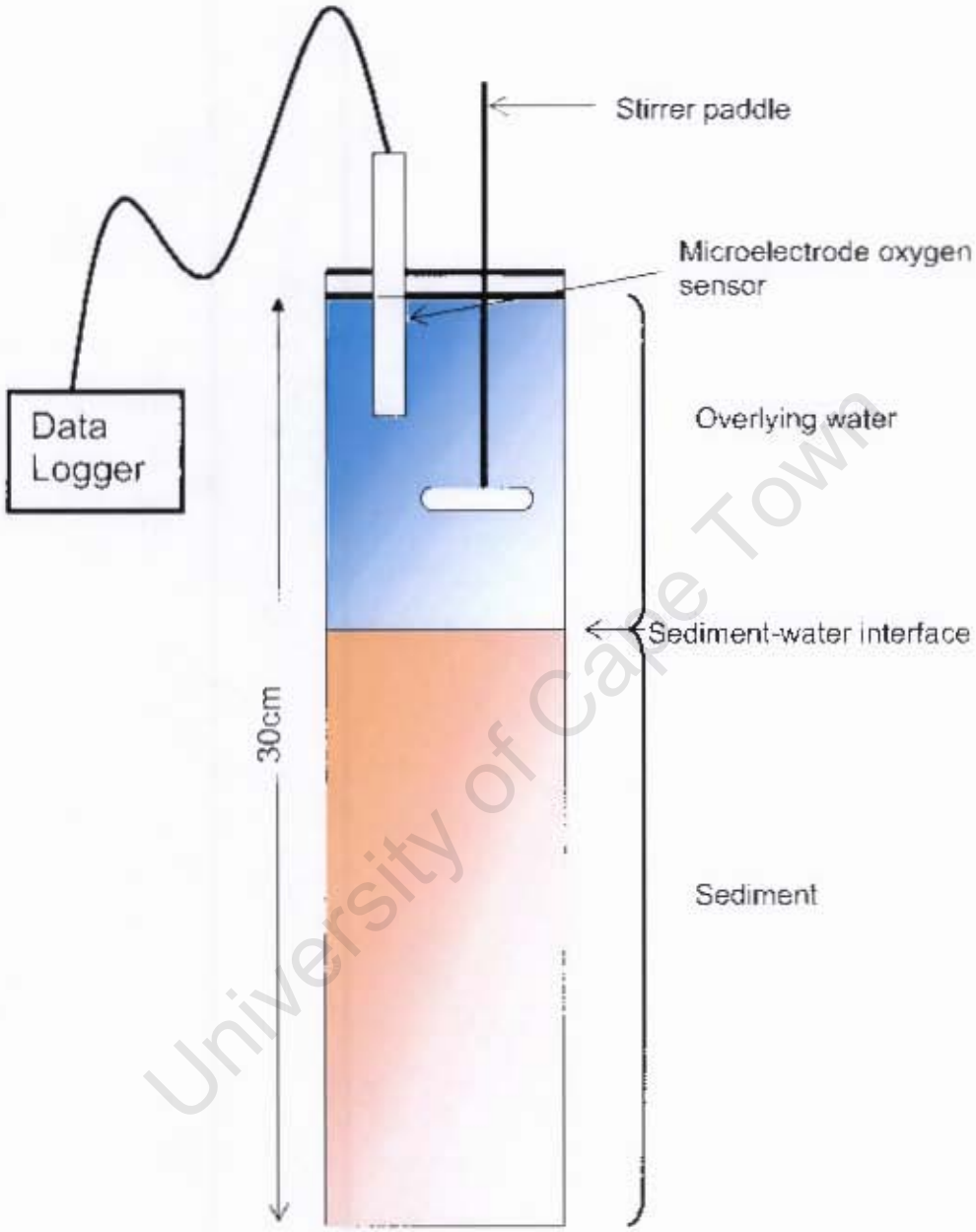

Figure. 2.3: Schematic diagram of sediment core oxygen incubation measurements. Oxygen concentrations were monitored in the overlying water over a period of 24 hours. The diagram is not to scale.

2.5 Interstitial water.

Sediment cores designated for interstitial water profiles were frozen and sectioned into 2 cm slices (for the top 10 cm) and 4 cm slices thereafter. The frozen sediment cores were sliced under nitrogen atmosphere (to avoid the air-oxidation of H_2S). The sections were placed in pre-labelled sample bags. The interstitial water was then squeezed out of the sediments using positive pressure applied through an inert gas (N_2; 5.0 instrument grade)) in a Teflon squeezing apparatus (see Figure 2.4). The inert gas was applied onto a latex diaphragm placed on the sediment forcing the interstitial water through a filter directly into a syringe to minimise the exposure to oxygen.

Figure 2.4 Reeburgh Teflon squeezing apparatus (Rheeburgh, 1967).

The interstitial water was then immediately sub-sampled for nutrients and sulphate and hydrogen sulphide analysis. These samples were frozen until analysed (using standard methods described in ***Appendix A***.) for solute concentration within 2 weeks of collection. Profiles were used for calculating sediment fluxes at the sediment-water.

2.6 Diffusive fluxes at the sediment water interface.

Diffusive fluxes of solutes at the sediment water interface were calculated using Fick's 1st law of diffusion. Sediment porosity was approximated from weight loss after heating the sediment at 80°C until for 12 hours. Porosity values of ~0.95 were obtained from this procedure similar to values reported by Glud *et. al.* (1994). Fossing *et. al.* (1999) reported average values of 0.85 for Namibian slope sediments. For the diffusive flux calculations, porosity was chosen as 0.9. Sediment diffusivity (D_{sed}) was calculated from molecular diffusion coefficients (D_o) after Li and Gregory, (1974) using eq. (17), with tortuosity equal to 1.1 (Berner 1980). Sediment diffusivities were corrected for *in situ* temperature, salinity and pressure using the Stokes-Einstein relationship (eq. 19). Concentration gradients for ammonium, nitrate, sulphate, phosphate and silicate were calculated between the solute concentration in the benthic boundary layer and the concentration at 1 cm below the interface.

Hydrogen sulphide concentration gradients were calculated using the gradient down the length of the core up to where the concentration gradient changed, as these gave a better reflection of fluxes from the sediment to the water column. The top few centimetres of hydrogen sulphide profiles appeared to have mixed layer with low concentrations characteristics, and an increase in sulphide concentration was observed below this depth. The lack of benthic infauna observed in this study and by others (Copenhagen 1953, Bailey 1991), rules out advection caused by bioturbation.

However, methane bubbling from the sediments is suggested to cause enhancedl advective flux of solutes to the water column. The effect of methane at the sediment-interface is acknowledged but was not explicitly measured in this study.

2.7 Sediment core incubations.

Incubations of nutrient fluxes were also monitored in the sediments. The nutrient cores were treated similarly to the cores used for oxygen incubations (*in situ* temperature, no light and air-tight). Here, three cores (with overlying water intact) fitted with a bung and stirrer (3 ¾ rpm) and two holes; one for extracting sample and the other for replacing water. Nutrient sub-samples (60 mL aliquots) were extracted at 3 hour intervals for a period of 24 hours. To compensate for pressure, as the sample was extracted, replacement water (collected in Niskin bottles before the collection of the sediment) was replaced into the reactor using a double plunger mechanism. A time series of nutrient fluxes were determined, taking into account a correction factor for the addition of the replace water.

2.8 Brief description of analytical methods used for determining solute concentrations.

Oxygen concentrations were measured in the overlying water using a YSI membrane electrode after a two point calibration. Samples prepared for nitrate, ammounium, sulphate, hydrogen sulphide, phosphate and silicate samples were filtered through 0.45µm membrane filters and stored frozen until analysis. Nutrient concentrations were determined colourimetrically using methods described by Grasshoff *et. al.* (1983) and the hydrogen sulphide were determined using the method described by Cline (1969). Organic content was determined through elemental analysis. Quality

control was performed by using the appropriate reference standards as well as comparing results for samples analysed independently by NatMIRC. A detailed description of methods used is provided in ***Appendix A***.

2.9 Particulate Organic Carbon (POC) and Particulate Organic Nitrogen (PON).

Particulate organic carbon (POC) and nitrogen (PON) were determined in each of the core sections. For POC analysis, roughly one gram of sample was oven-dried and acidified with ~ 5 mL organic-free 1 M HCl to remove the inorganic carbon fraction in the sediment. After acidification the samples were rinsed with de-ionised water and oven dried at 100°C. No acidification was carried out for PON samples, as acidification would remove the ammonia associated with the organic fraction of the sediment. POC and PON were analysed with a Euro CHN Elemental Analyser instrument. A standard reference material (MBSS-1) was treated exactly as the samples as quality control for the analysis.

2.10 Sediment traps.

Two sediment traps, each containing four tubular units of internal diameter 69mm and length 620mm (Figure 2.5) were deployed at the sample station A to determine the flux of particulate organic matter at every two month interval. A 1mm^2 mesh at the top of the sediment trap tubes prevented entry by large nekton. The traps were suspended in the water column at 60m and 80m depth by means of a subsurface float at Station A. Each unit contained a 1% formalin solution for sample preservation. Retrieved sediment traps were filtered through pre-ashed Microsep

GF/F filters and the suspended material was oven dried at 100°C and organic carbon and nitrogen content were determined as per Section 2.11 and corrected for the small filter blank.

Figure 2.5 Retrieval of sediment traps deployed at Station A.

Chapter 3

Results

Results obtained from the 2003 yearlong sampling programme are presented in this chapter. It comprises of the following parts;

- sediment interstitial water profiles,
- the diffusive fluxes of dissolved species,
- particulate organic carbon fluxes and
- total sediment oxygen demand.

3.1 Sediment interstitial water profiles.

Vertical profiles of biogeochemical solute concentrations in interstitial water give valuable insight into remineralization pathways, fluxes and redox zones within the sediment. Interstitial water concentration profiles for ammonium, nitrate, sulphate, sulphide, phosphate and silicate from the top 30cm of surface sediments collected at Station A over the investigation period are presented here (Figure 3.1 – Figure 3.6). Concentrations are given in μM, and the bottom boundary layer water concentrations (Table 3.1) were chosen as the concentration at the sediment-water interface (Z = 0cm).

Table 3.1: Concentration of oxygen, ammonia, nitrate, sulphate and sulphide in the bottom boundary layer (BBL; <5m above sediment) collected with Niskin bottles during each sampling interval.

Month	O_2 µM	NH_4-N µM	NO_3-N µM	SO_4-S mM	H_2S-S µM	PO_4-P µM	SiO_4-Si µM
Oct-02	14.4	1.8	23.9	-	-	1.7	33.8
Nov-02	2.6	0.0	24.5	-	-	1.3	54.0
Dec-02	12.7	1.2	13.5	-	-	1.6	23.1
Feb-03	2.0	0.7	17.1	26.4	44.4	2.0	21.2
Mar-03	6.6	8.0	20.8	-	44.7	2.7	31.3
May-03	5.8	21.0	10.6	30.4	45.9	2.1	31.1
Jul-03	5.0	3.5	24.1	29.1	57.6	5.9	34.5
Sep-03	21.6	2.9	6.1	27.7	31.8	2.3	39.1
Nov-03	4.5	16.2	-	24.9	16.2	0.0	35.4

- indicate months when concentrations were not measured

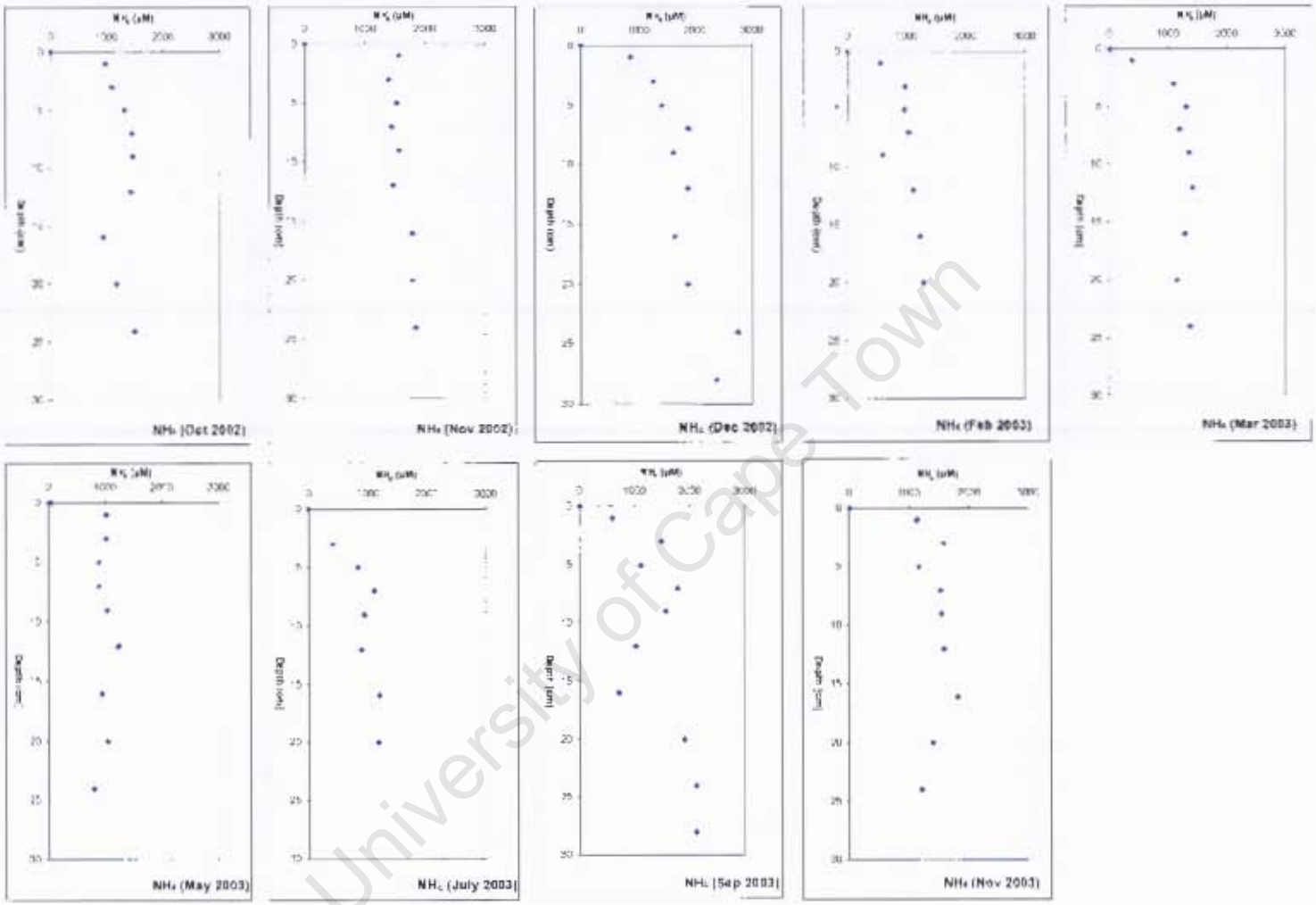

Figure 3.1: Interstitial water profiles of dissolved ammonium in sediment cores collected at Station A between Oct 2002 and Nov 2003. Ammonium concentrations of the overlying water were chosen at the sediment-water interface (Z = 0cm). Below Z = 0cm, ammonium concentrations were orders of magnitude greater than at the interface and indicated flux in the direction of the water column.

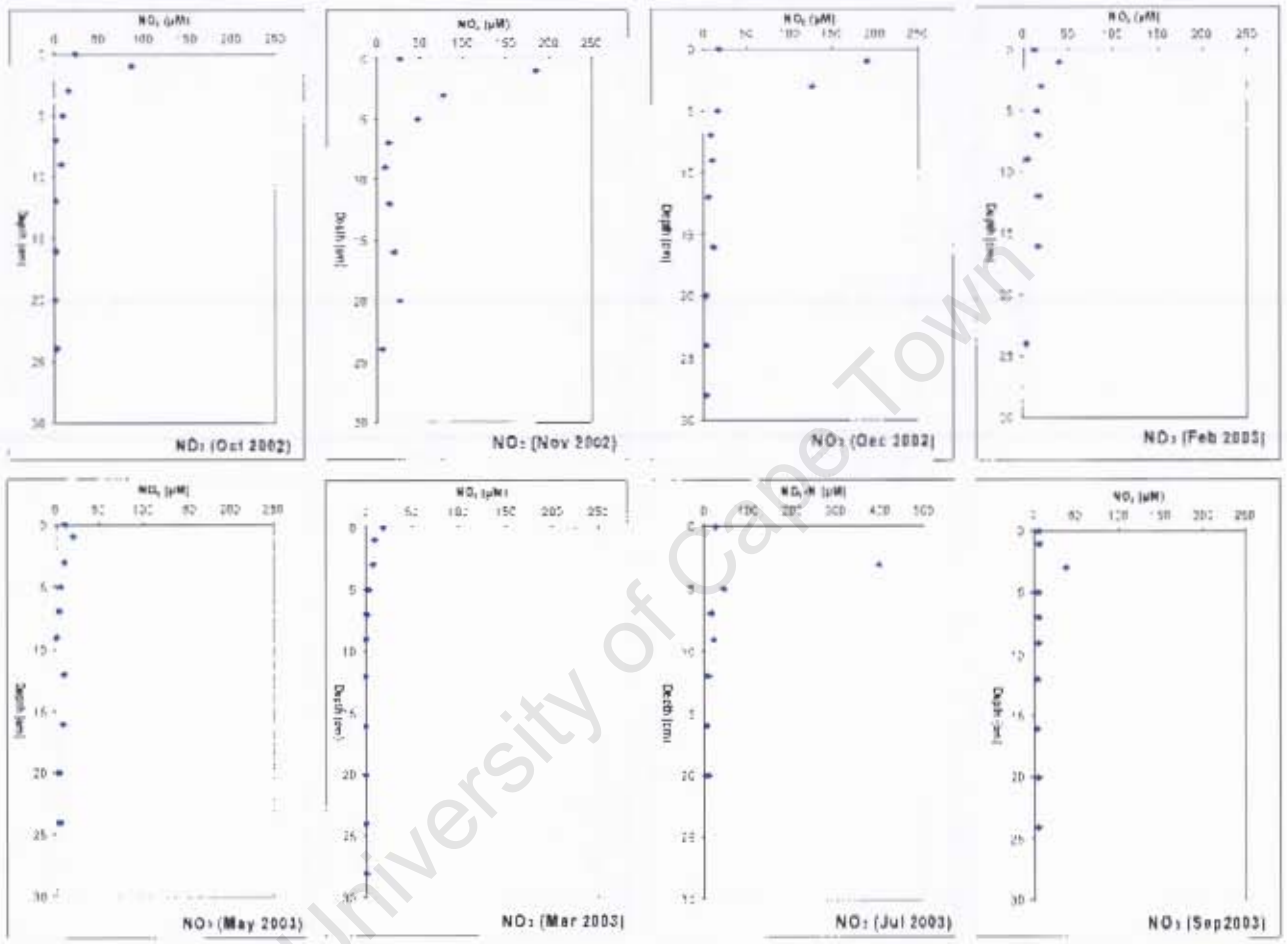

Figure 3.2: Interstitial water profiles of nitrate in sediment cores collected at Station A between Oct 2002 and Sep 2003. Nitrate concentrations of the overlying water were chosen at the sediment-water interface (Z = 0cm). Peak nitrate concentrations were observed between Z = 1cm and Z = 5 cm which were unexpectedly high in certain cases, possibly due to sample handling which introduced oxygen into the sediment cores.

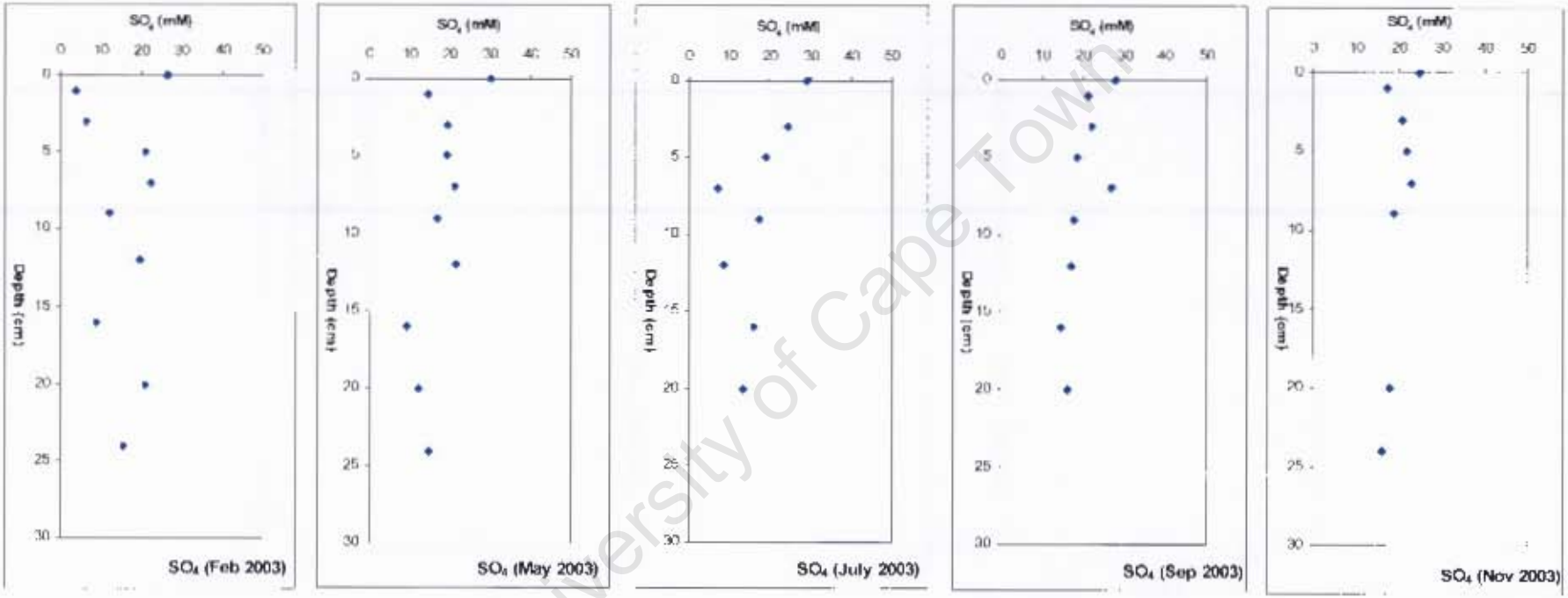

Figure 3.3: Interstitial water profiles of sulphate in sediment cores collected at Station A between Feb 2003 and Nov 2003. Sulphate concentrations at the sediment-water interface were chosen as the overlying water concentration. Higher sulphate concentrations in the water column indicated sulphate flux into the sediment.

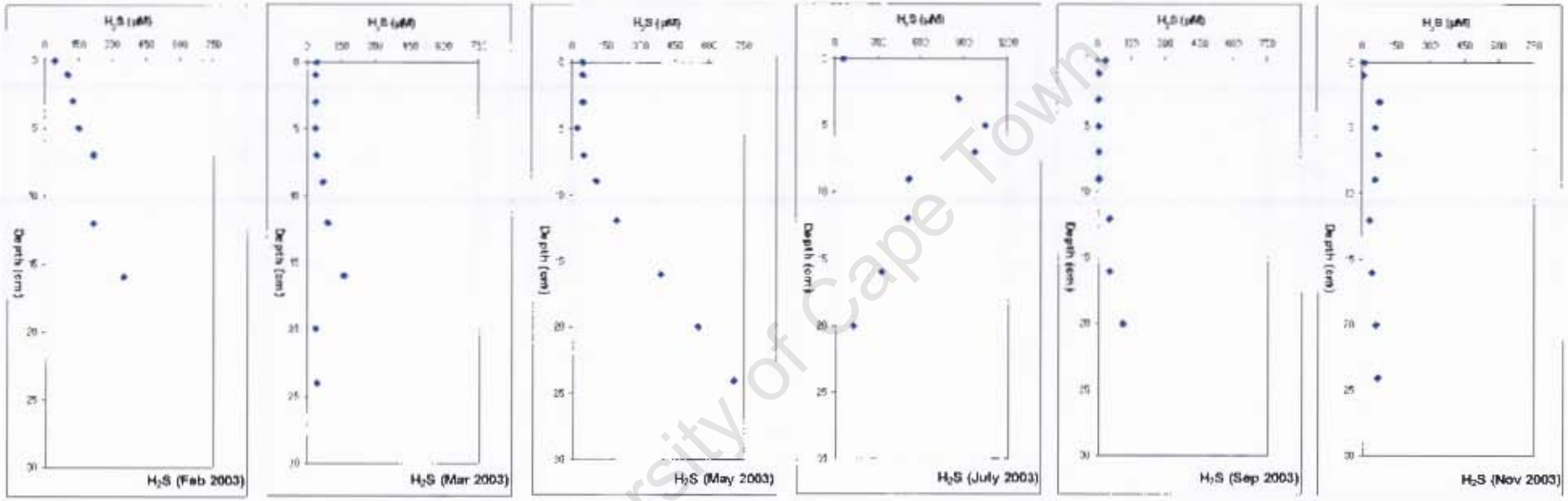

Figure 3.4: Interstitial water profiles of dissolved hydrogen sulphide in sediment cores collected at Station A between Feb 2003 and Nov 2003. Dissolved hydrogen sulphide concentrations increased towards the bottom of the cores from Feb 2003 – May 2003 and indicated fluxes in the direction of the water column. Sep 2003 and Nov 2003 showed little concentration variability with sediment depth. July 2003 shows an unexpected maximum in the concentration profile.

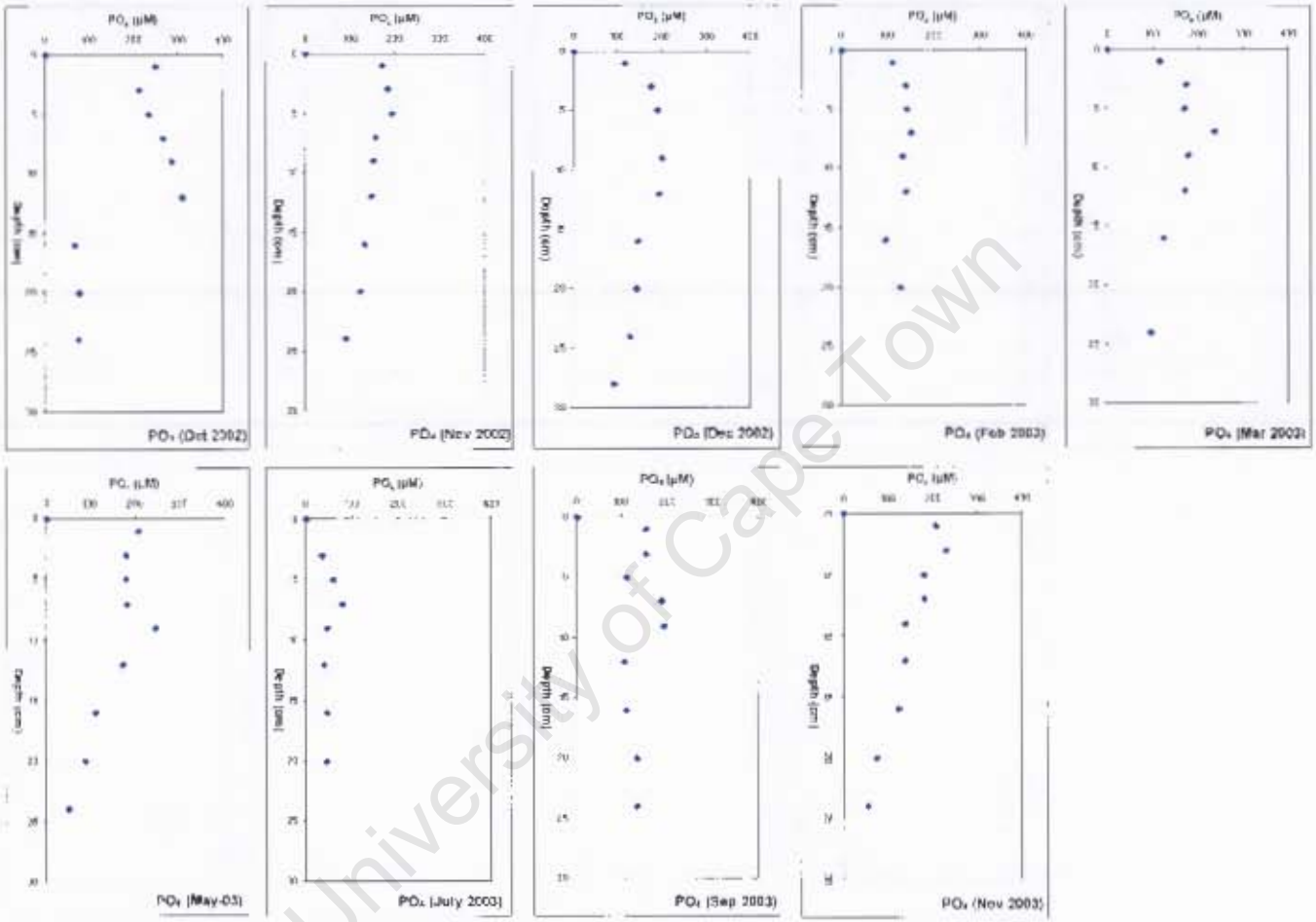

Figure 3.5: Interstitial water profiles of dissolved phosphate in sediment cores collected at Station A between Oct 2002 and Nov 2003. Phosphate concentrations within the sediment (below Z =1cm) were orders greater than at the sediment-water interface (Z = 0cm) which implied flux in the direction of the water column.

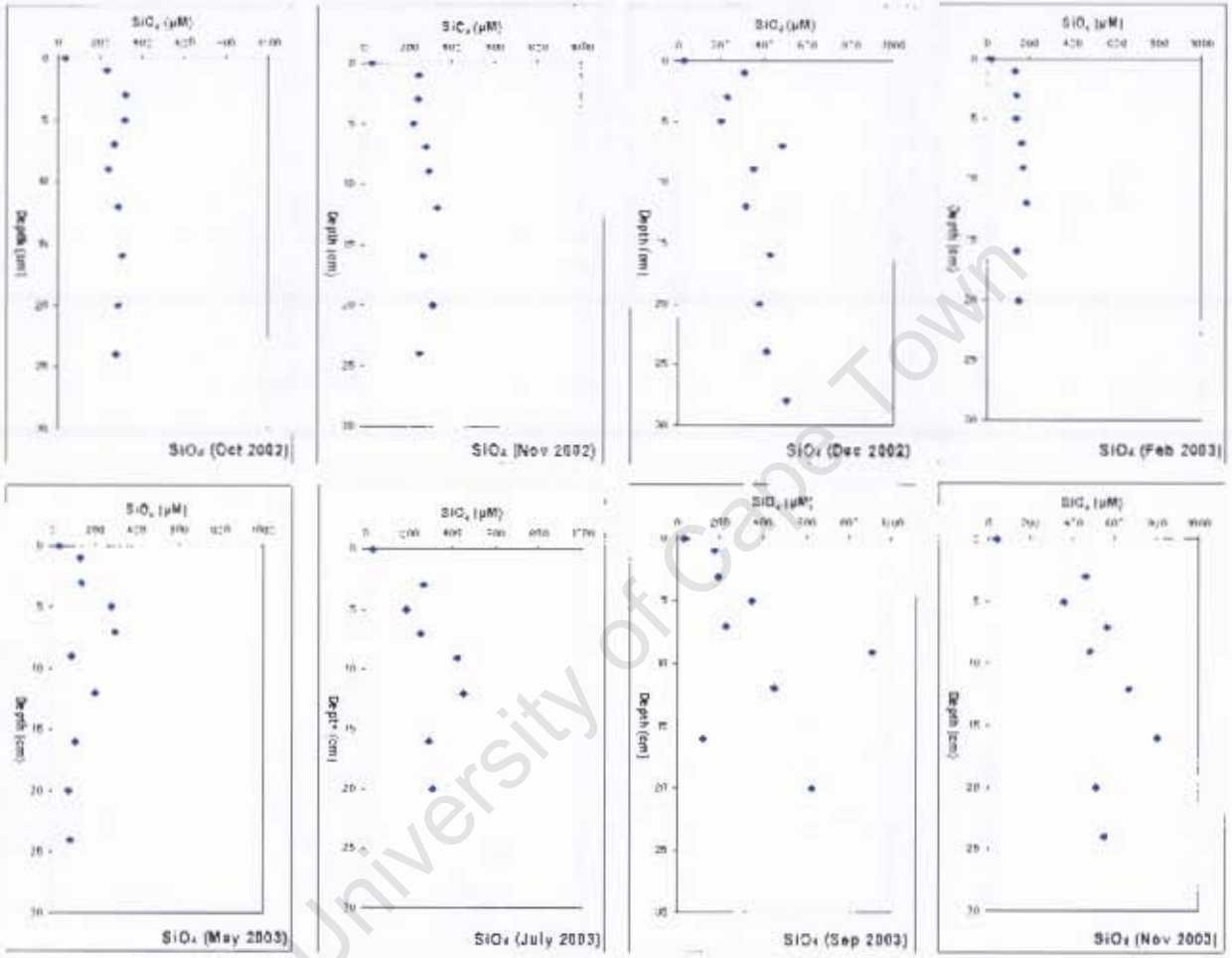

Figure 3.6: Interstitial water profiles of dissolved ortho-silicate in sediment cores collected at Station A between October 2002 and November 2003. Dissolved silicate concentrations within the sediment (below Z =1cm) were orders greater than at the sediment-water interface (Z = 0cm) which implied flux in the direction of the water column.

3.1.1 Ammonium porewater profiles.

Ammonium (NH_4^+) concentrations profiles for the period Nov 2002 – Nov 2003 are depicted in Figure 3.1. Down the length of the core, ammonium concentrations varied between 1-2 mM NH_4^+. In all cases, a marked difference (up to 1000 times greater) occurred at the sediment-water interface, stabilising below *Z* = 1cm in the sediment. The concentration gradient at the sediment-water interface reflected remineralization within the sediment and a net diffusional flux in the direction of the water column.

3.1.2 Nitrate porewater profiles.

As expected for anoxic sediments, Nitrate (NO_3^-) profiles (Figure 3.2) showed elevated concentrations up to 5 cm below the sediment-water interface throughout the whole year. Nitrate concentration profiles increased and peaked in the top 5 cm at levels of up to 200 µM NO_3^-. Below 5 cm in the sediment, the nitrate concentrations were below detection levels. Between *Z* = 0 cm and *Z* = 5 cm most nitrate profiles showed a maximum which were unexpectedly high during November 2002, December 2002 and July 2003 given the anoxic nature of the sediment.

3.1.3 Sulphate porewater profiles.

Sulphate (SO_4^{2-}) porewater profiles varied over a broad range of concentrations (10 – 30 mM SO_4^{2-}) in the top 30 cm of the cores (Figure. 3.3). The sediment-water gradient in the upper 1cm indicated sulphate flux into the sediment, possibly resulting from the removal of sulphate via sulphate reduction within the sediments. Below the sediment-water interface sulphate concentrations gradients were small, except for Feb. 2003, which showed unexpected variability with depth. The absence of benthic fauna from the sediment evidenced by the lack of burrows ruled out bioturbation for

the observed variation during Feb 2003 (Berner 1980). Analytical errors are proposed as a possible explanation for the Feb 2003 anomaly.

3.1.4 Hydrogen sulphide porewater profiles.

Hydrogen sulphide (H_2S) concentration profiles (in µM H_2S) are depicted in Figure 3.4. Concentrations of H_2S were comparable in the bottom water and at the sediment interface reaching up to 50 µM. Below the sediment-water interface concentrations increased with sediment depth indicating diffusion of hydrogen sulphide from deeper parts of the sediment. In July 2003 however, concentrations increased up to 5cm sediment depth and decreased below this depth. February to May 2003 concentrations reached up to 750 µM in the deeper layers. No significant increase in hydrogen sulphide concentrations was observed with depth during September and November 2003.

3.1.5 Ortho phosphate porewater profiles.

Dissolved phosphate (PO_4^{3-}) profiles are depicted in Figure 3.5. On all occassions concentrations ranged between 100 and 300 µM PO_4-P. Dissolved phosphate concentrations at the sediment-water interface (Z = 0cm) were low and increased sharply at *Z* = 1 cm resulting in steep gradients at the sediment-water interface and indicating dissolved phosphate fluxes are in the direction of the water column. Below *Z* = 1 cm all phosphate profiles remained constant or decreased slowly towards the bottom of the core.

3.1.6 Ortho silicate porewater profiles.

Dissolved silicate (SiO_2) profiles are depicted in Figure 3.6. Silicate concentrations ranged between 100 and 500 µM SiO_2. Similar to phosphate, silicate concentrations at Z = 0 cm were low, typical of seawater, causing a steep concentration gradient at the sediment-water interface which indicated fluxes of dissolved silicate into the water column. Below Z =1 cm silicate concentrations stabilised and indicated small gradients towards the bottom of the cores.

3.2 Particulate Organic Carbon (POC) and Particulate Organic Nitrogen (PON).

Particulate organic carbon (POC) and nitrogen (PON) profiles of the sediment cores collected over the time period are depicted in Figure 3.7 – Figure 3.12. POC and PON (wt%) showed a steady decrease towards the bottom of the sediment cores. Concentration ranged between 9 - 12 $\%C_{org}$ and 1 – 2 $\%N_{org}$ for POC and PON respectively. The lower POC and PON concentration in the deeper parts of the cores indicated that longer exposure to bacterial breakdown during burial caused lower C_{org} and N_{org} concentrations. C:N ratios (Table 3.2) ranged between 7 and 10 and tended to increase with depth. Higher C:N ratios (>7) indicate POC that has undergone early diagenesis of the most labile fraction rather than the input of fresh phytoplankton origin (Redfield ratio of 106:16). The observed seasonal C:N variability is coherent with the observed ammonium diffusive fluxes which peaked during summer months (see section 3.3.1). The lowest C:N ratios (~7) which indicated the input of fresh organic matter, were observed during Feb 03 and Mar 03 (late austral summer), slightly out of phase with the highest POM fluxes observed in Nov 02 and Dec 02 (late spring/early summer) (see section 3.4).

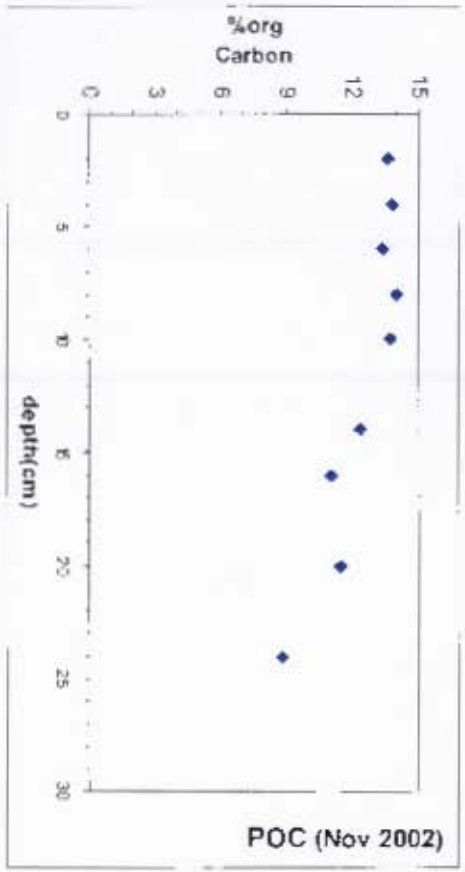

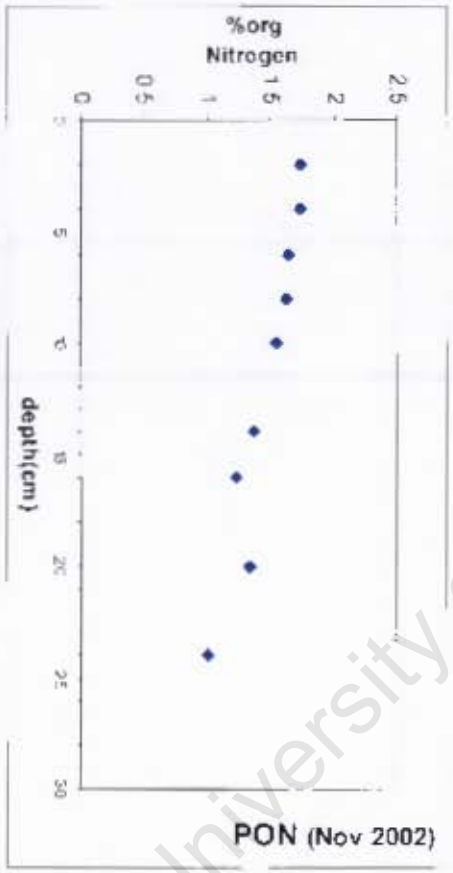

Figure 3.7 Depth profiles of % organic carbon and nitrogen of sediment cores collected on the Namibian inner shelf in November 2002.

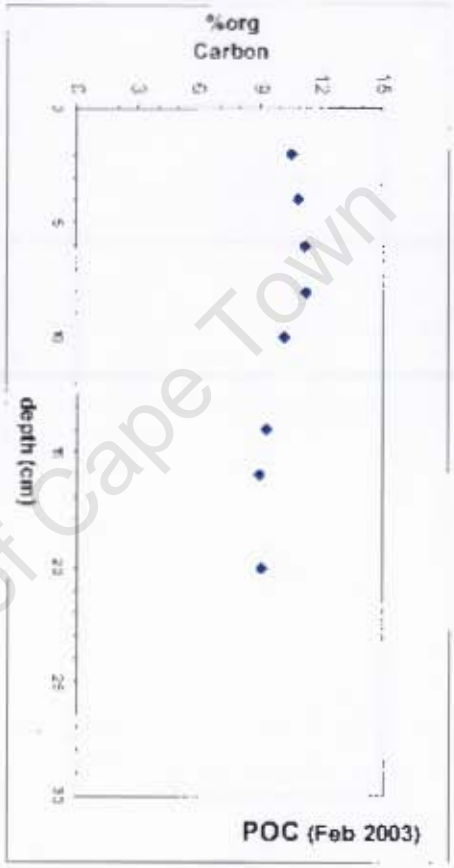

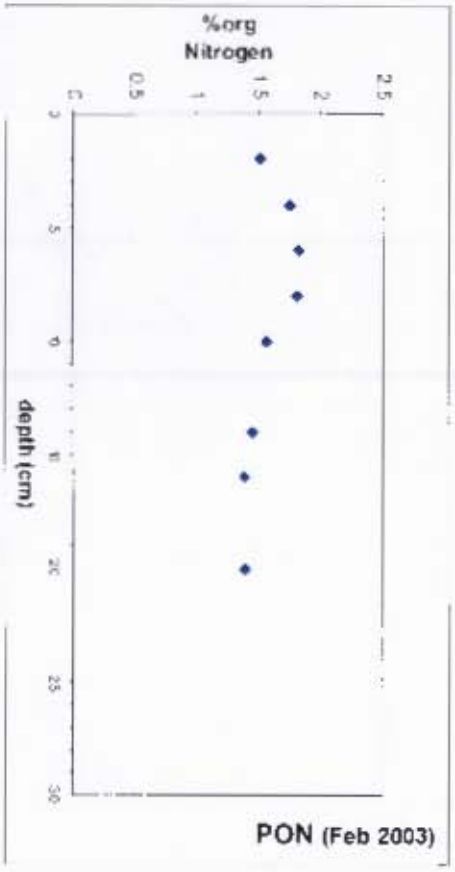

Figure 3.8 Depth profiles of % organic carbon and nitrogen of sediment cores collected on the Namibian inner shelf in February 2003.

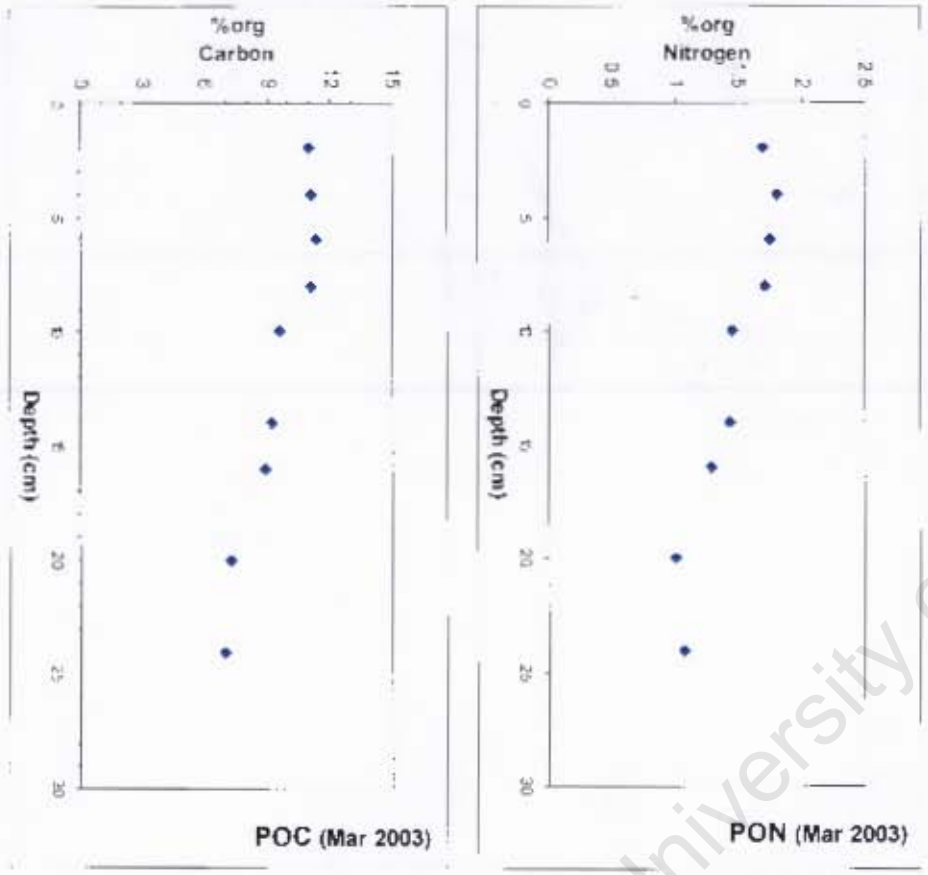

Figure 3.9 Depth profiles of % organic carbon and nitrogen of sediment cores collected on the Namibian inner shelf in March 2003.

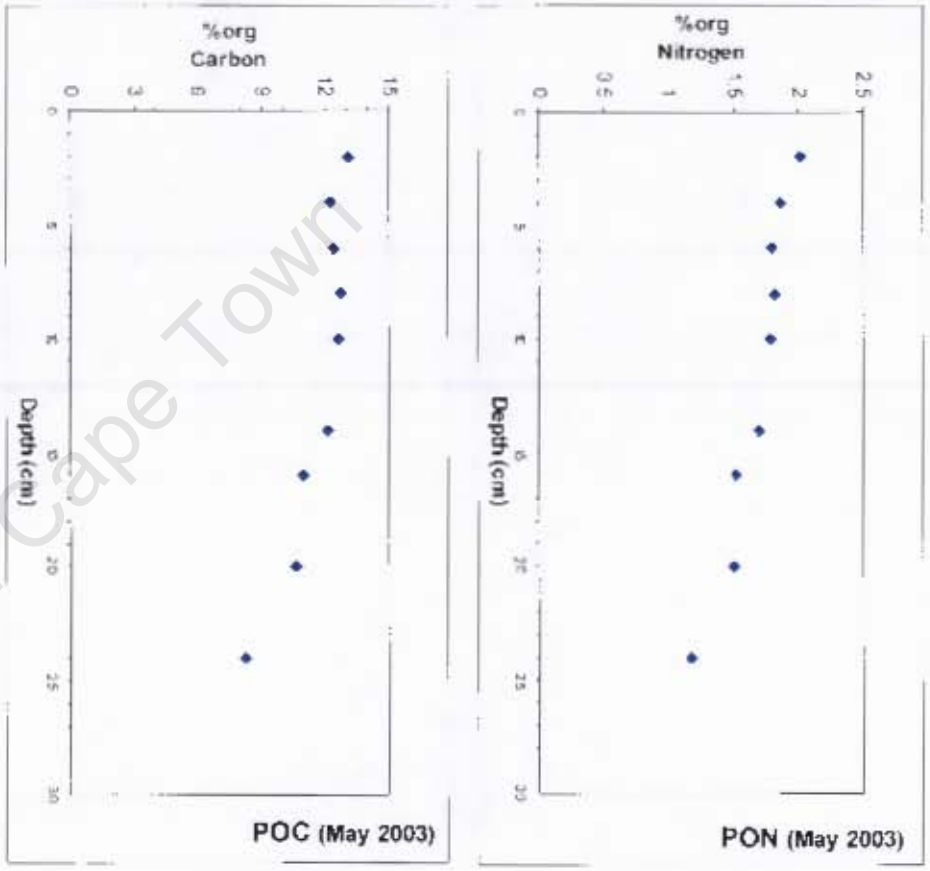

Figure 3.10 Depth profiles of % organic carbon and nitrogen of sediment cores collected on the Namibian inner shelf in May 2003.

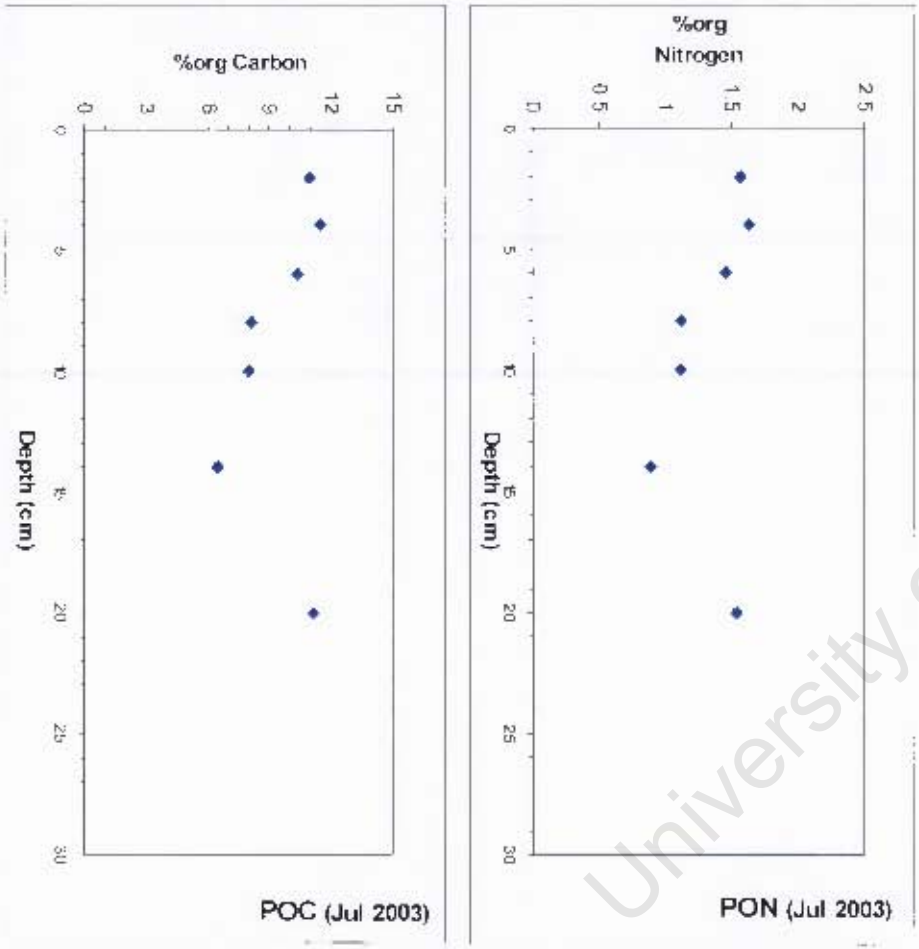

Figure 3.11 Depth profiles of % organic carbon and nitrogen of Sediment cores collected on the Namibian inner shelf in July 2003.

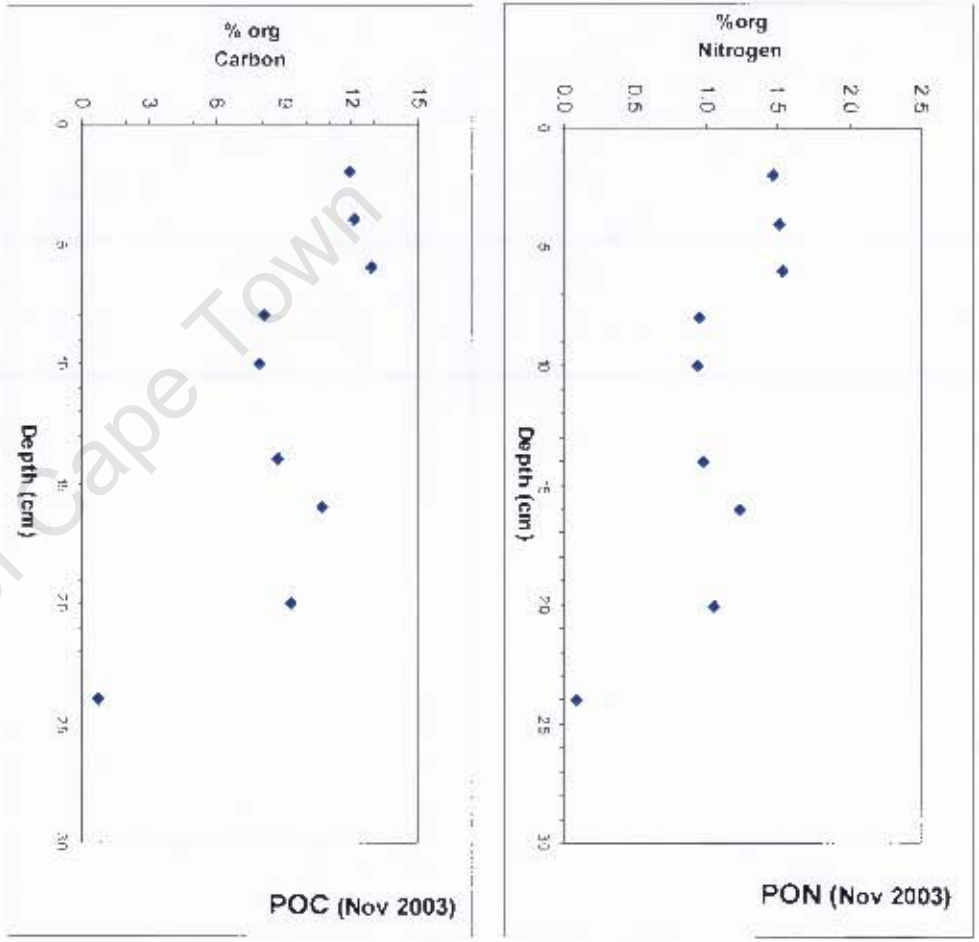

Figure 3.12 Depth profile of % organic carbon and nitrogen of sediment cores collected on the Namibian inner shelf in Nov 2003.

Table 3.2: C:N molar ratios down the depth of the sediment cores over the course of the year (Nov 2002 – Nov 2003). Highest ratios (>9), observed during summer months (Nov 2002 and Nov 2003), indicated relict organic matter.

Month Depth(cm)	Nov-02 C:N	Feb-03 C:N	Mar-03 C:N	May-03 C:N	Jul-03 C:N	Nov-03 C:N
2	9.18	8.16	7.53	7.59	8.16	9.46
4	9.32	7.27	7.19	7.66	8.17	9.43
6	9.52	7.24	7.51	8.07	8.27	9.85
8	10.08	7.27	7.54	8.13	8.40	10.04
10	10.40	7.59	7.65	8.27	8.39	9.74
14	10.51	7.53	7.55	8.34	8.53	10.39
16	10.42	7.47	7.97	8.46	8.66	10.01
20	9.98	7.61	8.37	8.28	8.36	10.21
24	10.21	-	7.60	8.15	-	9.50

3.3 Calculated diffusive fluxes of dissolved species.

Diffusive fluxes at the sediment-water interface were calculated using Fick's 1st law of diffusion (Eq. 11). Diffusive fluxes of oxidants and reduced species at the sediment-water interface were calculated using the concentration gradient between Z = 0 cm and Z = 1 cm unless stated otherwise. A summary of parameters, concentration gradients and calculated diffusive fluxes are presented in Table 3.3.

Table 3.3: Summary of calculated diffusive fluxes calculated using Fick's 1st Law. For concentration gradients (dC/dx), *interface* indicated gradients calculated from the difference between Z = 0 cm and Z =1cm while for the *gradient* the linear slope down the length of the core were used. Negative flux rates refered to diffusive flux in the direction of the water column while positive values implied flux in the direction of the sediment.

	NH_4 flux (mmol N /m^2/day)	**NO_3 flux** (mmol N /m^2/day)	**SO_4 flux** (mmol S/m^2/day)	**H_2S flux** (mmol S/m^2/day)	**PO_4 flux** (mmol P/m^2/day)	**SiO_4 flux** (mmol Si/m^2/day)
Average porosity (ø)	0.9	0.9	0.9	0.9	0.9	0.9
D_{sed} (cm^2/d)*	0.75	0.73	0.39	0.71	0.22	0.39
dC/dx	*interface*	*interface*	*interface*	*gradient*	*interface*	*interface*
Month						
Oct-02	-3.29	-0.21	-	-	-0.24	-0.36
Nov-02	-5.30	-0.49	-	-	-0.27	-0.27
Dec-02	-2.96	-0.58	-	-	-0.11	-0.51
Feb-03	-1.70	-0.08	55.67	-0.10	-0.11	-0.19
Mar-03	-1.29	0.04	-	-0.04	-0.11	-
May-03	-3.37	-	39.31	-0.18	-0.20	-0.19
Jul-03	-0.68	-0.61	5.63	-0.86	-0.03	-0.21
Sep-03	-2.04	-0.11	16.27	-0.03	-0.15	-0.24
Nov-03	-3.79	-	19.01	-0.04	-0.21	-0.66

* Calculated for 11°C based on the data from Boudreau (1996).

3.3.1 Ammonium diffusive fluxes.

Seasonal diffusive fluxes of ammonium are depicted in Figure 3.13 and ranged between -0.68 and – 5.30 mmolN.m^{-2}.d^{-1}. Concentration gradients of ammonium at the sediment water interface always indicated a flux in the direction of the water column. The highest flux was observed in Nov 2002 (- 5.30 mmolN.m^{-2}.d^{-1}) and the lowest flux was observed in July 2003 (-0.68 mmolN.m^{-2}.d^{-1}). Seasonally during the study period, ammonium diffusive flux peaked during the austral summer months (Nov 2002 and Nov 2003) and was lower during winter. This followed the observed fluxes of POC and PON (see section 3.4).

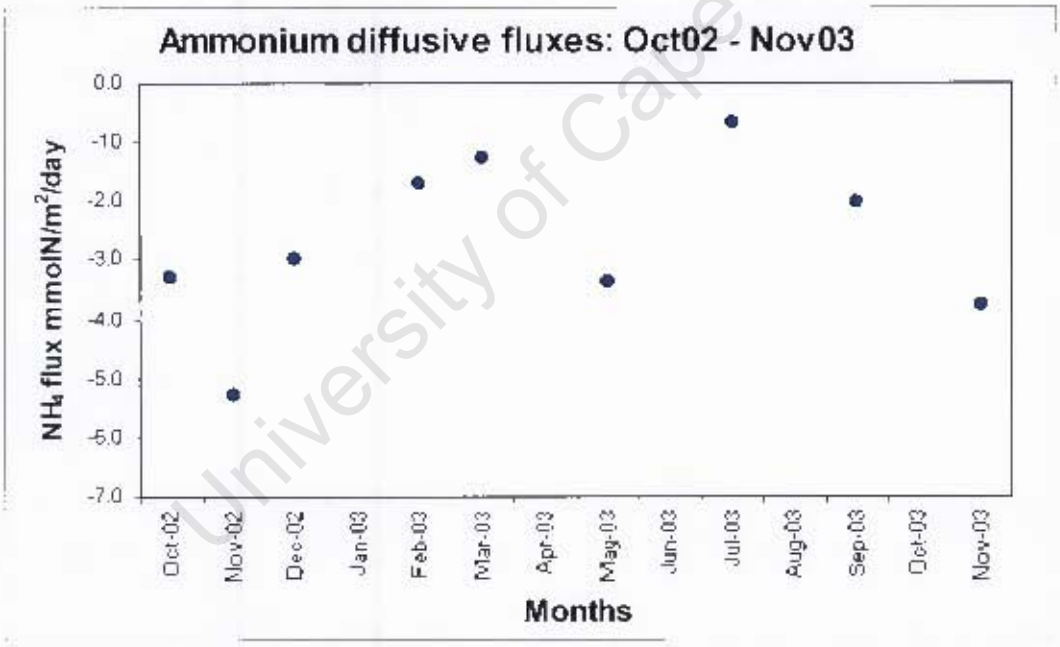

Figure 3.13: Plot of diffusive ammonium flux on the Namibian inner shelf sediments from Oct 2002 to Nov 2003. Diffusive fluxes are expressed in mmolN.m^{-2}.d^{-1}. Data suggests highest ammonium flux in summer months (Nov 2003 and Nov 2003) and lowest ammonium flux in winter months (Mar 2003 and Jul 2003). Negative scale indicated flux towards the water column.

3.3.2 Nitrate diffusive fluxes.

Nitrate diffusive fluxes are depicted in Figure 3.14 and ranged between + 0.04 and -0.61 mmol $N.m^{-2}.d^{-1}$. Most of the diffusional nitrate fluxes were in the direction of the water column, except March 2004, where flux was in the direction of the sediment. The flux of nitrate from the sediment into the water column was unexpected in an anoxic sediment environment. Flux of nitrate into the water column would indicate that nitrate is being formed within the sediments, possibly through the oxidation of ammonium with oxygen. Due to the anoxic environment of the sediment, oxidation of ammonium with oxygen was unlikely. The unexpected high subsurface nitrate concentrations could possibly be a natural phenomenon, or during sample handling, oxygen was introduced to the sediments. This paradox is revisited in the discussion section.

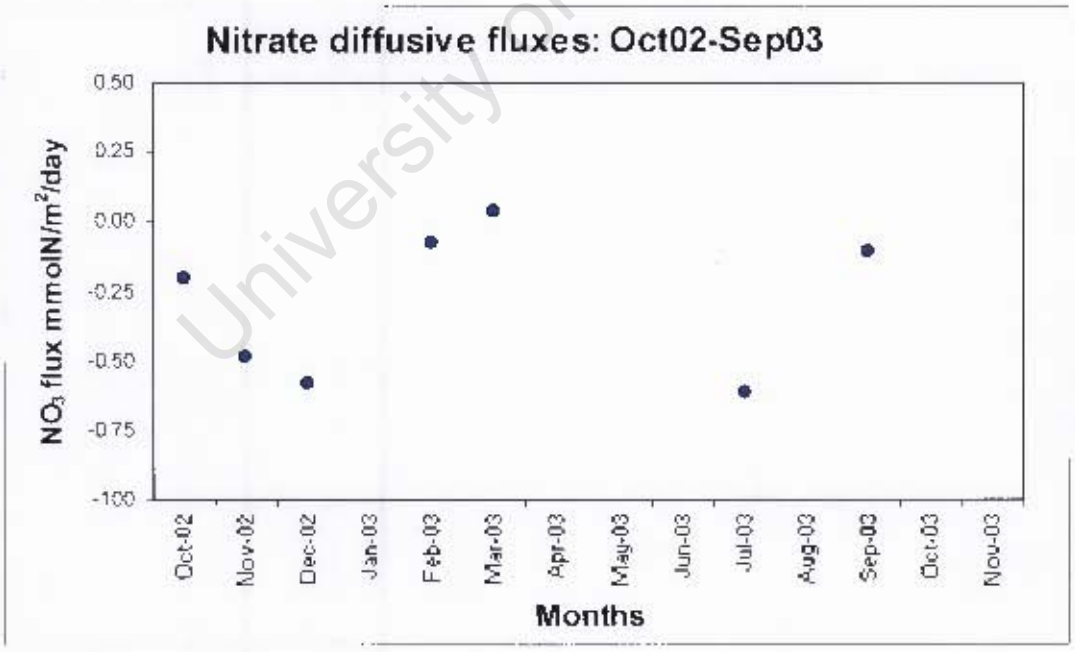

Figure 3.14: Plot of diffusive nitrate flux on the Namibian inner shelf sediments from Oct 2002 to Nov 2003. Diffusive fluxes are expressed in $mmolN.m^{-2}.d^{-1}$. The data show no clear seasonal trend in nitrate flux. Negative scale indicated flux to the water column which was unexpected in the anoxic environment.

3.3.3 Sulphate diffusive fluxes.

Diffusive sulphate fluxes are depicted in Figure 3.15 and ranged between 5.6 and 55.7 mmol $S.m^{-2}.d^{-1}$ at the sediment water interface. Sulphate concentration gradients indicated fluxes from the water column into the sediment. Although sampling started in October 2002, sulphate and sulphide concentrations were only measured from February 2003 onwards. Highest calculated sulphate fluxes were observed in Feb 2003 and May 2003, and the lowest flux in July 2003.

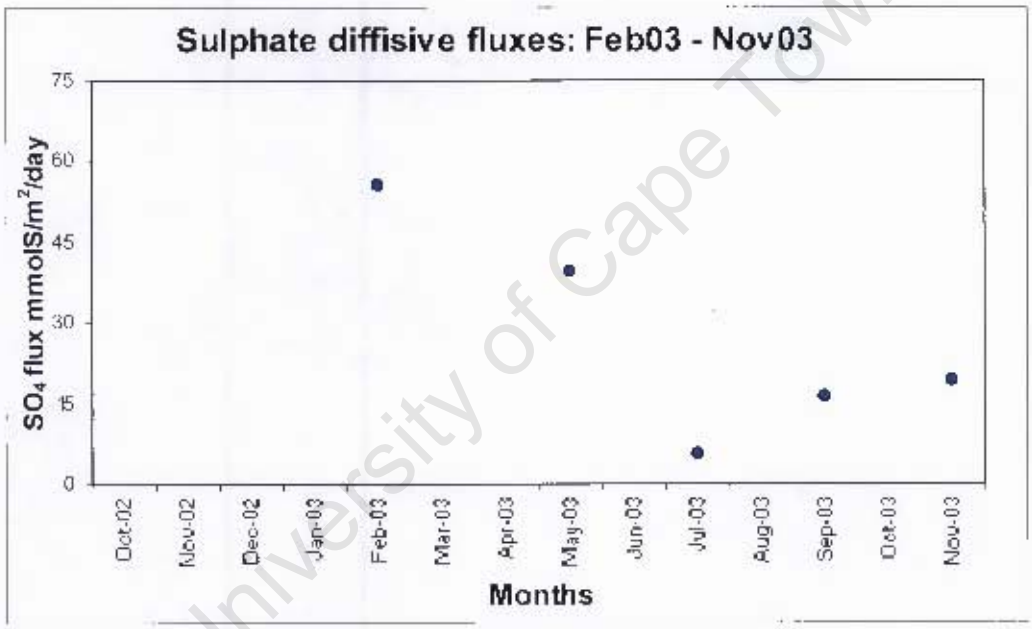

Figure 3.15: Plot of diffusive sulphate flux on the Namibian inner shelf sediments from Feb 2003 to Nov 2003. Diffusive fluxes are expressed in $mmolS.m^{-2}.d^{-1}$. Highest fluxes were observed from May 2003 – Sep 2003. Positive scale indicates flux into the sediment.

3.3.4 Hydrogen sulphide diffusive fluxes.

Hydrogen sulphide concentration gradients were calculated using the section of the concentration profiles where the concentration gradient changed, as there was seldom any concentration gradient at the sediment-water interface and sulphide concentrations increased at greater sediment depths. Diffusive hydrogen sulphide fluxes depicted in Figure 3.16 ranged between – 0.03 and – 0.86 mmol $S.m^{-2}.d^{-1}$ and were always from the sediment into the water column. Diffusive hydrogen sulphide remained low throughout the year fluxes and only a spike in the diffusive flux of sulphide was observed in July 2003 (- 0.86 mmol $S.m^{-2}.d^{-1}$)

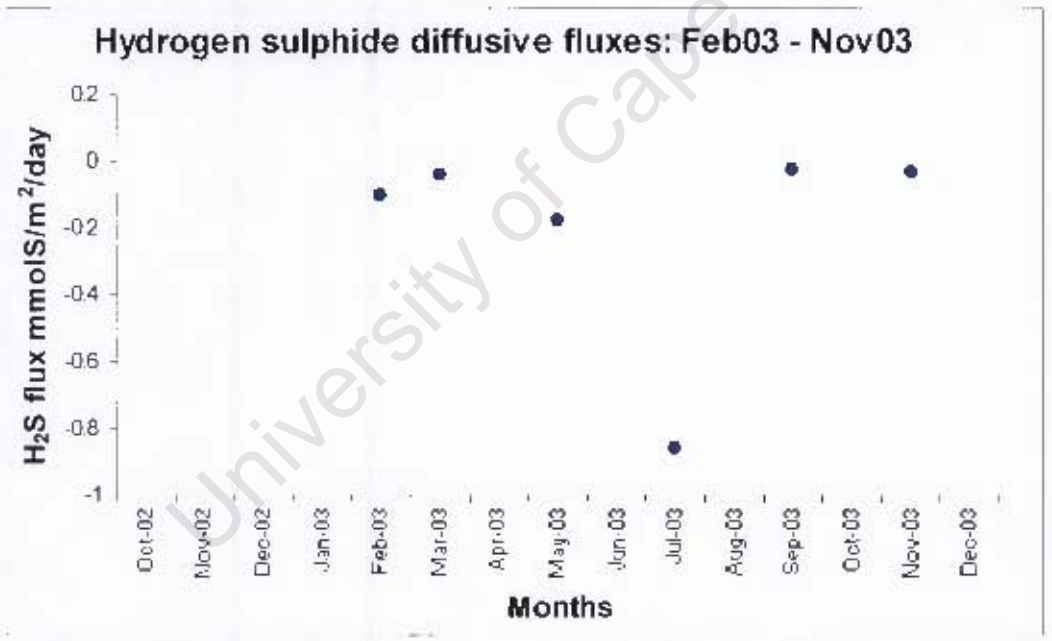

Figure 3.16: Plot of diffusive hydrogen sulphide flux on the Namibian inner shelf sediments from Feb 2003 to Nov 2003. Diffusive fluxes are expressed in $mmolS.m^{-2}.d^{-1}$. No seasonal trend was observed in hydrogen sulphide fluxes only a spike was of elevated sulphide flux in July 2003. The negative scale indicated fluxes toward the water column.

3.3.5 Phosphate diffusive fluxes.

Diffusive phosphate fluxes are depicted in Figure 3.17 and ranged between - 0.03 and - 0.27 mmol $P.m^{-2}.d^{-1}$. Concentrations of phosphate at the sediment-water interface were always less than concentrations at Z = 1cm and below, indicated phosphate flux in the direction of the water column. The highest diffusional flux rates were observed during austral summer months when the highest POM fluxes were also observed.

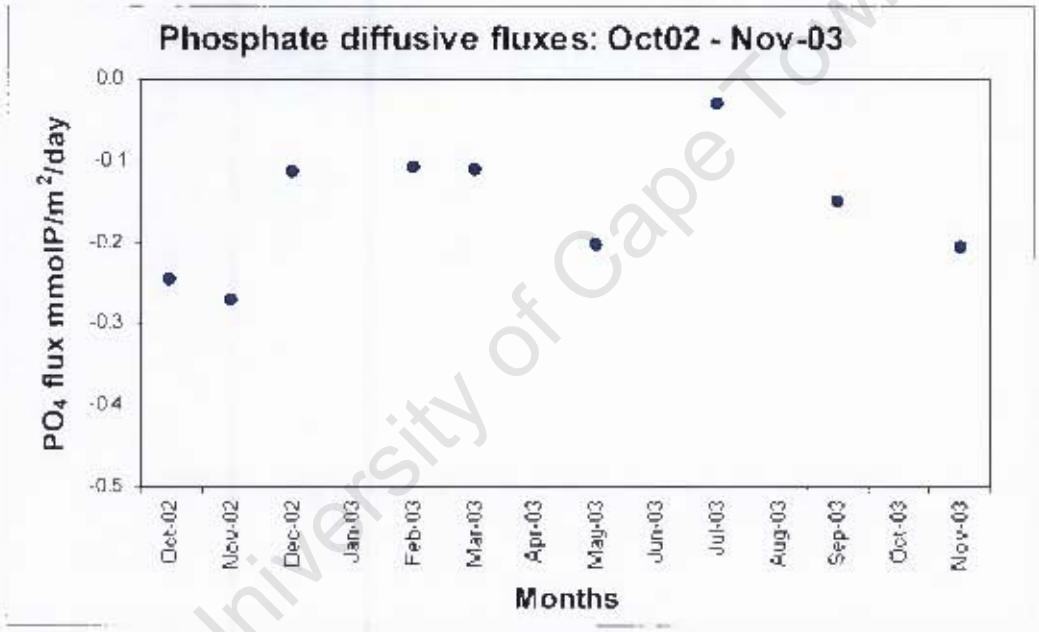

Figure 3.17: Plot of diffusive phosphate flux on the Namibian inner shelf sediments from Oct 2003 to Nov 2003. Diffusive fluxes expressed in $mmolP.m^{-2}.d^{-1}$. The negative scale indicated fluxes toward the water column.

3.3.6 Dissolved silicate diffusive fluxes.

Diffusive silicate fluxes are depicted in Figure 3.18 and ranged between -0.19 and -0.66 mmolSi.m^{-2}.d^{-1}. Concentrations of silicate at Z = 0 were always less than concentrations at Z = 1cm and below, indicated that silicate flux in the direction of the water column. The highest flux was observed during the summer months.

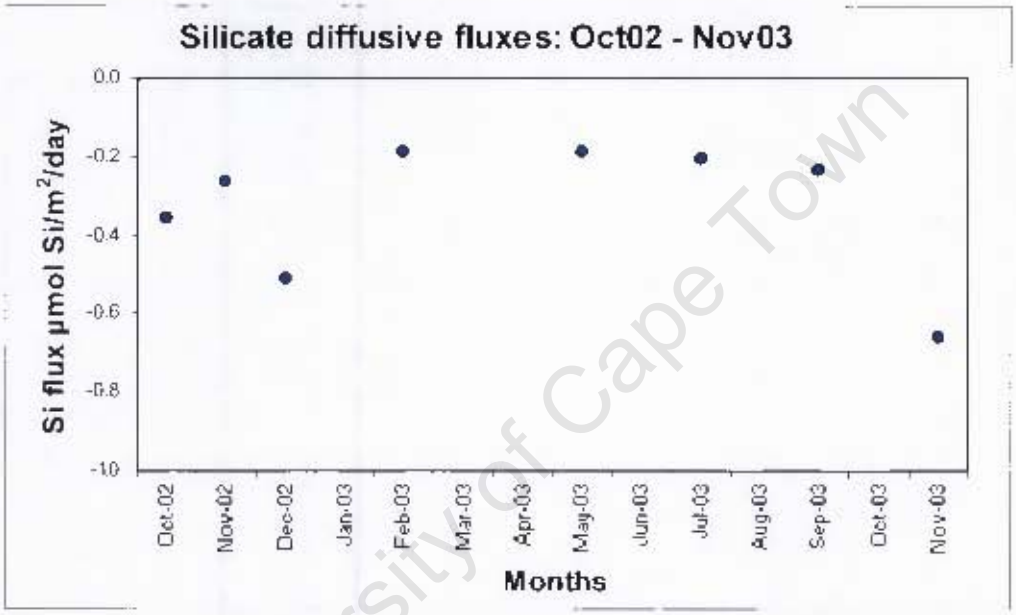

Figure 3.18: Plot of diffusive silicate flux on the Namibian inner shelf sediments from Oct 2003 to Nov 2003. Diffusive fluxes are expressed in mmolSi.m^{-2}.d^{-1}. The negative scale indicated fluxes toward the water column.

3.4 Sedimentation fluxes of particulate organic carbon (POC) and nitrogen (PON).

The fluxes of both particulate organic carbon and nitrogen POC and PON from sediment traps moored at the sampling station are shown in Figure. 3.19. POC and PON fluxes for Station A were at a maximum during summer months (Nov – Feb). Throughout the year POC ranged between 1.95 – 7.37 mmol $Cm^{-2}day^{-1}$, while PON ranged between 0.22 – 1.18 mmol N $m^{-2}day^{-1}$. POC flux concentrations observed in this study are comparable with flux concentrations at the Walvis Ridge (20°S, 09°E), Wefer and Fischer (1992) observed POC flux up to 9.2 $mmolC.m^{-2}.d^{-1}$.

Observed POC fluxes indicated higher primary production rates in the water column during the austral summer (Nov 2002 – Dec 2002 and Nov 2003). C:N ratios of the < 200 µm fraction, the detrital particles which exclude the mezo- and macro zooplankton, are presented in Table 3.4. The C:N ratios ranged between 5.2 – 8.7 with an average C:N ratio of 7.1 (std dev =1.16). Highest ratios were observed from late summer till spring (Feb 2003 – Aug 2003). The lowest C:N ratios were observed in Nov 02 and Nov 03.

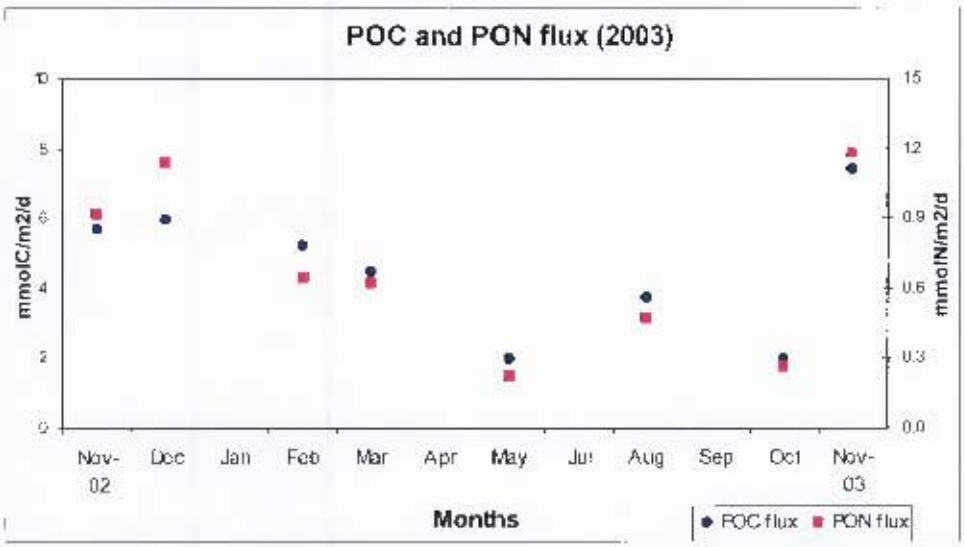

Figure 3.19: Plot of depositional C_{org} and N_{org} flux on the Namibian inner shelf from Nov 2002 to Nov 2003. Fluxes of both C_{org} and N_{org} peaked during summer months. Rates are expressed in mmol $Cm^{-2}day^{-1}$.

Table 3.4: Quasi-monthly depositional flux (total suspend solids, POC flux and PON flux) from sediment traps moored at Station A (22°59'S 14°03'E). The <200 µm fraction results are presented in both $mg.m^{-2}.d^{-1}$ and $mmol.m^{-2}.d^{-1}$.

	TSS(<200µm)	*POC flux*		*PON flux*		*C:N*
Month	$g/m^2/day$	$mmol/m^2/d$	$mg/m^2/d$	$mmol/m^2/d$	$mg/m^2/d$	
Nov-02	0.788	5.69	68.32	0.92	12.89	6.18
Dec-02	1.007	5.96	71.48	1.14	15.99	5.21
Feb-03	0.348	5.22	62.60	0.64	9.02	8.10
Mar-03	0.227	4.45	53.41	0.62	8.71	7.15
May-03	0.116	1.97	23.60	0.22	3.15	8.74
Aug-03	0.302	3.71	44.51	0.47	6.61	7.85
Oct-03	0.403	1.95	23.43	0.27	3.74	7.31
Nov-03	0.416	7.37	88.48	1.18	16.49	6.26

3.5 Total sediment oxygen demand.

Sediment oxygen uptake fluxes from sediment cores collected quasi-monthly from Nov 2002 to Nov 2003 are depicted in Figure 3.20. A clear seasonal trend in oxygen consumption was observed which peaks in May to Sep 2003. The plot shows that the total sediment oxygen demand (TSOD; aerobic + anaerobic) ranged from 4.27 – 20.10 mmol O_2 $m^{-2}day^{-1}$.

As was described in the sampling methods, oxygen concentrations in the overlying water of the incubated cores were artificially elevated and do not necessarily reflect the *in situ* water column oxygen concentrations. The actual water column oxygen concentrations from a CTD oxygen profile are shown in Figure 3.21. The plot show water column dissolved oxygen concentrations of less than 22.3 µM overlying the sediment throughout the year.

During the oxygen incubations, oxygen concentrations were measured in the water overlying the sediment over a period of 24 hrs. A volumetric oxygen consumption rate was observed, which was converted to an areal oxygen consumption rate by using the area of sediment in contact with the overlying water during core incubations. The calculation was done as follows using May2003:

Volumetric TSOD rate: 210.38 µmol $O_2.dm^{-3}.day^{-1}$

Volume of water overlying sediment: 0.33 L

Area of sediment in contact with water: 31.17 cm^2

The volumetric rate was converted to a molar rate of consumption by multiplication with the overlying water volume and thereafter it was converted to an areal rate through division by the sediment area.

Molar rate: 69.43 µmol.day^{-1}

Areal oxygen consumption rate: 22.27 mmol $O_2.m^{-2}.day^{-1}$.

Where multiple core incubations were measured, the average of the areal rates is presented. A summary table of all the calculations are presented in ***Appendix B***.

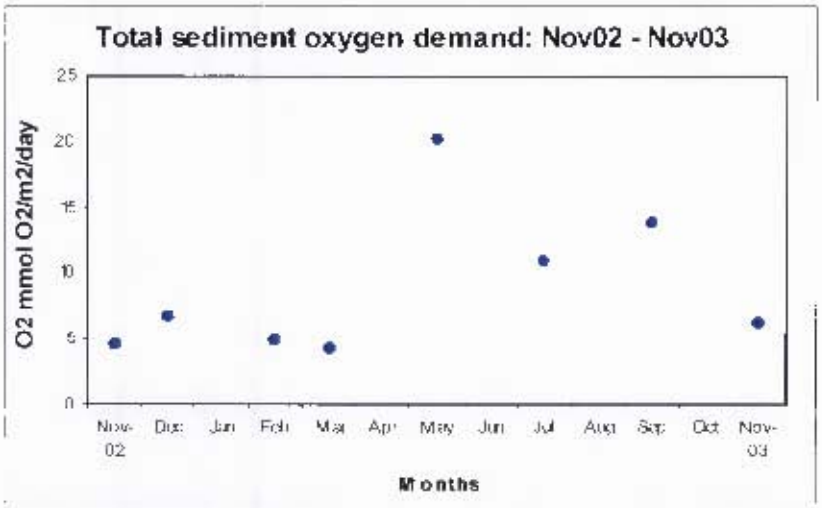

Figure 3.20: Plot of total oxygen consumption on the Namibian inner shelf between Nov 2002 and Nov 2003. TSOD peaked between May 2003 and Sep 2003.

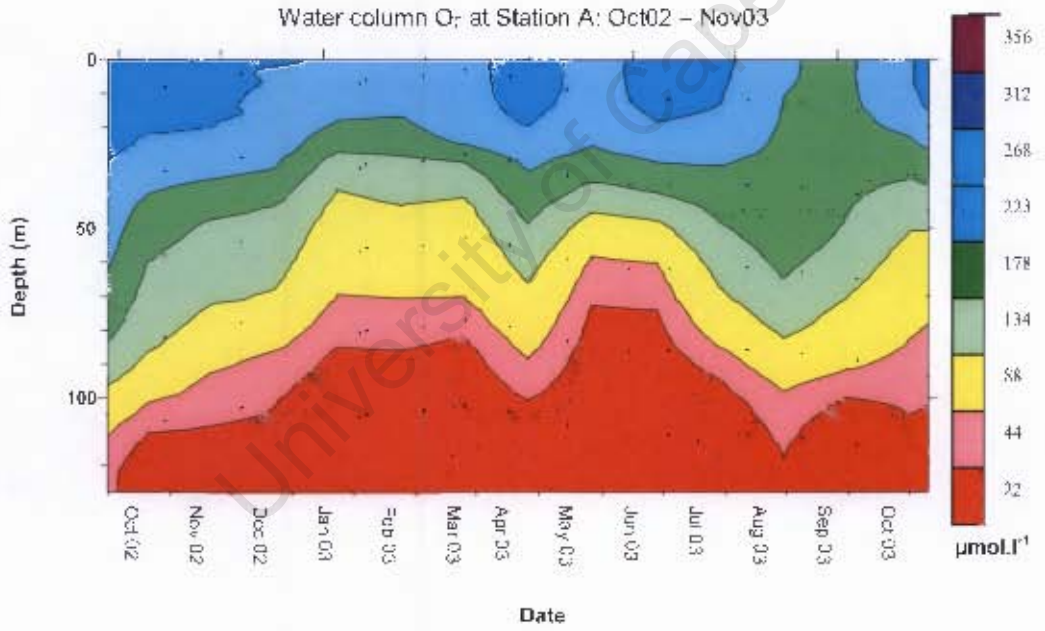

Figure 3.21: Water column dissolved oxygen profile time series at sample Station A from Oct 2002 – Nov 2003. Water depth (m) is plotted on the y-axis and oxygen concentration per individual month on the x-axis. It shows that anoxic conditions peaked between Feb 2002 and Jul 2003 while hypoxic conditions prevailed during summer months. (Data courtesy of NATMIRC).

3.6 Fluxes of dissolved species measured in incubation experiments.

Initially the biogeochemical fluxes were measured via incubations of species concentrations in sediment cores. Due to uncertainties from sample handling of core incubations, it was decided that calculated diffusive fluxes from porewater concentration gradients (presented in Section 3.3) would be used for comparison purposes instead of the measured fluxes from incubation experiments. Nonetheless, results obtained from measured incubations of biogeochemical species fluxes are presented here but were not used in the discussion due to poor reproducibility evidenced by standard deviations in brackets. Incubation fluxes of ammonium, nitrate, sulphate, hydrogen sulphide, phosphate and silicate are summarised in Table 3.5.

Table 3.5: Areal flux of ammonium, nitrate, sulphate, hydrogen sulphide, phosphate and silicate measured in sediment cores collected on the Namibian inner shelf sediments from Nov 2002 till Nov 2003. Negative rates indicate decrease in concentration while positive rates indicate increase. Standard deviations in brackets suggest that the replicate samples were not reproducible.

Month	**NH_4 flux** mmol N /m^2/day	**NO_3 flux** mmol N /m^2/day	**SO_4 flux** mmol S /m^2/day	**H_2S flux** mmol S /m^2/day	**PO_4 flux** mmol P /m^2/day	**SiO_4 flux** mmol Si /m^2/day
Nov-02	-2.92 (2.30)	-	-	-	-1.05 (0.83)	-16.71 (13.5)
Dec-02	-	-	-	-	-	-3.44 (3.7)
Feb-03	-3.70 (3.08)	-0.12 (0.01)	118.04 (28.8)	-0.40	-0.02 (0.001)	-
Mar-03	-3.85 (2.64)	0.08 (0.10)	-88.20 (23.9)	-1.95 (0.3)	-0.09 (0.10)	-
May-03	-3.99 (0.89)	-0.09 (0.002)	-32.87 (31.3)	-2.53 (1.08)	-0.08 (0.10)	-1.88 (0.9)
Jul-03	-1.88 (0.48)	-0.09	-73.42 (36.8)	-1.20 (0.25)	-0.24 (0.07)	-0.83 (0.8)
Sep-03	-2.33	-	33.63 (33.8)	-0.44 (0.18)	-0.34	-0.92
Nov-03	-2.80 (0.39)	-0.05 (0.02)	136.20 (78.4)	-2.45 (0.16)	-0.35 (0.12)	-2.30 (0.7)

Chapter 4

Discussion

Temporal variability in sediment oxygen demand and biogeochemical fluxes

Historically, the Namibian shelf is seen as one of the main areas of formation of low oxygen water (LOW) conditions in the Benguela system (Chapman and Shannon 1985). This study focussed on the role of biogeochemical fluxes on seasonal variability of total sediment oxygen demand (TSOD) in the Central Benguela inner shelf. The approach adopted was to measure quasi-monthly TSOD through incubated sediment cores and balance it with the export flux of particulate organic carbon (POC) as well as calculated diffusional sediment fluxes of the main dissolved species (NO_3^{2-}, NH_4^+, PO_4^{3-}, SiO_4^{4-}, SO_4^{2-} and HS^-). This chapter discusses the seasonal variability of TSOD observations and the role of the main biogeochemical drivers affecting TSOD.

4.1 Seasonal oxygen and oxygen flux variability.

A seasonal trend in TSOD was observed during the study period (Nov 2002 – Nov 2003) which peaked in austral winter (May 2003 to September 2003) (Figure 4.1a). During this period, TSOD was up to four times greater than the austral summer months (Nov 2002 – Dec 2002). Throughout the study period, water column oxygen profile indicated that DO concentration remained below 22.3µM (Figure 4.1b) in the bottom boundary layer (BBL; 0 – 20m off the seafloor) consistent with the semi-permanent anoxic water over the shelf sediments (Bailey 1991). In austral winter

months, increased TSOD caused the anoxic bottom boundary layer water with DO <22.3µM to extend up to 30m further into the water column.

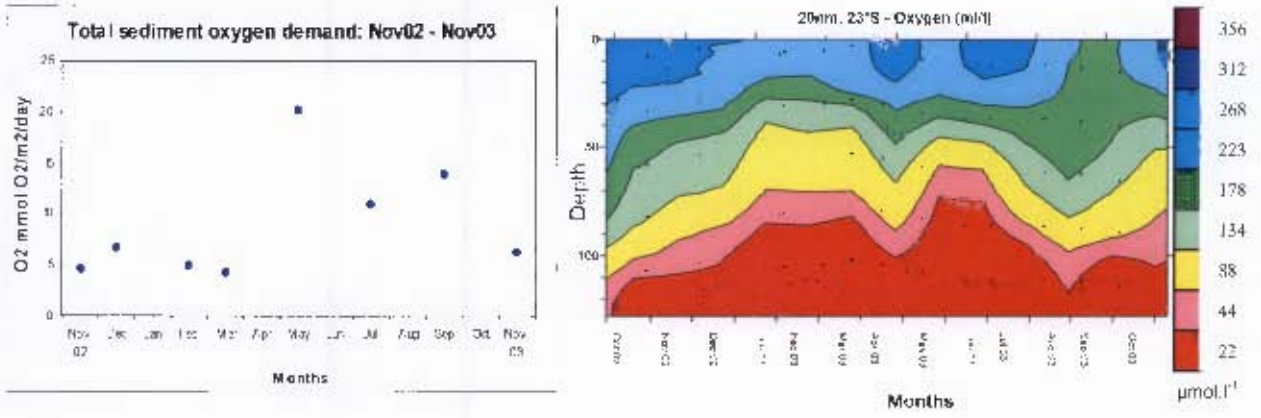

Figure 4.1:*a*) Plot of total oxygen demand on the Namibian inner shelf between Nov 2002 and Nov 2003. TSOD peaked between May 2003 and Sep 2003. Rates are expressed in mmol $O_2 m^{-2} day^{-1}$; *b*) Water column dissolved oxygen profile time series at sample Station A from Oct 2002 – Nov 2003. It showed the maximum anoxia is in winter months.

The historical view on the biogeochemical basis for hypoxia/anoxia was that SOD follows primary productivity in line with maximum upwelling activity mid to late summer in the Benguela (Bailey 1991). Due to the persistent intensity of upwelling at the Lüderitz cell (Shannon and Nelson 1996), some authors have suggested a constant flux of POC and related TSOD (Bailey 1991), however this not confirmed with data. The data presented in the current study exhibits seasonal variability in TSOD. The discussions that follow will examine the possible role of POC fluxes as well as reduced metabolite fluxes on the variability of TSOD.

4.2 Seasonal POC/PON fluxes.

High primary productivity in the Central Benguela continental shelf area is responsible for the high sedimentation rates of organic detritus (Bremner 1983; Probyn 1992; Monteiro *et.al.* 2005). POC fluxes in the current study peaked during austral summer months (Nov – Feb) ranging between 5 – 7 $mmol.m^{-2}.d^{-1}$. The POC

fluxes from this study were higher than fluxes of 1.16 mmolC.m^{-2}.d^{-1} observed by Giraudeau *et. al.* (2000) Sep1989 and Jan 1990 on the upper slope off Walvis Bay (23°S, 13°E; 595m water depth) during active upwelling. The authors observed a maximum POC flux and proposed a direct relationship of POC flux to the seaward extension of newly upwelled waters. The higher fluxes from the current study were expected as the sampling station from the current work was closer inshore and less water column degradation of POC occurs in the shallower water column.

The average C:N ratio of 7.1 (range 5.2 – 8.7; std dev 1.16) is typical of fresh marine derived phytoplankton (Libes 1992) according to Redfield stoichiometry. Seasonally, the C:N molar ratios show that highest C:N ratios (>8) in sediment trap samples were observed during the austral winter period (Feb 2003 – May 2003) although the higher fluxes of POC/PON were observed during austral summer months (Nov 2002 and Nov 2003) (Figure 4.2). Higher C:N ratios observed during winter months indicate a loss of the most labile nitrogen fraction of OM (Monteiro *et. al.* 2005). It indicates that during the summer higher productivity period, a higher portion of nitrogen is exported from the euphotic zone to the sediment.

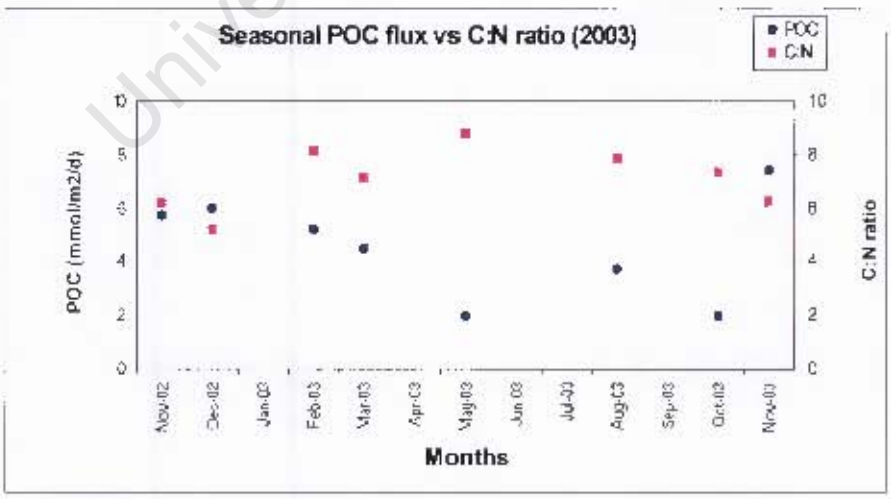

Figure 4.2: Plot of seasonal relationship between POC export flux and C:N molar ratios: 2002 – 2003. It shows highest input of fresh POC fluxes (C:N ~7) during summer months, while winter months showed the slowest POC fluxes with higher C:N ratios. POM with higher C:N ratios is and indication of 'older' relict POM.

A seasonal scale comparison of the POC fluxes and TSOD measurements during 2003 are illustrated in Figure. 4.3. During austral summer months, (Nov 2002 – Feb 2003 and Nov 2003) TSOD and POC fluxes were comparable. However, during winter and early spring (May03 – Sep03) POC fluxes remained low, while increased TSOD fluxes were observed. The stoichiometric relationship for aerobic respiration is illustrated by the following simplified equation:

$$CH_2O + O_2 \rightarrow CO_2 + H_2O \qquad (20)$$

During summer months the good agreement between POC flux and TSOD flux (almost 1:1) suggested that POC flux is the major driver of TSOD during this part of the year. During austral winter months however, TSOD were not related directly to POM flux, and reduced metabolites are hypothesised to play a more significant role.

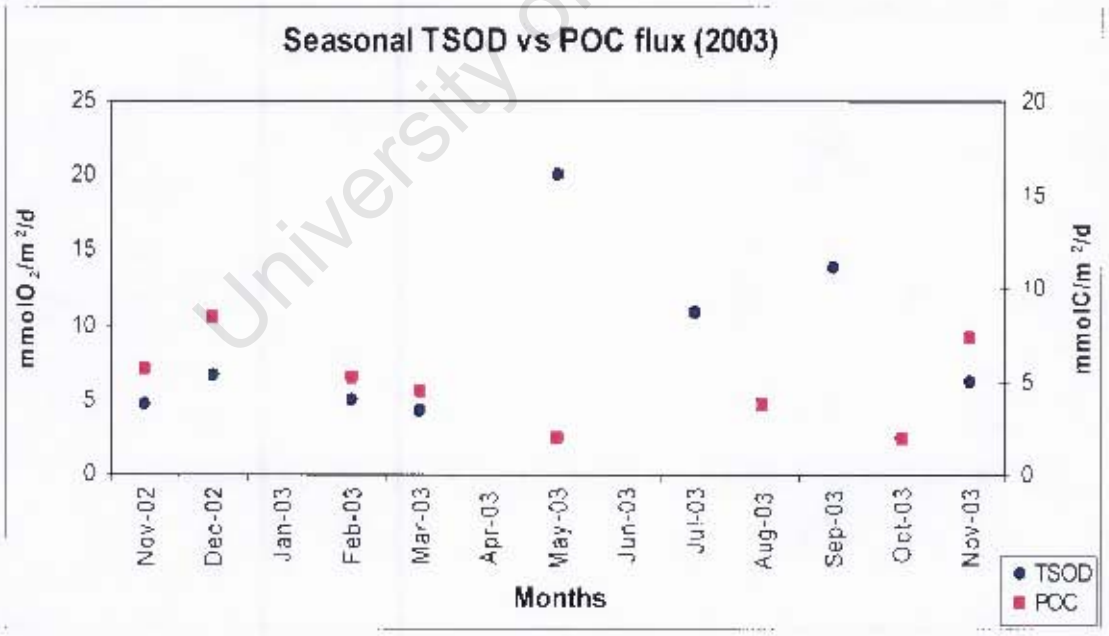

Figure 4.3: Plot comparing TSOD and POC flux during 2002 – 2003. It shows that peak POC fluxes during summer months (Nov 2002 – Mar 2003) do not coincide with peak TSOD during winter to early spring (May 2003 – Sep 2003).

4.3 Reduced metabolite diffusional fluxes.

Reduced metabolites play a significant role in sediment oxygen demand processes, particularly in anoxic sediments (Froelich *et. al.* 1979; Berner 1980; Ferdelman *et. al.* 1999). In this section the fluxes of ammonium resulting from de-amination and hydrogen sulphide resulting from sulphate reduction are compared with TSOD fluxes measurements for 2003.

4.3.1 Diffusive ammonium fluxes.

Ammonium is a product of aerobic and anaerobic remineralization (hydrolysis) of organic matter through deamination, as well as a byproduct of nitrate reduction (only seldom) (Berner 1980; Stumm and Morgan 1981). High concentrations of ammonium (up to 2.5 mM) were observed in the porewater profiles starting 1cm below the sediment-water interface. At the sediment water interface (Z = 0cm) ammonium concentrations were always low, but typical of seawater. High concentrations below the sediment-water interface indicated high rates of ammonium production within the sediments through anaerobic remineralization of organic matter.

Large concentration gradients at the sediment water interface indicated high calculated diffusional fluxes in the direction of the water column. Ammonium fluxes to the water column peaked during austral summer months (Figure 3.13) coinciding with peak POC fluxes (Figure 3.19). The seasonal trend of ammonium diffusive flux however did not follow the seasonal TSOD measurements. This suggested that sediment fluxes of ammonium alone cannot explain the seasonal TSOD variability observed on Namibian inner shelf sediments, particularly the winter inverse in POC and TSOD. The stoichiometric relationship for nitrification is 1 NH_4^+: 2 O_2 via Eq 21.

$$1/8\ NH_4^+ + ¼\ O_2 \rightarrow 1/8\ H_2O + NO_3^- + ¼\ H^+ \quad (21)$$

If all the ammonium is oxidised via this reaction, then in November 2002, when the diffusional flux of ammonium was -2.74 mmol $N.m^{-2}.d^{-1}$, it would require an oxygen supply of 5.48 mmol $O_2.m^{-2}.d^{-1}$ (see Table 4.1 for a summary). The oxygen supply required for nitrification is higher than the measured TSOD for November 2002 (4.61 mmol $O_2.m^{-2}.d^{-1}$) indicating that nitrification of ammonium could play a role in sediment oxygen demand within these sediments during the summer. However, the fact that seasonal ammonium diffusive fluxes cannot account for the increased TSOD in winter months, when ammonium flux is at a minimum, suggests that ammonium also does not govern SOD.

Remineralised ammonium in the sediment is a direct result of the hydrolysis of the PON flux. However, the observed flux of PON (~0.6 mmol $N.m^{-2}.day^{-1}$) was significantly less than the diffusional ammonium flux (1 – 6 mmol $N.m^{-2}.day^{-1}$) at the sediment-water interface (Figure 4.4). Two processes could explain this anomaly. Adsorbed ammonium in the particulate phase, which is in equilibrium with the interstitial water phase, could account for more than 90% of the total ammonium concentration (Monteiro *pers. commun.*). Through equilibrium it could maintain, in the short term, a high porewater concentration. Alternatively, ammonium could be recycled near the sediment-water interface; the water-column ammonium concentrations and the gradient calculations would then result in an overestimation of calculated diffusive ammonium fluxes. The latter model would explain why ammonium plays a minimal role in oxygen demand and eliminate the problem of replacing the losses that would follow from the first model.

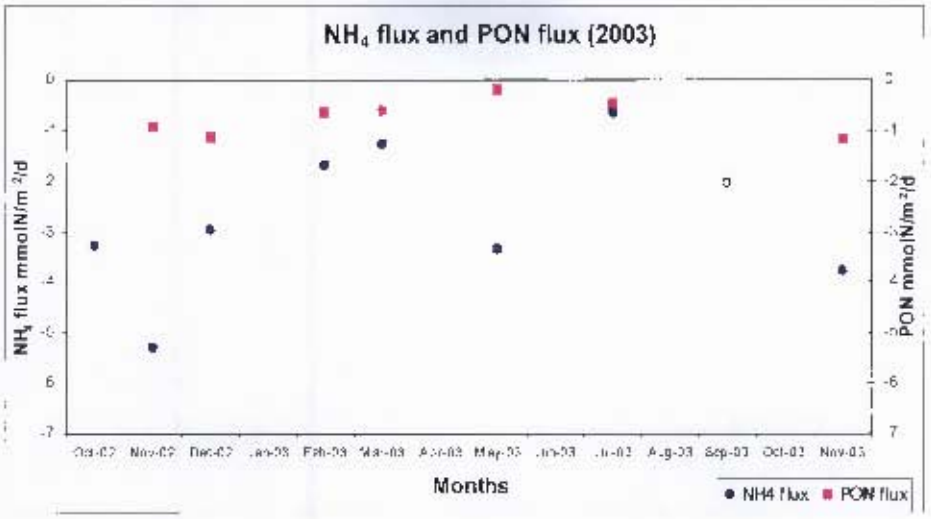

Figure 4.4: Comparison of PON flux and NH_4 flux at the sediment water interface. It shows that PON fluxes are smaller than NH_4 fluxes.

4.3.2 Diffusive hydrogen sulphide fluxes.

Hydrogen sulphide (H_2S) flux from the sediment diffuses to the overlying water column and has been shown to play a role in maintaining low dissolved oxygen via its oxidation (Ferdelman *et. al.* 1999; Brüchert *et. al.* 2003; Van der Plas *et. al.* in press). Ferdelman *et. al.* (1999) found that the oxidation of sulphide oxidation may account for 20 – 96 % of total oxygen uptake and proposed that the high volumetric rates of oxygen consumption at the sediment-water interface reflect the kinetics of sulphide oxidation. Hydrogen sulphide oxidation via Eq 22 has a stoichiometric relationship to oxygen of 2:1.

$$1/8\ H_2S + ¼\ O_2 \quad \cdot \quad 1/8\ SO_4^{2-} + ¼\ H^+ \qquad (22)$$

Hydrogen sulphide concentrations reached 57 µM in the BBL and up to 1000 µM in the porewater in July 2003. The profiles show low H_2S concentrations in the top 5cm, with a gradient increase below this depth indicating flux from deeper sediment layers

from Feb 2003 – July 2003). The highest diffusional flux of hydrogen sulphide from the sediment into the water column was calculated for July 2003 (-1.30 mmol $S.m^{-2}.d^{-1}$). Although increased hydrogen sulphide fluxes were expected during winter months, little seasonal variability was observed, only a spike in hydrogen sulphide flux in July 2003 which coincided with the winter maxima in TSOD. Data aliasing is proposed for the observed H_2S flux variability. H_2S flux data therefore also do not agree with seasonal TSOD variability on the Namibian inner shelf sediments, and it is still expected that increased H_2S fluxes play a more important role in TSOD during winter months.

Brüchert *et. al.* (2003) observed spatial distribution of H_2S fluxes ranging between 1.2 – 7.7 $mmolS.m^{-2}.d^{-1}$ along a 100m isobath on the Namibian shelf. The lowest H_2S flux in the Brüchert *et. al.* (2003) study were comparable with the highest flux (July 2003) of the current study. All the remaining months showed H_2S fluxes were an order of magnitude lower than those observed by Brüchert *et. al.* (2003). Also, the calculated H_2S fluxes were an order of magnitude lower than ammonium diffusive fluxes. It is possible that H_2S fluxes were underestimated as a result of the following three reasons:

- Difficulty in determining the hydrogen sulphide fluxes due to outgassing during sampling of sediments and porewater extraction could lead to an underestimation of these fluxes.
- Precipitation of hydrogen sulphide as iron or organic sulphides (Bailey, 1979; Fossing et. al. 1999). However, low reactive iron content in these sediments limit iron sulphide precipitation and sulphide oxidation by iron (Schultz *et. al.* 1994; Brüchert *et. al.* 2003).

- Anaerobic oxidation of hydrogen sulphide with nitrate by *Thiomargarita spp* which potentially remove up to 90% of the sulphide flux (Brüchert *et. al.* 2003).

Both POM fluxes and reduced metabolite fluxes play a role in sediment oxygen demand processes. However, seasonal variability in TSOD could not be related directly to either seasonality in POC flux or the flux of reduced metabolites. Some other possibilities influencing TSOD, not considered in this study, are the role of methane fluxes and its effect on sulphide fluxes. High rates of methane ebullition could contribute not only to accelerated transport and losses of hydrogen sulphide, but also weak residual gradients.

Monteiro *et. al.* (*in press*) investigated a high temporal resolution biogeochemical mooring data set for *in situ* oxygen, methane, temperature and salinity situated at Station A at 80m water depth from Oct 2002 – Nov 2003. The study found increased methane concentrations in the bottom boundary layer (BBL) from May 2003 – Aug 2003. The increased concentrations in the BBL were proposed to be linked to increased methanogenic activity and methane ebullition and diffusion. Increased methane activity was first observed when the system switches from hypoxic to anoxic. The periods of increased *in situ* methane concentrations observed at the mooring coincided with increased TSOD measured in core incubations. It is hypothesised that CH_4 bubbles increase the mass transfer rate of hydrogen sulphide. TSOD fluxes would therefore respond to increased fluxes of reduced compounds from the sediments.

4.3.3 Diffusive Sulphate flux.

Sulphate reduction is considered to be the dominant remineralization process on the Namibian inner shelf (Ferdelman *et. al.* 1999; Fossing *et. al.* 1999; Brüchert *et. al.* 2003). Sulphate fluxes calculated at the sediment-water interface, in all instances indicated flux into the sediment, and ranged between 5.6 – 55.7 mmol $S.m^{-2}.d^{-1}$. This is comparable to areal sulphate fluxes ranging between 9 – 52 mmol $S.m^{-2}day^{-1}$ along the 100m isobath of the Namibian continental shelf (Brüchert *et. al.* 2003). The available sulphate flux data show that the highest sulphate fluxes were observed in Feb and Mar 2003, however, sulphate fluxes showed little correlation with hydrogen sulphide fluxes (Figure 4.5). Hydrogen sulphide is a direct result of sulphate reduction, related 1:1 in its stoichiometry (Eq. 23).

$$CH_2O + \tfrac{1}{2} SO_4 + \tfrac{1}{2} H^+ \rightarrow CO_2 + \tfrac{1}{2} HS^- + H_2O \qquad (23)$$

The discrepancy between sulphate and hydrogen sulphide fluxes further supports the argument that analytical problems with the hydrogen sulphide data set were encountered, possibly during preservation of hydrogen sulphide samples or exposure to air during sampling.

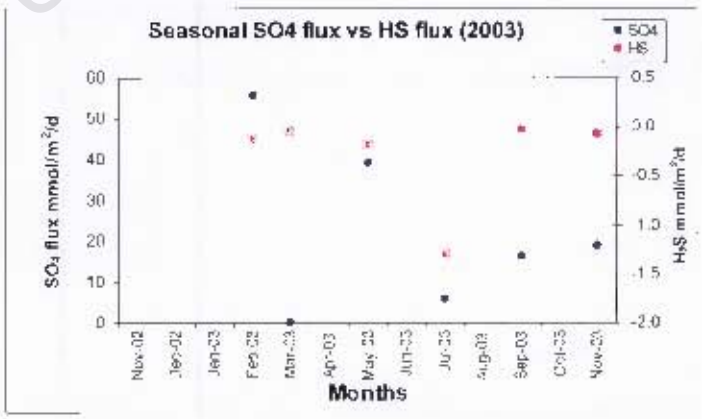

Figure 4.5: Plot showing the hydrogen sulphide and sulphate diffusive fluxes (in mmol $S.m^{-2}.d^{-1}$) between Feb 2003 and Nov 2003. It shows that the highest sulphide fluxes into the water column (Jul 2003) had little relation to sulphate fluxes over the period.

4.4 Fluxes of other metabolites.

Diffusional fluxes of nitrate, phosphate and silicate that do not contribute directly to the sediment oxygen demand were also measured in this study and are they will be discussed in the following section.

4.4.1 Diffusive nitrate flux.

From the porewater concentration profiles, a zone of unexpectedly high nitrate concentrations (up to 400 µM) were observed in the top 5 cm of sediments (Figure 3.2) and nitrate concentrations below detection thereafter. The high nitrate concentrations in this zone could indicate the formation of nitrate possibly through nitrification. Because of the anoxic redox environment, dissimilatory nitrate reduction is expected within the sediments and it is unlikely that nitrate would form through nitrification of ammonium. Water column nitrate concentrations within the BBL seldom reached concentrations >20 µM (Van der Plas *et. al. in press*; Tyrell and Lucas, 1997). The highest nitrate concentration observed in the BBL in the current study was 25 µM (See Table 3.1 for a summary). Nitrification of ammonium with oxygen is only possible if oxygen was introduced to the sediment as a result of sample handling or some other mechanism for the high nitrate concentrations observed.

Schultz *et. al.* (1999) identified giant nitrate storing sulphur bacteria (*Thiomargarita namibiensis*) on the Namibian inner shelf. Most cells have diameters of 100 – 300 µm and 98% of its biovolume consisted of a liquid vacuole. Each cell had nitrate accumulated in its vacuole of 0.1 – 0.8 M and was only present in the top 10 cm of the sediment. It was proposed that these specialised bacteria utilized the stored nitrate for the oxidation of sulphide, coupling the sulphur and the nitrogen cycles

Schultz *et. al.* (1999). It is possible that the high nitrate concentrations observed in the upper 5 cm of the sediment could be released from the rupturing of these bacteria during the porewater squeezing method of sampling.

4.4.2 Diffusive phosphate flux.

Phosphate is a by product of remineralization and in many ways similar to that of ammonia. It is liberated into solution during decomposition of organic matter by bacteria, however unlike ammonia, it does not undergo oxidation in the presence of oxygen (Berner 1980). Its Redfield stoichiometric relationship (C:N:P) in organic matter is 106:16:1. Phosphate is strongly adsorbed to on ferric oxides, therefore upon removal of oxygen and reduction of iron, phosphate is liberated to the water column (Berner 1980). The major processes controlling phosphate concentrations in unbioturbated, anoxic sediment are; diffusion, deposition, adsorption, OM remineralization and authigenic mineral precipitation.

The dissolved phosphate concentrations within the sediment were several orders higher than that observed at the sediment-water interface, due to high anaerobic mineralization organic matter within the sediments. As a result, fluxes at the sediment-water interface were in the direction of the water column with the highest fluxes observed during the austral summer months and in May 2003. This trend is similar to that observed for ammonium diffusive fluxes result. The average NH_4:PO_4 ratio of fluxes was calculated as 17.5 (stdev 4.7), showing typical Redfield behaviour. Figure 4.6 shows the linear relationship between ammonium and phosphate flux which result from remineralization of organic matter in the sediments.

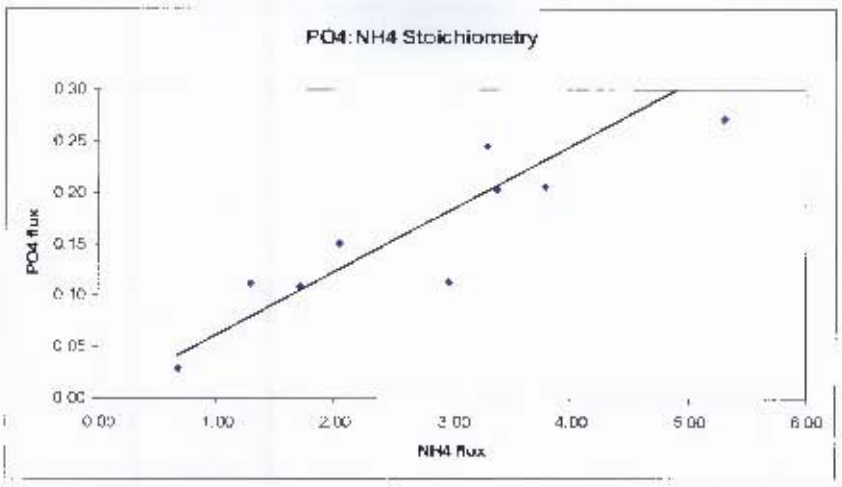

Figure 4.6: Plot of phosphate diffusive flux vs ammonium diffusive flux. It shows the linear relationship between ammonium and phosphate. The line represents the 16:1 N:P Redfield stoichiometry. It shows the linear relationship between ammonium and phosphate flux and its typical Redfield behaviour.

4.4.3 Diffusive silicate flux.

At the pH and ionic strength of seawater, the dominant dissolved species of silicon is silicic acid (H_4SiO_4). Planktonic diatoms and radiolaria living in surface waters produce skeletons consisting of opaline silica (or opal) through the polymerization of silicic acid molecules. Dissolved silicon concentrations are highest in regions subject to upwelling (Libes 1992). When these siliceous tests die and settle on the sediments, they undergo dissolution rather than remineralization. Elevated concentrations of dissolved silica in the sediment porewaters relative to the overlying water are evidence of dissolution.

The sediments on the Namibian inner shelf are mainly diatom ooze (Bremner 1983; Bailey 1991; Monteiro *et. al.* 2005) typical of upwelling active coastal areas. Similar to phosphate, silicate profiles showed a steep gradient between the sediment and the water column which indicated diffusive fluxes of dissolved silicate to the water

column. Little evidence of seasonal variability was apparent from calculated diffusional silicate fluxes. Silicate concentrations in the BBL ranged between 20 - 55 µM Si over the study period consistent with observations from Dittmar and Birkicht, (2001) and Van der Plas *et .al.* (*in press*). Biogenic opal contributes between 10 and 20% of the total particulate flux on the Namibian slope sediments (Giraudeau *et. al.* 2000).

Chapter 5

Findings and Conclusions

This study focused on the role of sediment fluxes on the seasonal variability of dissolved oxygen on the Namibian inner shelf sediments. Using the findings from this study, proposed answers to the two key questions posed in the Introduction are presented in this chapter.

1.) What are the characteristics of seasonal variability of sediment oxygen demand on the Namibian inner shelf mud belt?

Sediment oxygen demand (TSOD) from the core incubations peaks during austral winter/early spring (May to Sep 2003). The maximum TSOD of 20.10 mmol $O_2.m^{-2}.day^{-1}$ observed in May 2003 (austral winter) was roughly five times higher than SOD measurements during the austral summer months (Nov – Feb). The seasonal pattern observed in this study was found to be different to the previous understanding of the Benguela coastal system, which links local formation of low oxygen water (LOW) to primary productivity (Chapman and Shannon 1985; Bailey 1991). New production derived particulate organic carbon (POC) fluxes peaked during early austral summer months (Nov – Dec) at 7 – 10 $mmolC.m^{-2}.d^{-1}$. During summer months a good stoichiometric agreement between POC flux and TSOD was observed, however during winter months, TSOD increased beyond the oxidation of POC/PON (Figure 5.1). It was concluded that the link between POC and TSOD is limited under aerobic conditions to the austral summer period. The anomaly in the austral winter period suggested that SOD controls lie in a biogeochemical response of the sediment and not in POC forcing.

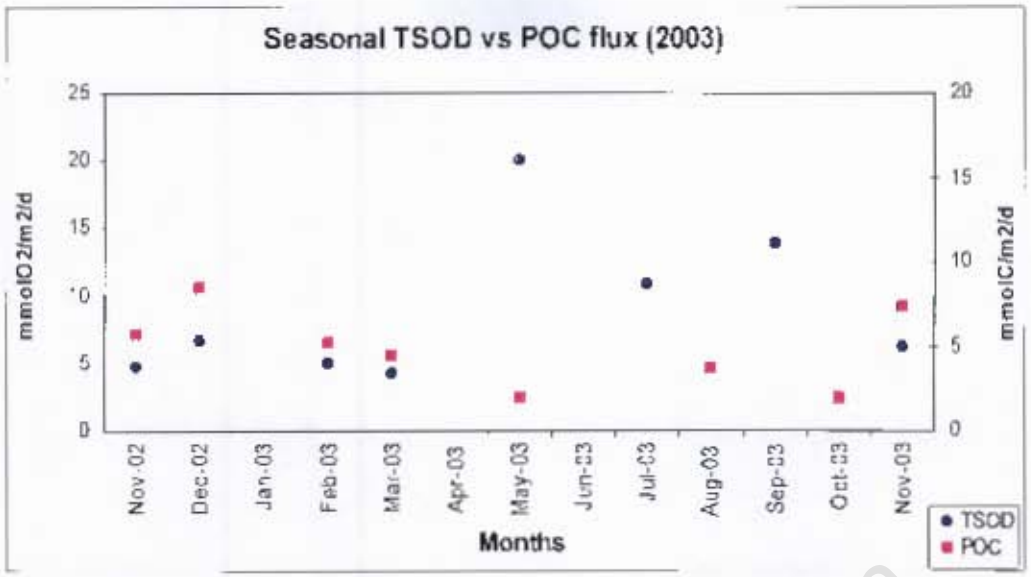

Figure 5.1: Plot comparing TSOD and POC flux during 2002 – 2003. It shows that peak TSOD (winter to early spring; Mar - Sep) does not coincide with peak POC fluxes (during summer months; Nov - Feb).

2.) How are the vertical sediment biogeochemical fluxes related to the variability in sediment oxygen demand?

The fluxes of reduced compounds resulting from anaerobic remineralization were then considered as an alternative major driver of sediment oxygen demand. Ammonium diffusive fluxes also peaked during austral summer (Nov – Dec) months at 3 – 5 $mmolN.m^{-2}.d^{-1}$ in the direction of the water column indicating highest remineralization rates during these months. Seasonal ammonium fluxes followed POC/PON fluxes rather than seasonal SOD variability. It was concluded that although ammonium fluxes contributed to SOD it is not the major driver during winter months.

Small concentration gradients of hydrogen sulphide were observed with little seasonal variability in hydrogen sulphide fluxes. Given that sulphate reduction is

considered the dominant organic matter remineralization process in these sediments (Ferdelman *et. al.* 1999) and the high sulphate fluxes into the sediment observed, the data suggested an underestimation of sulphide fluxes. Aeration of hydrogen sulphide samples during sampling and *in situ* ebullition with methane from sediments were suggested as possible explanations for the low sulphide fluxes. They remain open questions.

This study clarifies some of the important biogeochemical characteristics of seasonal variability in sediment oxygen demand on the Namibian inner shelf. Although POC flux and fluxes of reduced metabolites play a role in maintaining hypoxia/anoxia on the Namibian inner shelf in austral summer months, neither of these fluxes drive the observed seasonal characteristics of TSOD. During the winter months, it is proposed that the biogeochemical response of the sediments to remotely forced hypoxic water (Monteiro, *et. al. in press*), controls TSOD variability.

References:

Anrosti, C. and Homer, M., 2003, Carbon cycling in a continental margin sediment: contrasts between organic matter characteristics and remineralisation rates and pathways, *Estuarine, Coastal and Shelf Science*, **58**, 197 – 208.

Bailey, G.W. 1979. Physical and Chemical aspects of the Benguela current in the Luderitz Region, M.Sc thesis, University of Cape Town.

Bailey, G.W. 1987. The role of regeneration from sediments in the supply of nutrients to the Euphotic zone in the southern Benguela system. *South African Journal of Marine Science,* **5**, 273 - 285.

Bailey, G.W., 1991. Organic carbon flux and development of oxygen deficiency on the modern Benguela continental shelf south of 22°S: spatial and temporal variability. In Tyson, R.V., Pearson, T.H. (Eds.), Modern and Ancient Continental Shelf Anoxia, **58**, 171-183

Bailey, G.W., De B. Beyers, C.J. and Lipschitz, S.R. 1985. Seasonal variation of oxygen deficiency in waters of Southern South West Africa in 1975 and 1976 and its relation to the catchability and distribution of the Cape Rock Lobster *Jasus Lalandii. South African Journal of Marine Science,* **3**, 197 - 214

Bailey, G.W., Boyd, A.J., Duncombe-Rae, C.R., Mithcell-Innes, B. and Van Der Plas, A., 2001, Synthesis of marine science research in the Benguela current system during cruises linked to the BENEFIT training programme in 1999, *South African Journal of Marine Science*, **97**, 271 - 274.

Berner, R.A., 1980, Early diagenesis: A theoretical approach, Princeton series in geochemistry, Princeton University Press, NJ.

Boudreau, B.P., 1996, Diagenetic models and their implementation. Modelling transport and reactions in aquatic sediments, Springer-Verlag, Berlin, ISBN 3-540-61125-8.

Bremner, J. M., 1983. Biogenic sediments on the South West African (Namibian) continental margin. In *Coastal Upwelling: Its sedimentary record, Part B: Sedimentary records of ancient coastal upwelling* (eds. J. Thiede and E. Suess), 73 – 104, Plenum.

Brüchert, V., Jørgensen, B.B., Neumann, K., Riechmann, D., Schlösser, M and Schulz, H., 2003, Regulation of bacterial sulfate reduction and hydrogen sulfide fluxes in cental Namibian coastal upwelling zone. *Geochimica et. Cosmochimica Acta,* **67** (23), 4505 - 4518.

Brüchert, V., Lass, U., Endler, R., Dübecke, A., Julies, E., Leipe, T. and Zitzmann, S., 2006, Shelf anoxia in the Namibian upwelling system: An Integrated assessment of shelf anoxia and water column hydrogen sulphide in the Benguela coastal upwelling system off Namibia, *In press.*

Bubnov, V.A. 1972. Structure and characteristics of the oxygen minimum layer in the Southeastern Atlantic. *Oceanology,* **12**, 193 - 201.

Chapman, P. and Shannon, L.V. 1985. The Benguela Ecosystem Part II. Chemistry and Related Processes. *Oceanography and Marine Biology: An Annual Review*, **23**, 183 - 251.

Cline, J. D., 1969, *Limnology and Oceanography*, **17**, 454 - .

Copenhagen, W.J.,1953, The periodic mortality of fish in the Walvis Bay region: a phenomenon within the Benguela current. *Investigational Report, Division Fisheries Union of South Africa,* **14,** 1-35.

Devol. A.H., 2003, Solution to a marine mystery, *Nature*, **422**, 575 - 576

Dittmar, T. and Birkicht, M., 2001, Regeneration of nutrients in the northern Benguela upwelling and the Angola-Benguela Front areas, *South African Journal of Science*, **97**, 239 – 246.

Ferdelman, G. F., Fossing, H. and Neumann, K. 1999. Sulphate reduction in surface sediments of the Southeast Atlantic continental margin between 15°38'S and 27°57'S (Angola and Namibia). *Limnology and Oceanography,* **44**, 650 - 661.

Fossing, H., Ferdelman, T.G. and Berg, P., 2000, Sulphate reduction and methane oxidation in conctinental margin sediments influenced by irrigation (South East Atlantic off Namibia), *Geochimica et. Cosmochimica Acta,* **64** (5), 897 – 910.

Froelich, P.N., Klinkhammer, G.P., Bender, M.L., Luedtke, N.A., Heath, G.R., Cullen, D., and Dauphin, P., 1979, Early oxidation of organic matter in pelagic sediments in the equatorial Atlantic: suboxic diagenesis. *Geochimica et Cosmochimica Acta*, **43**, 1075 – 1090.

Giraudeau, J., Bailey, G.W. and Pujol, C., 2000. A high resolution time-series analysis of particle fluxes in the Northern Benguela coastal upwelling system:

carbonate record of changes in biogenic production and particle transfer processes. *Deep-Sea Research II*, **47**, 1999 – 2028.

Glud, R.N., Gundersen, J.K., Jørgensen, B.B., Pevsbech, N.P. and Schulz, H.D., 1994., Diffusive and total oxygen uptake of deep-sea sediments in eastern South Atlantic Ocean: *in situ* laboratory measurements. *Deep-Sea Research,* **41,** 1767 -1788.

Grasshoff, K., Kremling, K. and Ehrhardt, M., 1983, Methods of seawater analysis. Second, revised and extended edition, VerlagChemie, ISBN 3-527-25998-8.

Hart, T.J., and Currie, R.I., 1960. The Benguela Current. *"Discovery" Rep,* **31**, 123 – 298.

Hamukuaya, H., O'Toole, M., Woodhead, P.M.J., 1998, Observations of severe hypoxia and off-shore displacement of Cape hake over the Namibian shelf in 1994. In; Benguela dynamics: Impacts of variability on sea-shelf environments and their living resources. *South African Journal of Marine Science*, **23**, 397 – 417.

Hocutt C.H. and Verheye H.M., 2001, BENEFIT marine science in the Benguela Current region during 1999: Introduction, *South African Journal of Science*, **97**, 195 – 198.

Hutchings, L., 1992, Fish harvesting in a variable, productive environment – searching for rules or searching for exceptions? *South African Journal of Marine Science*, **12**, 297 – 318.

Lee, C., 1992, Controls of organic carbon preservation: The use of stratified water bodies to compare intrinsic rates of decomposition in oxic and anoxic systems. *Geochimica et. Cosmochemica Acta*, **56**, 3323 – 3335.

Li, Y. and Gregory, S., 1974, Diffusion of ions in sea water and in deep-sea sediments, *Geochimica et Cosmochimica Acta*, **38**, 703 – 714.

Libes, S.M., 1992, An introduction to marine biogeochemistry, John Wiley & Sons, New York, ISBN 0-471-50946-9.

Kuypers, M.M.M., Sliekers, A.O., Lavik, G., Schmid, M., Jorgensen, B.B., Kuenen, Sinninge Damste, J.S., Strous, M., Jetten, M.S.M., 2003, *Nature*, **422**, 608 – 611.

Middelburg, J.J., Vlug, T. and Van der Nat, F.J.W.A., 1993, Organic matter mineralization in marine systems, *Global Planetary Change*, **8**, 47 – 58.

Mohrholz, V., Schmidt, M., and Lutjeharms J.R.E., 2001, The hydrography and dynamics of the Angola Benguela frontal zone and environment in 1999, *South African Journal of Science,* **97**, 199 – 208.

Monteiro, P.M.S and Van der Plas, A.K., Bailey, G.W., Fidel, Q., 2004, Low oxygen Variabilility in the Benguela Ecosystem: A review and new understanding. CSIR REPORT ENV-S-C 2004-075. CSIR Stellenbosch, Republic of South-Africa.

Monteiro, P.M.S., Nelson, G., Van der Plas, A.K., Mabille, E., Bailey, G.W., Klingelhoeffer, E., 2005, Internal-tide shelf topography interactions as a

forcing factor governing the large scale distribution and burial fluxes of particulate organic matter (POM) in the Benguela upwelling system. *Continental Shelf Research*, **25**, 1864 – 1876.

Monteiro, P.M.S., Van der Plas, A.K., Mohrholz, V., Mabille, E., Pascall, A., Joubert, W.R., 2006 The variability of natural hypoxia and methane production in a coastal upwelling system: oceanic physics or shelf biology? *Geophysical Research Letters* (*in press*).

Ogrinc, O., Faganeli, J., Pezdic, J., 2003, Determination of organic carbon remineralization in near-shore marine sediments (Gulf of Trieste, Northern Adriatic) using stable carbon isotopes. *Organic Chemistry,* **34**, 681-692

Probyn, T.A., 1992, The inorganic nitrogen nutrition of phytoplankton in the Southern Benguela: New production, phytoplankton size and the implications for pelagic foodwebs. *South African Journal of Marine Science*. **12**: 411 – 420.

Redfield, A.C., Ketchum, B.H. and Richards, F.A., 1963, The influence of Organisms on the Composition of Seawater. In *The Sea*, Vol. 2, M.N. Hill, Ed., Wiley-Interscience, New York.

Rheeburgh, W.S., 1967, An improved interstitial water sampler, *Limnology and Oceanography*, **12**, 163 – 165.

Schultz, H.D., Dahmke, A., Schinzel, U., Wallmann, K and Zabel, M., 1994, Early diagenetic processes, fluxes and reaction rates in sediments of the South Atlantic, *Geochimica et Cosmochimica Acta*, **58** (9), 2041-2060.

Schultz, H.N. Brinkhoff, T. Felderman, T.G. Hernandez Marine, M. Teske, A and Jørgensen, B.B. 1999. Dense populations of giant sulphur bacterium in Namibian Shelf Sediments. *Science,* **284**, 176-192.

Shannon, L.V. and Nelson, G., 1996, The Benguela: Large scale features and processes and system variability. In: Wefer, G., Berger, W.H., Siedler, G., Webb, D. (Eds.), The South Atlantic: Present and Past Circulation. Springer, Berlin.

Stumm, W. and Morgan, J.J., 1996, Aquatic Chemistry. Chemical equilibria and rates in natural waters, 3rd Edition, Wiley-Interscience, New York. ISBN 0-471-51185-4.

Sundby, S., Boyd, A. J., Hutchings, L., O'Toole, M. J., Thorisson, K., & Thorsen, A. (2001). Interaction between cape hake spawning and the circulation in the northern Benguela upwelling ecosystem. *A Decade of Namibian Fisheries Science. South African Journal of Marine Science 23*, 317-336.

Tyrrel, T. and Lucas, M.I., 2002, Geochemical evidence of denitrification in the Benguela upwelling system, *Continental Shelf Research,* **22**, Issue 17, 2497 - 2511.

Visser, G.A., 1970, The oxygen – minimum layer between the surface and 1000m in the North-Eastern South Atlantic, *Fisheries Bulletin S. Afr.*, **6**, 10 – 22.

Van der Plas, A.K., Monteiro, P.M.S. and Pascall, A., 2005, The cross shelf biogeochemical characteristics of sediments in the central Benguela and its

relationship to overlying water column hypoxia. *Continental Shelf Research, in press.*

Wang, Y. and Van Cappellen, P., 1996, A multicomponent reactive transport model of early diagenesis: Application to redox cycling in coastal marine sediments. *Geochimica et Cosmochimica Acta*, **60** (16), 2993 – 3014.

Wattenberg, H., 1938 *Wiss. Ergebn. Dt. Atlant. Exped. 'Meteor',* 1925-1927, **9,** 1-132.

Woodhead, P.M., Hamukuya, H., O'Toole, M.J and McEnroe, M., 1998, Effects of oxygen depletion in shelf waters on hake populations off central and northern Namiba. In: International Symposium, *Environmental variability in South East Atlantic.* (eds. Shannon V. and O'Toole M.J.) 10 pp. NATMIRC, Namibia

Web references:

1.) www.bclme.org

Appendix A - **Description of analytical methods**

- Dissolved Oxygen.

  Dissolved oxygen was measured *in-situ* using the instrumentation described in Section 3.5. The membrane electrode method (field measurement) from Standard Methods for the examination of Water and Wastewate was used. Oxygen diffuses through a permeable membrane on a polarographic oxygen electrode. The diffusion current produced by the electrode is linearly proportional to the concentration of molecular oxygen. The instrument is calibrated according to manufacturer's specifications using the air saturation method. The calibrated electrode is used to measure the dissolved oxygen concentration in the ovelying water column.

- Dissolved Nitrate.

  In the absence of a suitable reaction for the direct colourimetric determination of nitrate, nitrate is reduced to nitrite by passing the standards and samples through a cadmium reduction column. The resulting nitrite produced is reacted with a diazo-coupled colour reagent and measured at 540nm. This treatment of the sample determines both nitrate and nitrite together and nitrite has to be determined separately and subtracted from this total amount to obtain the nitrate. An AutoAnalyser II (AAII) instrument was used in the procedure (method by Grasshoff *et. al.* 1983 based on the method described by Kirkwood, 1994).

- Dissolved Total Ammonium.

  Under alkaline conditions ammonia reacts with hypochlorite and forms monochloramine, which, in the presence of phenol and excess hypochlorite, forms indo-phenol blue. This colourometric method measures the total ammonia nitrogen i.e. unionised NH_3-N as well as NH_4-N. A citrate buffer solution is added to the

samples and standards respectively, mixed, and then a phenol solution is added and mixed and finally the alkaline oxidant solution is added and mixed. The resulting turquoise-blue solution is passed through a photometer (630nm; AAII) and the sample absorbances are compared to the standard solution absorbances (method by Grasshoff *et. al.* 1983 based on the method described by Kirkwood, 1994).

- Dissolved Reactive Phosphate.

The automated colourometric determination of dissolved inorganic phosphate is based on the reaction of ortho-phosphate and acidified molybdate reagent to form a dodecaheteropoly acid, which is subsequently reduced to an intense blue compound. An ascorbic acid solution is added to the samples and standards respectively, mixed, and then a molybdate reagent solution is added and mixed. The resulting blue coloured solution is passed through a photometer (880nm; AAII) and the sample absorbances are compared to the standard solution absorbances absorbances (method by Grasshoff *et. al.* 1983 based on the method described by Kirkwood, 1994).

- Dissolved Reactive Silicate.

The automated colourometric determination of dissolved silicate is based on the reaction of reactive silicate and acidified molybdate reagent to form a silicomolybdic acid, which is subsequently reduced with methol to form an intense blue heteropoly silicate compound. The resulting blue coloured complex solution is passed through a photometer (810nm; AAII) and the sample absorbances are compared to the standard solution absorbances absorbances (method by Grasshoff et. al. 1983 based on the method described by Strickland and Parsons 1972).

- Sulphate.

A turbidimetric Method was used to determine sulphate (SO_4^{2-}) concentrations. Sulphate ion (SO_4^{2-}) is precipitated in an acidic medium with barium chloride ($BaCl_2$) so as to form barium sulphate crystals. An AutoAnalyser II (AAII) instrument was used in the procedure. A buffer solution is added to the samples and standards respectively, mixed, and then the barium chloride solution is added and mixed. The resulting turbid solution is passed through a spectrophotometer (420nm; AAII) and the sample absorbances are compared to the standard solution absorbances. Method described in Standard Methods for the examination of Water and Wastewater.

- Hydrogen sulphide.

A spectrophotometric method with methylene blue as colour reagent was used for determination of hydrogen sulphide. Hydrogen sulphide samples were preserved with 20% Zinc acetate solution. After acidification with 6*N* HCl, hydrogen sulphide was condensed with di-methyl-*p*-phenylenediamine with Iron(*III*) chloride as the oxidant. Absorbances of colour development was mearured with UV/Vis spectrophotometer (670nm, 1cm cuvette) and the sample absorbances were compared to the standard solution absorbances (method by Grasshoff et. al. 1983 based on the method described by Cline 1969).

Appendix B – Raw data for Chapter 3.

Table B.1: Porewater concentrations of sediment cores collected in 2003.

NH_4-N (µM)	Date								
Depth (cm)	*Oct-02*	*Nov-02*	*Dec-02*	*Feb-02*	*Mar-02*	*May-02*	*Jul-02*	*Sep-02*	*Nov-03*
0	2	0	0	1	10	42	4	3	16
1	978	1569	879	559	390	1020	-	607	1138
3	1105	1387	1275	975	1092	1020	404	1495	1571
5	1318	1523	1425	962	1309	896	833	1121	1174
7	1457	1434	1871	1044	1188	882	1098	1786	1536
9	1469	1565	1617	590	1351	1036	939	1561	1548
12	1438	1470	1875	1113	1423	1232	899	1035	1571
16	930	1789	1645	1223	1285	952	1204	727	1814
20	1190	1779	1878	1291	1152	1050	1177	1909	1404
24	1496	1851	2756	-	1375	812	-	2131	1223
28	-	-	2380	-	-	-	-	2118	-
NO_3-N (µM)									
0	23.9	26.7	18.2	13.1	18.7	10.1	27.2	6.1	-
1	86.7	185.4	190.7	40.0	9.3	20.0	-	7.5	-
3	15.9	76.6	127.0	20.9	7.1	10.0	396.2	38.4	-
5	8.6	47.7	16.4	16.0	1.9	5.1	45.6	5.6	-
7	1.8	13.8	8.4	16.4	0.9	3.7	16.3	5.4	-
9	7.8	9.7	10.1	5.3	0.5	0.0	22.4	5.2	-
12	0.9	14.2	5.9	17.5	0.4	9.7	8.0	4.6	-
16	0.9	19.7	10.5	16.5	0.0	7.5	5.0	4.2	-
20	1.7	27.4	2.4	-	0.0	4.0	7.1	4.8	-
24	2.8	6.4	2.6	3.8	0.5	5.3	-	5.0	-
28	-	-	2.8	-	0.7	-	-	-	-

Table B.1: Continued from previous page.

SO_4-S (mM) Depth (cm)	Date								
	Oct-02	*Nov-02*	*Dec-02*	*Feb-02*	*Mar-02*	*May-02*	*Jul-02*	*Sep-02*	*Nov-03*
0	-	-	-	26.4	-	30.4	29.1	27.7	24.9
1	-	-	-	4.0	-	14.5	-	21.1	17.2
3	-	-	-	6.5	-	19.4	24.5	22.2	20.6
5	-	-	-	20.9	-	19.4	19.1	18.8	21.7
7	-	-	-	22.4	-	21.2	7.0	26.9	22.8
9	-	-	-	12.1	-	16.6	17.2	17.6	18.8
12	-	-	-	19.7	-	21.5	8.5	17.2	-
16	-	-	-	9.0	-	9.4	16.0	14.6	-
20	-	-	-	20.9	-	12.3	13.3	16.2	18.0
24	-	-	-	15.7	-	14.8	-	-	15.8
H_2S-S (µM)									
0	-	-	-	44.4	44.7	45.9	57.6	31.8	16.2
1	-	-	-	100.0	40.0	46.5	-	4.6	11.7
3	-	-	-	126.5	39.4	48.8	861.1	2.4	75.5
5	-	-	-	148.2	40.0	24.7	1044.4	5.4	56.1
7	-	-	-	214.1	42.4	51.2	972.2	5.5	72.7
9	-	-	-	-	72.4	102.4	511.1	6.1	58.3
12	-	-	-	214.1	90.0	194.4	505.6	52.9	34.9
16	-	-	-	350.0	161.8	388.9	327.8	52.2	42.8
20	-	-	-	-	37.1	550.0	128.2	109.0	62.2
24	-	-	-	-	40.6	705.6	-	-	66.9
28	-	-	-	-	-	-	-	-	-

Table B.1. Continued from previous page

PO_4-P(µM) Depth (cm)	Date								
	Oct-02	*Nov-02*	*Dec-02*	*Feb-02*	*Mar-02*	*May-02*	*Jul-02*	*Sep-02*	*Nov-03*
0	1.7	1.2	1.6	1.8	1.2	1.3	2.6	2.3	0.0
1	249.2	171.8	116.3	111.8	115.0	207.9	-	154.0	207.4
3	212.4	185.0	177.6	139.3	174.0	179.2	36.1	154.0	230.4
5	233.7	193.0	191.9	143.0	169.8	180.6	59.6	110.0	180.5
7	267.5	156.8	419.3	152.1	237.7	182.8	78.9	188.2	180.5
9	286.5	152.1	201.4	133.8	178.3	247.3	45.6	192.0	139.3
12	308.8	146.6	193.5	139.3	169.8	172.1	38.2	106.3	139.3
16	70.2	133.5	146.0	97.1	123.4	112.2	45.6	110.0	124.6
20	78.8	123.5	143.5	128.3	-	87.7	45.6	135.6	73.0
24	77.1	89.6	128.2	-	94.0	52.4	-	135.6	53.8
28	-	-	92.9	-	-	-	-	-	-
SiO_4-Si(µM)									
0	33.8	35.8	29.4	21.2	-	31.1	34.5	39.1	35.4
1	236.0	251.2	313.3	130.5	-	138.0	-	174.5	-
3	317.3	248.6	234.9	140.4	-	140.0	268.2	192.0	462.1
5	319.6	226.9	205.1	138.4	-	283.2	187.8	349.0	359.4
7	268.7	284.0	482.1	162.2	-	299.4	258.5	226.9	564.8
9	237.8	297.4	352.2	166.1	-	90.0	421.9	909.8	479.2
12	290.7	339.7	319.4	187.9	-	205.0	453.6	453.7	667.5
16	304.0	268.2	429.4	144.4	-	110.0	292.6	122.2	804.4
20	287.6	318.1	383.8	150.3	-	80.0	307.2	628.2	513.5
24	274.1	257.1	416.0	-	-	86.0	-	-	547.7
28	-	-	500.6	-	-	-	-	-	-

- Indicate months for which no data are available.

Table B.2: Areal oxygen uptake rates calculated from raw data.

	Length(cm)	L(meters)	volume (dm^3)	measured gradient ($mmol/dm^3/min$)	mmol/min	$\mu mol/m^2/min$	TSOD $mmol/m^2/day$	Ave TSOD
Nov-02	9.0	0.090	0.28	-0.0000356	-9.99E-06	-3.20	-4.61	4.61
Dec-02	9.0	0.090	0.28	-0.0000430	-1.21E-05	-3.87	-5.57	6.70
	9.0	0.090	0.28	-0.0000604	-1.69E-05	-5.43	-7.82	
Feb-03	8.4	0.084	0.26	-0.0000446	-1.17E-05	-3.74	-5.39	4.93
	9.2	0.092	0.29	-0.0000338	-9.70E-06	-3.11	-4.48	
Mar-03	8.4	0.084	0.26	-0.0000392	-1.03E-05	-3.30	-4.75	4.27
	6.2	0.062	0.19	-0.0000426	-8.22E-06	-2.64	-3.80	
May-03	8.6	0.086	0.27	-0.0001463	-3.92E-05	-12.58	-18.12	20.10
	10.5	0.105	0.33	-0.0001461	-4.78E-05	-15.34	-22.09	
Jul-03	9.2	0.092	0.29	-0.0000937	-2.69E-05	-8.62	-12.41	10.89
	8.9	0.089	0.28	-0.0001026	-2.85E-05	-9.13	-13.15	
	9.2	0.092	0.29	-0.0000536	-1.54E-05	-4.93	-7.10	
Sep-03	12.7	0.127	0.40	-0.0001118	-4.43E-05	-14.20	-20.45	13.82
	10.3	0.103	0.32	-0.0001209	-3.88E-05	-12.45	-17.93	
	6.5	0.065	0.20	-0.0000329	-6.67E-06	-2.14	-3.08	
Nov-03	9.4	0.094	0.29	-0.0000653	-1.91E-05	-6.14	-8.84	6.12
	6.8	0.068	0.21	-0.0000347	-7.35E-06	-2.36	-3.40	

Table B.3: Particulate organic carbon (POC) and particulate organic nitrogen (PON) concentration profiles with sediment depth from November 2002 to November 2003.

Month	Nov-02		Feb-03		Mar-03		May-03		Jul-03		Nov-03	
Depth(cm)	%POC	%PON	%POC	%PON	%POC	%PON	%POC	%PON	%POC	%PON	%POC	%PON
2	13.68	1.74	10.52	1.50	10.96	1.70	13.10	2.01	10.91	1.56	5.46	0.78
4	13.81	1.73	10.92	1.75	11.11	1.80	12.20	1.86	11.47	1.64	12.16	1.50
6	13.35	1.64	11.26	1.81	11.32	1.76	12.43	1.80	10.30	1.45	12.95	1.53
8	13.98	1.62	11.24	1.80	11.08	1.71	12.74	1.83	8.10	1.12	8.14	0.95
10	13.76	1.54	10.15	1.56	9.59	1.46	12.66	1.79	8.06	1.12	7.88	0.94
14	12.37	1.37	9.32	1.44	9.20	1.42	12.17	1.70	6.51	0.89	8.70	0.98
16	10.99	1.23	8.91	1.39	8.83	1.29	10.98	1.51	-	-	10.66	1.24
20	11.42	1.33	9.03	1.38	7.21	1.00	10.65	1.50	11.09	1.55	9.28	1.06
24	8.80	1.01	-	-	7.03	1.08	8.25	1.18	-	-	0.73	0.09